AN INTEGRATED STUDY OF THE RESERVE ESTIMATION OF NARSHINGDI GAS FIELD

MD. MAHFUZUL HOQUE

DEPARTMENT OF PETROLEUM AND MINERAL RESOURCES ENGINEERING

BANGLADESH UNIVERSITY OF ENGINEERING AND TECHNOLOGY

DHAKA, BANGLADESH

AN INTEGRATED STUDY OF THE RESERVE ESTIMATION OF NARSHINGDI GAS FIELD

A Thesis by

MD. MAHFUZUL HOQUE

Submitted to the

Department of Petroleum and Mineral Resources Engineering

Bangladesh University of Engineering and Technology

In partial fulfillment of the requirements for the degree of

MASTER OF SCIENCE IN PETROLEUM ENGINEERING

January, 2015

RECOMMENDATION OF THE BOARD OF EXAMINERS

The undersigned certify that they have read and recommended to the Department of Petroleum & Mineral Resources Engineering, for acceptance, a thesis entitled **"AN INTEGRATED STUDY OF THE RESERVE ESTIMATION OF NARSHINGDI GAS FIELD"** submitted by **MD. MAHFUZUL HOQUE** in partial fulfillment of the requirements for the degree of MASTER OF SCIENCE in PETROLEUM ENGINEERING.

Chairman (Supervisor) ……
Afifa Tabassum Tinni
Assistant Professor
Department of PMRE, BUET, Dhaka.

Member (Ex-Officio) ……..
Dr. Mohammad Tamim
Professor and Head
Department of PMRE, BUET, Dhaka.

Member ……
Mohammad Mojammel Huque
Assistant Professor
Department of PMRE, BUET, Dhaka.

Member (External) ……
Md. Jahangir Kabir
Deputy Manager (Reservoir Engg.)
Petrobangla

Date: 3rd January, 2015

ABSTRACT

Demand of natural gas is always higher than the supply in Bangladesh. Correct estimation of reserve is important for the development of the gas fields, design of production facilities and preparation of the gas contracts. Narshingdi is one of the gas fields of Bangladesh Gas Field Company Limited (BGFCL). This field was discovered by Petrobangla in 1990. The objective of this study was to estimate the Gas Initially In Place (GIIP), remaining reserve, reservoir boundary, and various petrophysical data of Narshingdi gas field.

There are two gas sands, Upper Gas Sand (UGS) and Lower Gas Sand (LGS) in this field. Gas production started in 1996 and presently the two producing wells (NAR-1 and NAR-2) are producing gas from LGS at a rate of 17 and 11 MMSCFD respectively. Seventeen years of production data (1996 to 2013) have been analyzed to perform material balance and advanced decline curve analysis. Monte Carlo simulation approach was also performed to estimate proved, probable and possible reserve. Reservoir simulation using ECLIPSE 100 black oil simulator was performed for the purpose of history matching and production forecast. Different forecast scenarios were designed to investigate the effect of additional vertical well and gas compression on recovery.

The regular pressure survey of the field was not conducted and therefore Flowing Gas Material Balance an alternative to conventional material balance was performed. In the absence of pressure transient test (e.g., buildup, drawdown) data, advanced decline curve analysis was performed to calculate the reservoir potentiality (permeability, skin), reservoir area, GIIP and the ultimate recovery of the field.

This study shows that the reservoir is depletion type and the pressure decline is significant. Adding more well in the lower gas sand will not be beneficial.

ACKNOWLEDGEMENT

My deepest appreciation goes to my supervisor Ms. Afifa Tabassum Tinni, Assistant professor, Department of Petroleum and Mineral Resources Engineering for her valuable guidance and supervision throughout the entire work. I would like to thank Ms. Farhana Akter, lecturer, Department of PMRE, for her cooperation and time to time help, to complete this work. My sincere appreciation is for Dr. M. Tamim, Professor and Head of PMRE department for his valuable suggestion and support to accomplish this work. I express my gratitude to Dr. Mahbubur Rahman (On Leave), Associate Professor, PMRE department for his initial guidance to start this work and learn the necessary software. I would like to thank Mohammad Mojammel Huque, Assistant Professor, department of PMRE for his advice to complete this work. I would like to thank the staff of PMRE department for their kind help.

I would like to thank to the officials of Petrobangla and BGFCL for helping me to collect necessary data to complete this work. I would like to thank Mr. Amir Faisal, Deputy General Manager, Md Jahangir Kabir, Deputy Manager, Ahsanul Hoque, Deputy Manager (reservoir and data management division) Petrobangla for their advice and help to complete this work. My unequivocal gratitude and praise to the almighty Allah by whom and through whom all things consist, for the life, grace, favor, strength, wisdom and understanding to come this far in the life and continue onwards. All glory to him forever.

TABLE OF CONTENTS

LIST OF FIGURES

FIGURE **Page**

LIST OF TABLES

TABLES **Page**

CHAPTER 1
INTRODUCTION

The volume of hydrocarbons is difficult to quantify. It is estimated by means of various methods at different stages of exploration and development. The accuracy of estimation increases with the number and reliability of the available data on the reservoir geological model, fluid and rock properties as well as the recovered fluid volumes. The amount of gas in a subsurface reservoir is called gas in place (GIP). Only a fraction of this gas can be recovered from a reservoir. This fraction is called the recovery factor. The portion that can be recovered is considered to be a reserve[1].

The information of gas reserve is crucial for the development of production strategy, contract preparation and valuation of reserves. Classically reserves are estimated in three ways volumetric, material balance and production decline[2]. Volumetric and material balance methods estimate original gas in place and production decline yields an estimate of recoverable gas. Volumetric method attempts to determine the amount of gas in place by using the size of the reservoir as well as the physical properties of its rocks and fluids. An assumed value of recovery factor is used to get the amount of recoverable reserve[1].

Material balance methods provide a simple but effective, alternative to volumetric methods for estimating not only original gas in place but also gas reserves at any stage of reservoir depletion. A material balance equation is simply a statement of principal of conservation of mass. When sufficient production and pressure data are available; application of material balance method can provide the predominant drive mechanism of the reservoir[3].

The decline curve analysis offer an alternative to volumetric and material balance method and history matching with reservoir simulation for estimation original gas in place and gas reserves. Application of gas reserve techniques to gas reservoirs is most appropriate when more conventional volumetric or material balance techniques are not accurate or sufficient data are not available to justify the complex reservoir simulation[3].

The Narshingdi Gas field is located near Narshingdi town approximately 50 km. northeast of Dhaka. The Narshingdi structure is a subsurface anticline directed NNW-SSE (North-northwest-South-southeast) and is about 60 sq km in size. This is northern most culmination of the greatest Bakhrabad anticline and was named A2 culmination by Shell in early 1960s[4].

There are two exploration wells penetrating the Narshingdi structure, Narshingdi-1 (NAR-1) and Narshingdi-2 (NAR-2), which were drilled in 1990 and late 2006, early 2007 respectively. Gas has been encountered at two horizons, which are referred to as the Upper Gas Sand (UGS) and Lower Gas Sand (LGS). Currently both wells are producing gas from the Lower Gas Sand[4].

Previous Reserve Estimation:

Pre drill:

Pre drill GIIP estimation was made by Bangladesh Oil Gas and Mineral Corporation (BOGMC) based on a seismic interpretation and sand thickness from nearby fields. They estimated the potential for 2.1 TCF gas that is far greater than any of the post drill estimates. In 1992, Intercomp Kanata Management (IKM) estimated that proved, probable and possible reserve of LGS to be 64.8, 110.7, 148.5 BCF respectively[5].

Post drill:

In 2003, Petrobangla's Reservoir Study Cell estimated GIIP and Recoverable reserve for the LGS using both deterministic volumetric and material balance methods. According to this study, the proved reserve of the LGS is 137.25 BCF and proved plus probable reserve is 248.46 BCF and the GIIP using the Material Balance method is 295 BCF[5].

In 2003 reserve report, the Hydrocarbon Unit Bangladesh and Norwegian Petroleum Directorate (HCU-NPD) made an estimation of GIIP for both UGS and LGS of Narshingdi gas field using the deterministic volumetric method. The result of this study is shown in the Table 1.1

Table 1.1: HCU-NPD 2003 Reserve Estimate-Narshingdi Gas Field[5]

Sand	Proved GIIP (BCF)	Probable GIIP (BCF)	Possible GIIP (BCF)	Proved + Probable (BCF)	Proved + Probable +Possible (BCF)
Upper Sand		71.7		71.7	71.7
Lower Sand	46.46	189.04	79.8	235.5	315.3
Field Total	46.46	260.74	79.8	307.2	387

In addition a material balance study using the MBAL software package was performed by HCU-NPD. This material balance study used shut-in well head pressure data and converted that data to shut in bottom hole pressure (SBHP) using the pressure gradient information. This study indicates that a GIIP of 315 BCF for the lower gas sand[5].

In November 2009 RPS Energy estimated the GIIP to be 369 BCF and 365 BCF using the reservoir simulation and volumetric method respectively[5].

According to the report by HCU-NPD, entitled "Bangladesh Gas Reserve Estimation 2003" which was updated in 2011 summarized the proved, proved plus probable, proved plus probable pus possible GIIP are 247.6, 344.6, 444.6 BCF respectively. They also showed that Material Balance and Approximate Well Material Balance (AWMB) estimates of GIIP to be 314 BCF 415 BCF respectively[5].

Akter F. conducted Reserve Estimation Study of Narshingdi gas Field using Eclipse 100, and the history match result of LGS is 284 BCF[6].

The reserve estimated by different companies/agencies has been summarized in Table 1.2

Table 1.2: Reserve Estimate by Different Companies /Agencies

Estimating Company/Agency	Estimated GIIP in BCF	Year of Estimation
Intercomp Kanata Management (IKM)	Proven 64.8 Probable 110.7 Possible 148.5	1992
Petrobangla Reservoir Study Cell	Proven 137.25 Proven + Probable 248.46 Material Balance 295	2003
Hydrocarbon Unit Bangladesh and Norwegian Petroleum Directorate (HCU-NPD)	Proven 46.46 Proven + Probable 307.2 Proven+ Probable +Possible 387 Material Balance 315	2003
RPS Energy	Reservoir simulation 369 Volumetric method 365	2009
Hydrocarbon Unit	P_{90} 247.6 P_{50} 344.6 P_{10} 444.6 Material Balance 314 AWMB 415	2011

CHAPTER 2

SCOPE OF THE STUDY

2.1 Objectives of the study

The objective of this study is to perform an extensive reservoir engineering study of Narshingdi field to understand the behavior and predict its future performance utilizing the available information. Reservoir performance predicted by simulation or analytical models can be verified by actual reservoir performance. This study has been subdivided as follows:

- Revising and updating the GIIP, recoverable reserves and remaining reserves.
- History matching of well production and pressure data by reservoir simulation.
- Predicting future performance for different future development scenarios.

2.2 Methodology

The geological, geophysical data, rock and fluid properties, production history, completion and well test data, were collected from Petrobangla and Bangladesh Gas Field Company Limited (BGFCL).

- Probabilistic reserve estimation using the Monte Carlo Simulation approach performed to find P_{90}, proven reserve, P_{50}, proven + provable reserve, and P_{10}, proven+ provable + possible reserve.
- Conventional material balance (Using the software MBAL of IPM Suits) and Flowing gas material balance used to estimate the GIIP, reserve, recovery factor and drive mechanism of the reservoir.
- Advanced decline curve analysis (using the software Topaze and Fekete R.T.A) accomplished to predict ultimate gas recovery at some future reservoir abandonment pressure or economic production rate.
- A dynamic reservoir simulator “ECLIPSE 100” (Black oil simulator) used to perform a history match and evaluates future development scenarios; do nothing, drilling additional wells (vertical/horizontal).

The working procedure is shown in the Figure 2.1

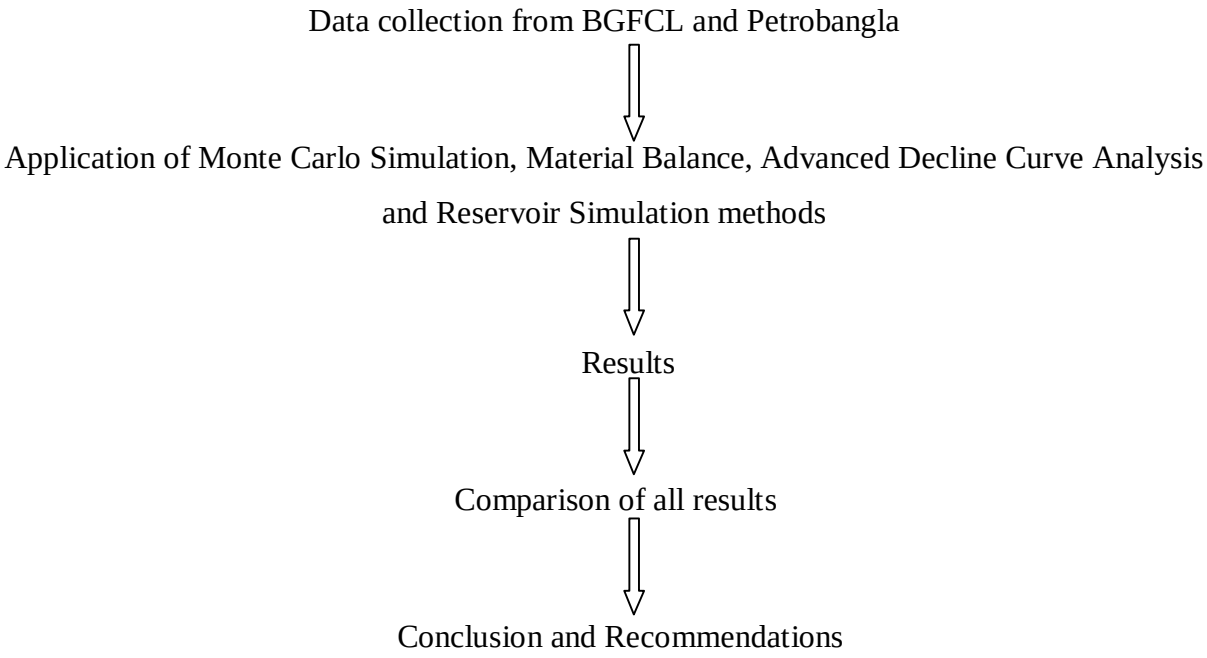

Figure 2.1: Work procedure flow diagram.

CHAPTER 3

GENERAL INFORMATION OF THE FIELD

Narshingdi gas field is located in northeastern part of Bangladesh in the western edge of the eastern fold belt in the northern portion of Block 9. The field is located on the northernmost culmination of greater Bakhrabad structure that includes the Meghna and Bakhrabad gas fields to the south. The field is about 40 km. north of Bakhrabad field and approximately 32 km west of Titas gas field[5]. Location of the field is shown in Figure 3.1

Figure 3.1: Location Map of Narshingdi Gas Field

3.1 Structure

The Narshingdi Field is an anticline with a simple four-way dip closure at the northern end of the Bakhrabad-Meghna-Narshingdi structure trend, the main axis of this structural trend lies NNW-SSE, curving slightly NNE toward the northern end where the Narshingdi structure is located. The structure lies on the southern fringes of the Surma Basin which is located at the western margin of the North-South trending Chittagong-Tripura folded belt. The structural dip at the Narshingdi closure is quite gentle, estimated to be in the range of only 1-2 degrees. The structure was first mapped by Shell in 1960 with a single fold seismic grid[4].

3.2 Stratigraphy

Stratigraphically, the Narshingdi gas field area is located in the southern part of the Surma Basin. The lithological succession penetrated in the Narshingdi area is comprised of Neogene deposits from recent alluvium to sedimentary rocks of the upper Bhuban. The sediment source was initially in the North-West and North but in later times, following the uplift of the Tripura folds; sediments were also derived from an uplifted landmass in the East[4].

Geological and petrophysical evidence convincingly indicate that the gas sands of the Narshingdi area are of the mouth bar type. The areal extents of the mouth bars by their very nature are widely variable. Optical seismic resolution is critical for a reliable definition of these sand bodies.

The sedimentary sequence encountered during the drilling of the Narshingdi structure is listed below.

TIPAM GROUP (Late Miocene-Pliocene): The Tipam Group consists of Girujan Clay and Tipam Sandstones. The Tipam Sandstone is the lower member of the Tipam Group and is predominately arenous sequence with clay pebble beds at its base. It is characterized by highly cross bedded, very course grained sands with pebbles, mica granules, and fossil wood as common constituents. The environment of deposition is Fluvial. Although the Tipam Sandstone has the excellent reservoir characteristics and is a producing interval in the Asam Valley of India, it is not productive anywhere in Bangladesh. This is probably due to lack of consistent regional seal[4].

BOKABIL FORMATION (Middle-Late Miocene): The Bokabil Formation encountered in the Narshingdi structure mainly consists of sandstones, shales and siltstones. The presence of abundant foraminiferal micro-fauna indicative of marginal to shallow marine conditions. The shales are light to medium grey, occasionally dark grey with minor coal insulations, soft, silty, micromicaceous and calcareous. The Sandstones are light grey, very fine to fine grained and generally calcareous lamination, slightly calcareous and sandy. The depositional environment is interpreted as being a lower delta plain[4].

BHUBAN FORMATION (Middle Miocene): This zone mainly consists of very fine to medium grained, well stored, subangular to subrounded, calcareous sandstone. Interbedded grey shales are common with laminations of siltstone.

3.3 Reservoir

Only two gas bearing sands were encountered in Narshingdi gas field and were named as Upper Gas Sand and Lower gas Sand. The two gas sand and other associated nonproductive sands in the gross stratigraphic interval were interpreted to be mouth bar sands in the IKM study on the basis of connate water salinity and position in the Middle/Late Miocene depositional basin.

The Upper Gas Sand is about 17 m thick with the gas saturated portion being about 9.4 m (gross sand) and containing 7.3 m of net sand. The Upper Gas Sand interval contains interlaminated shales and siltstones along with the sands. The lower gas sand is about 13.7 m thick (completed gas bearing interval) and contains 12.5 m of net sand. The two productive intervals are separated stratigraphically by 266 m of non-reservoir section. Lithologically, the productive sand ranges in grain size from coarse silts to medium-grained sands are composed predominantly of quartz with secondary amounts of feldspar and rock fragments. Porosity ranges 7-26% and the average permeability is 42 and 32 md for the UGS and LGS respectively. In general, the reservoir quality is considered to be poor to moderate[4, 5].

3.4 Exploration and Field Development[5]

Narshingdi structure was identified by Pakistan Shell Oil Company (PSOC) and named as project A2. Production from this field commenced on 25 July, 1996 from the LGS. At the start of production, daily flow rate was 25 MMSCFD. However the rate was reduced to about 20 MMSCFD within a year. Daily production from the single well remained relatively constant for the next several years and was still at a level of 20 MMSCFD when NAR-2 well was completed at the lower gas sand and began production in February 2007. With the addition of gas production from NAR-2, the total daily production from the field jumped to about 35 MMSCFD. At the end of December 2013, combined daily production from the two wells was still at about 28 MMSCFD.

3.5 Well wise and Sand wise Production History

Figure 3.1 graphically present the well-wise production history for Narshingdi gas field. Figure 3.1 shows that NAR-1 accounts the major share of the gas that has been produced from this field till the end of 2013. NAR-2 began producing in February 2007 and is producing gas at a rate slightly less than the NAR-1. The cumulative production from the Lower Gas Sand was about 150 BCF as of December 2013. NAR-1 has produced 114.2582 BCF or approximately 76% of the field total production.

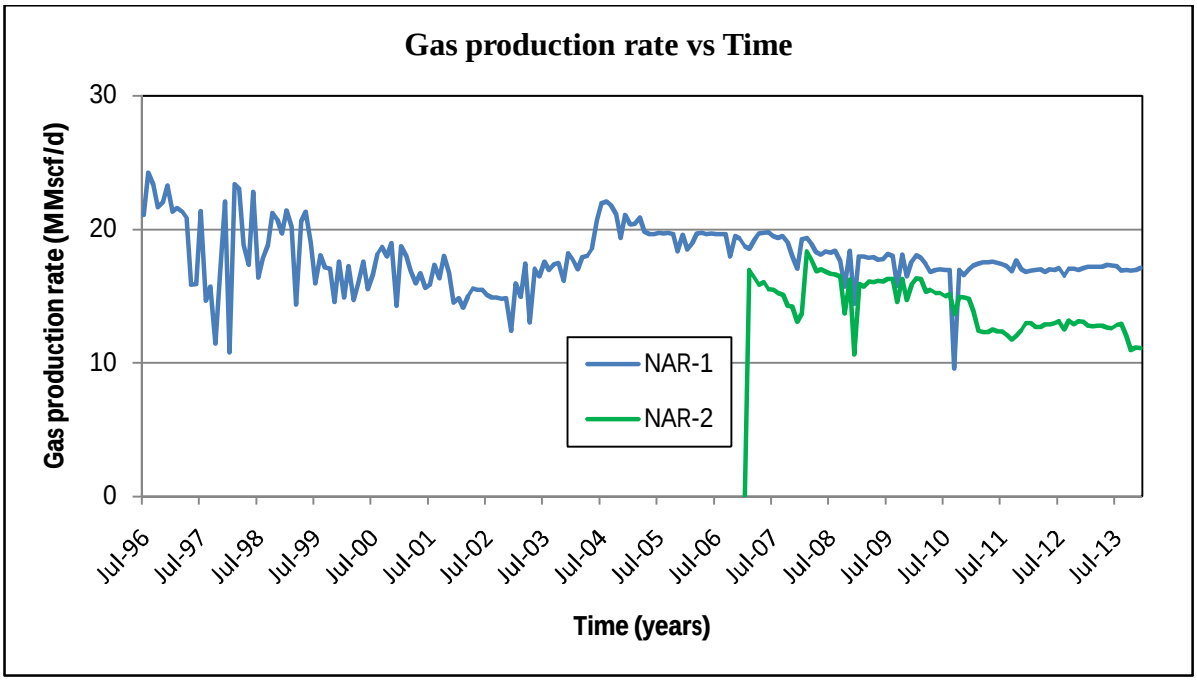

Figure 3.1: Gas production history (NAR-1 and NAR-2)

3.6 Reservoir Parameters

Summary of the reservoir parameters is shown in Table 3.1 and Table 3.2

Table 3.1: Summary of the reservoir parameters

Parameter	NAR-1	NAR-2
Well type	Vertical	Vertical
Well depth	3450 m	3285 m
Perforation interval	3169.76-3183.78m	3178-3191m
Well status	Producing	Producing
Tubing size	3-1/2 inch	4-1/2 inch
Completion date	14 October 1990	14 January 2007
Start of production	July 1996	Feb 2007
Initial production rate	25 MMscf/d	17 MMscf/d
Production rate at December 2013	17 MMscf/d	11 MMscf/d
Cumulative gas production up to December 2013	114.2582 BCF	35.9655 BCF
Initial reservoir pressure	4575 psia	3550 psia
Initial shut in well head pressure	3480 psia	2857 psia
Tubing head pressure at December 2013	1443 psia	1330 psia
Initial reservoir temperature	205 ºF	163 ºF
Condensate gas ratio (December 2013)	2 bbl/MMscf	1.96 bbl/MMscf
Water gas ratio (December 2013)	0.8 bbl/MMscf	1.15 bbl/MMscf

Table 3.2: Properties of rock

Porosity	07-22 %
Permeability	35 md
Gas saturation	65%

CHAPTER 4

LITERATURE REVIEW

4.1Volumetric Method

Volumetric estimation is the only mean available to assess hydrocarbons in place prior to acquiring sufficient pressure and production information to apply material balance techniques. Recoverable hydrocarbons are estimated from the in place estimates and a recovery factor that is estimated from analogue pool performance and/or simulation studies. Therefore, volumetric methods are primarily used to evaluate the in-place hydrocarbons in new, non-producing wells and pools and new petroleum basins[7].

The volumetric method is useful in reserve work for estimating gas in place at any stage of depletion. During the development period before reservoir limits have been accurately defined, it is convenient to calculate gas in place per acre-feet of bulk reservoir rock. Later in the life of the reservoir when the reservoir volume is defined and performance data is available, volumetric calculations provide valuable checks on gas in place estimates obtained from material balance and other methods[8]. The formula for volumetric reserve calculation is

$$G\left(\frac{\text{scf}}{\text{acre}-\text{ft}}\right) = 7{,}758Ah\emptyset(1-S_{wi})\frac{1}{B_{gi}(\text{res bbl/scf})}$$

$$\text{or } G\left(\frac{\text{scf}}{\text{acre}-\text{ft}}\right) = 43{,}560Ah\emptyset(1-S_{wi})\frac{1}{B_{gi}(\text{res ft}^3/\text{scf})}$$

where, G = initial gas in place, scf

A = original productive area of reservoir, acres

h = net effective formation thickness, ft

$\emptyset$=porosity, fraction

S_{wi}= initial water saturation fraction

B_{gi}=initial gas formation volume factor

$B_{gi} = 5.02\frac{ZT}{P}$ (bbl/scf) where

Z=compressibility factor

T=reservoir temperature, R

P =reservoir pressure, psia

4.1.1 Monte Carlo Simulation

Monte Carlo Simulation is considered to be the best method for estimating Hydrocarbon reserves of reservoirs with high geological heterogeneity, especially at the initial life of the reservoir when not much production data are available[9].

Monte Carlo simulation is a stochastic modeling method to simulate real-world situations where there is uncertainty in the input variables. This uncertainty cannot be directly modeled using analytical solutions. While conceptually very simple, a trivial example provides the easiest route to developing an understanding of the Monte Carlo simulation procedure.

Expected Ultimate Recovery (EUR) is calculated as the product of the prospect area (*A*, acres), average net hydrocarbon thickness (*h*, feet), and recovery factor (*RF*). The algebraic expression of this simple model is:

$$EUR = A \times h \times RF$$

The deterministic approach would simply multiply the "best estimate" for each of these quantities to obtain a single value of EUR. The deterministic approach assumes that the most likely value of every input is encountered simultaneously, which is generally very unrealistic.

For each of the three input variables, *A*, *h*, and *RF*, independent cumulative probability distributions can be defined, describing the uncertainty in each of these variables. The Monte Carlo method can make use of these distributions to arrive at an overall cumulative probability distribution (overall uncertainty) for EUR. This analysis approach is superior to the single-valued deterministic approach because of the valuable insight gained into the "upside," "downside," "most likely outcome," and the "mean" level of reserves that would result from drilling a large number of similar prospects.

4.1.2 Advantages of Monte Carlo Simulation

Risk analysis is performed because there are uncertainties in the estimation of reserves. Quantifying that uncertainty with ranges of possible values and associated probabilities (i.e. with probability distribution) helps everyone understand the risks involved. There is always an underlying model, such as a volumetric reserve estimates; a production forecast cost estimation or a production sharing economical analysis[10].

Probabilistic reserves estimate using a generalized Monte Carlo approach has many advantages over simpler deterministic or other probabilistic methods. The particular method described deals more thoroughly with geologic structural dependency and at the same time allows for a high degree of accuracy. Data preparation is kept to a minimum, allowing seismic and other basic data to be used directly in calculations without the need of preparing time consuming area-depth graphs used in more conventional methods**.** A further advantage is the elimination of certain arbitrary decisions related to extreme structural scenarios based on geological mapping of a very limited number of possible situations. Sensitivities related to uncertainties and errors are handled in an easy manner. The approach related to gross rock volume calculations is different from more conventional probabilistic reserves simulations in that it involves the direct manipulation of all surfaces bounding the most likely rock volume. Such uncertainty, described by statistical distributions (e.g. seismic velocity error) and functional relationships involves geological horizons bounding individual sands (reservoirs), faults, and fluid contacts[11].

Probabilistic estimating of hydrocarbon volumes has its most important application when associated with development projects, particularly when dealing with large gas structures where reserves are directly related to a sales contact, possibly involving several billion dollars. Such simulations may be carried out by a Monte Carlo approach. This method that lends itself more easily to describing uncertainties associated with hydrocarbon volumes which have to be estimated. One can differentiate between “recoverable hydrocarbons” (oil or gas), a quantity which represents the maximum possible recovery essentially governed only by physical reservoir processes, and “reserves” which is the maximum quantity (usually less than recoverable hydrocarbons) that can be recovered with a certain development plan and production policy[11].

4.1.3 Monte Carlo Simulation Procedure

1. A random number between zero and one (representing the value of the cumulative probability) for each of the three input variables was generated.

2. The cumulative probability distribution for each input variable at their respective random number was entered to determine the "sampled" value for each input.

3. The three independent variable sampled values were multiplied to yield a sample reserve estimate[12].

An individual calculation or run to estimate a prospect size in this fashion is known as a "pass." By itself, the individual value of EUR generated by a pass is meaningless. In case of repeated a large number of times, a cumulative distribution for the EUR emerges.

The minimum number of passes required depends on the number of input variables that are risked. Generally, enough runs are needed to ensure that the entire domain of input variables is examined. The larger the number of input variables, the larger the minimum number of passes required.

Typically, 1000 or more passes comprise a single Monte Carlo simulation. As a qualitative rule, smooth Cumulative Density Function (CDF) of output variables is indication of an appropriate number of runs.

Once a Monte Carlo simulation run concludes, analysis of the results follows. Assuming a 1000 pass simulation run, results are processed as follows:

1. EUR results were arranged in ascending order.

2. The sorted EUR values were numbered from 1 to the total number of samples (e.g., 1000).

3. The cumulative probability was calculated of each value by dividing the sample number by the total number of samples (in this case, 1000).

4. The resultant cumulative probability function (Cumulative Probability vs. EUR) was plotted. Lacking a smooth distribution necessitates re-running the simulation with a larger number of passes.

5. The mean, variance, P_{10}, P_{50}, P_{90} and any other desired statistical parameters were calculated.

This analysis yields the statistical parameters desired for prospect analysis. Expect the values of these parameters to vary slightly with each simulation. An unacceptably large variation warrants an increase in the number of passes[12].

4.1.4 Generating Triangular Distributed Random Variates

Given a random variate U drawn from the uniform distribution in the interval (0, 1) then the variate

$$X = a + \sqrt{U(b-a)(c-a)} \quad \text{for } 0 < U < F(c)$$

$$X = b - \sqrt{(1-U)(b-a)(b-c)} \quad \text{for } F(c) \leq U < 1$$

Where $F(c) = \frac{(c-a)}{(b-a)}$

Here a is the Minimum value, b is the Maximum value and c is the most likely or most common value[13].

4.1.5 Probability Density Function (PDF) and Expectation Curves

A well recognized form of expressing uncertainty is the probability density function. Expectation curves are alternatively known as probability curves. The X axis on expectation curves (Figure 4.1) is typically the GIIP, UR or Reserves of a field. The slope of the expectation curve indicates the range of uncertainty; a broad expectation curve represents a large range of uncertainty and steep expectation curve represents a field with little uncertainty[7].

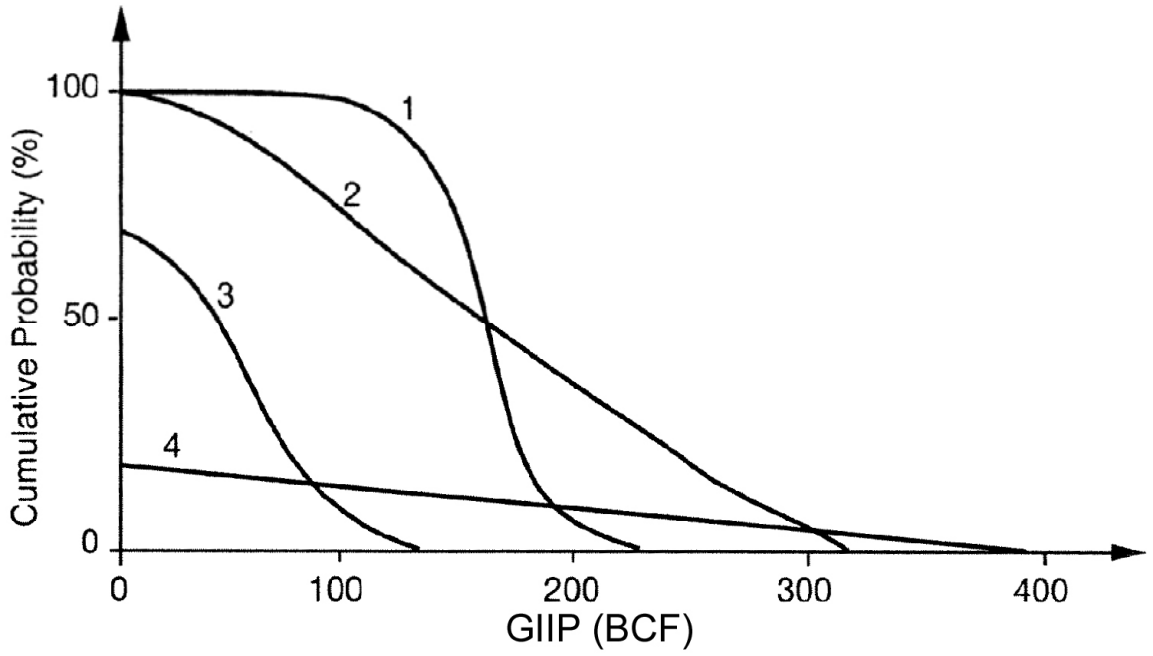

Figure 4.1: Expectation Curve

In the Figure 4.1 curves 1 and 2 represent discoveries, since they both have a 100% probability of containing a finite amount of gas. Case 1 is a well defined discovery and case 2 represents a poorly defined discovery. Case 3 has an estimated probability of gas present of 65%, i.e. low risk of failure to find gas (35%). Case 4 has a high risk of failure (85%) to find any gas.

A typical expectation curve for ultimate recovery is shown in the Figure 4.2

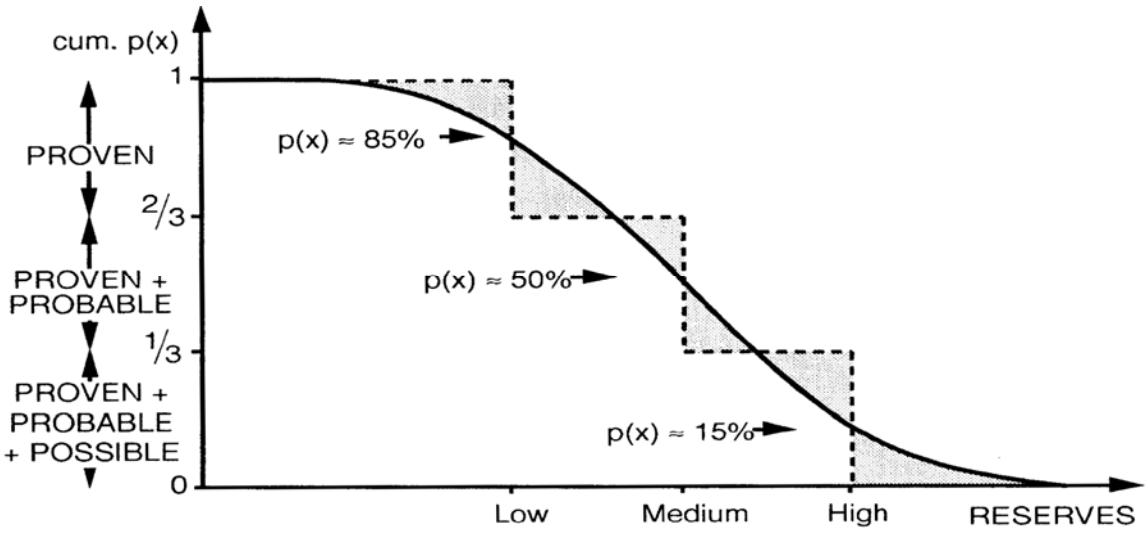

Figure 4.2: Expectation curve for a discovery

P_{90} is the low estimate, 90% cumulative probability of at least this reservoir. P_{50} is the medium estimate, 50% cumulative probability and P_{10} is the high estimate, 10% cumulative probability[7].

4.1.6 Limitation of Monte Carlo Simulation

In spite of its power and applicability Monte Carlo Simulation does not do the following [10]

1. It does not make decisions, it prepare for decision making.
2. It does not analyze data; there is companion software for that purpose
3. It does not optimize functions; the output distributions serve as ingredients for optimization
4. It does not provide ready-made models, every one builds their own.

The probabilistic methods have several inherent problems. They are affected by all input parameters, including the most likely and maximum values for the parameters. In such

methods, one cannot back calculate the input parameters associated with reserves. Only the end result is known but not the exact value of any input parameter. On the other hand, deterministic methods calculate reserve values that are more tangible and explainable. In these methods, all input parameters are exactly known; however, they may sometimes ignore the variability and uncertainty in the input data compared to the probabilistic methods which allow the incorporation of more variance in the data.

4.2 Material Balance

The Material Balance equation has long been regarded as one of the basic tools of reservoir engineering for interpreting and predicting reservoir performance. The material-balance equation is the simplest expression of the conservation of mass in a reservoir. The equation mathematically defines the different production mechanisms and effectively relates the reservoir fluid and rock expansion to the subsequent fluid withdrawal. Material balance methods of reserves estimation involve the analysis of pressure behavior as reservoir fluids are withdrawn, and generally result in more reliable reserves estimates than volumetric estimates. Reserves may be based on material balance calculations when sufficient production and pressure data is available. Confident application of material balance methods requires knowledge of rock and fluid properties, aquifer characteristics and accurate average reservoir pressures. In complex situations, such as those involving water influx, multi-phase behavior, multilayered or low permeability reservoirs, material balance estimates alone may provide erroneous results.

4.2.1 Conventional Material Balance Analysis

Assumptions:

1. A reservoir may be treated as a constant volume tank.
2. Pressure equilibrium exists throughout the reservoir, which implies that no large pressure gradient exists across the reservoir at any given time.
3. Laboratory pressure-volume-temperature (PVT) data apply to the reservoir gas at the average pressures used.
4. Reliable production and injection data and reservoir pressure measurements are available.

5. The change in volume of the interstitial water with pressure, change in porosity with pressure, and evaluation of gas dissolved in the interstitial water with decrease in pressure are negligible[8].

The general form for the material balance equation was first presented by Schilthuis in 1941. The equation is derived as a volume balance which equates the cumulative observed production, expressed as an underground withdrawal, to the expansion of the fluids in the reservoir resulting from a finite pressure drop. The volume balance can be evaluated in reservoir barrel as

Underground withdrawal (rb) = Expansion of oil and originally dissolved gas (rb) + Expansion of gas cap gas (rb) + Reduction in HCPV due o the connate water expansion and decrease in the pore volume (rb)

The general form of the material balance equation[15]

$$N_pB_o + (G_p - N_pR_s)B_g = NB_{oi}\left(\frac{(B_o-B_{oi})+(R_{si}-R_s)B_g}{B_{oi}}\right) + G(B_g - B_{gi}) + (NB_{oi} + GB_{gi})\left(\frac{c_{ws}S_{wc}+c_f}{1-S_{wc}}\right)\Delta p + (w_e - W_p) \quad (4.1)$$

When working with gas reservoirs, there is no initial oil; therefore, N and Np are equal to zero. The general material balance for a gas reservoir can then be obtained

$$G(B_g - B_{gi}) + GB_{gi}\left(\frac{c_{ws}S_{wc}+c_f}{1-S_{wc}}\right)\Delta p = G_pB_g - (W_e - W_p)B_w \quad (4.2)$$

For most gas reservoirs, the gas compressibility term is much greater than the formation and water compressibility, and the second term on the left hand side of the Equation 4.2 become negligible,

$$G(B_g - B_{gi}) = G_pB_g - (W_e - W_p)B_w \quad (4.3)$$

When there is neither water encroachment into nor water production from reservoir of interest, the reservoir is said to be volumetric. For a volumetric gas reservoir Equation 4.3 reduces to

$$G(B_g - B_{gi}) = G_pB_g \quad (4.4)$$

Substituting expression for B_g and B_{gi} into Equation (4.4) yields

$$G\left(\frac{P_{sc}ZT}{T_{sc}p}\right) - G\left(\frac{P_{sc}z_iT_i}{T_{sc}P_i}\right) = G_p\frac{P_{sc}ZT}{T_{sc}P} \quad \text{(4.5)}$$

Noting that production is essentially an isothermal process (i.e. the reservoir temperature is remain constant), then Equation 4.5 is further simplified to

$$G\left(\frac{Z}{P}\right) - G\left(\frac{Z_i}{P_i}\right) = G_p\left(\frac{Z}{P}\right) \quad \text{(4.6)}$$

$$\frac{P}{Z} = -\frac{P_i}{Z_iG}G_p + \frac{P_i}{Z_i} \quad \text{(4.7)}$$

SinceP_i, Z_i and G are constant for a given reservoir, plotting $\frac{p}{z} vs\ G_p$would yield a straight line. If $\frac{p}{z}$ is set equal to zero, that would represent the production of all gas from reservoir, then the corresponding G_p equal to G, the initial gas in place. Deviation from this straight line can caused by external recharge or offset drainage. In water drive reservoir the relation between G_p and $\frac{p}{z}$ is not linear, because of the water influx, the pressure drops less rapidly than under volumetric control.

Different approaches used in the study of Material Balance

In the material balance study, due to non-availability of needed pressure surveys, five approaches have been used using

(a) Static bottom hole pressure (SBHP) estimated from shut in well head pressure.
(b) Shut in well head pressure (SWHP).
(c) Flowing bottom hole pressure (FBHP), estimated from flowing well head pressure.
(d) Flowing well head pressure (FWHP)
(e) AWMB (Approximate well head material balance)

4.2.2 Static Bottom Hole Pressure, Estimated From Shut in Well Head Pressure

To record the static bottom hole pressure or the reservoir pressure by downhole gauge measurement, the well is required to shut-in for a few days for pressure build-up. This is not feasible due to critical demand-supply situation. But different wells of the field were shut-in from time to time because of production problems or any other reasons pressure build up data

were recorded in this situation. The shut in well head pressure was taken and corresponding bottom hole pressure was calculated. The calculated bottom hole pressure is however, not suitable for the data recorded from a properly designed well test program, particularly due to the uncertainty of the degree of pressure stabilization achieved during the shut-in wellhead pressure measurements. In the absence of any well-test program, this approach can be a good alternative. The following approach is used for estimating shut-in bottom hole pressure from shut in wellhead pressure. General formula for the vertical flow calculation is written as follows[1]

$$\int_2^1 \frac{\frac{ZT}{p}dp}{1+(6.7393*10^{-4} fLq_{sc}{}^2 Z^2 T^2)/(zp^2 d^5)} = 0.01875\gamma_g z \quad \text{(4.8)}$$

Where the units are p =psia,q_{sc} = $Mscfd$, d =in, T = °R and L, z =feet (z is the vertical elevation difference between the bottom hole, inlet point 1 and surface outlet point 2). The left integral of Equation 4.8 cannot be evaluated easily because z is a complex function of p and T, and temperature variation with depth is not easily defined. Various simplifying assumptions were made in the evaluation of this integral from the basis for the different methods that give results of varying degrees of accuracy.

Some methods for vertical flow assume an average temperature, in which case Equation 4.8 becomes

$$\int_2^1 \frac{\frac{Z}{p}dp}{1+(6.7393*10^{-4} fLq_{sc}{}^2 Z^2 T^2)/(zp^2 d^5)} = \frac{0.01875\gamma_g z}{T_{av}} \quad \text{(4.9)}$$

For a shut–in well, the flow rate, q_{sc} is equal to zero and Equation 4.9 simplifies to

$$\int_{p_{wh}}^{p_{ws}} \frac{ZT}{P} dp = 0.01875\gamma_g Z \quad \text{(4.10)}$$

Equation 4.10 describes the relationship between the pressure measured at the surface (or well head) and pressure at the bottom

In calculating the static bottom hole pressure of the wells, Average Temperature and Z factor method is used[16].

This method is used to simplify the left hand side of the Equation 4.10 as

$$Z_{av}T_{av}\int_{P_{wh}}^{P_{ws}}(\frac{dp}{p}) = 0.01875\gamma_g Z \quad (4.11)$$

Upon integration

$$ln\frac{P_{ws}}{P_{wh}} = \frac{0.01875\gamma_g}{Z_{av}T_{av}} \quad (4.12)$$

or

$$P_{ws} = P_{wh}\exp\left[\frac{0.01875\gamma_g Z}{Z_{av}T_{av}}\right] \quad (4.13)$$

Generally this is written as $P_{ws} = P_{wh}e^{s/2}$ where $s = \frac{0.01875\gamma_g}{Z_{av}T_{av}}$ ..... (4.14)

To determine the average temperature, the bottom hole temperature (BHT) and the surface temperature should be known. For the static column of the gas, an arithmetic average temperature is satisfactory to use. For calculatingZ_{av}, the average pressure is required. Thus a trial and error type solution is necessary. A good initial estimate of P_{ws} can be made using the equation

$$P_{ws} = P_{wh} + 0.25\left(\frac{P_{wh}}{100}\right)\left(\frac{Z}{100}\right) \quad (4.15)$$

4.2.3 Shut in Well Head Pressure

In this approach field recorded shut-in well head pressure are used to make a $\frac{P}{Z}$ versus cumulative production plot. The approach is based on the assumption that there is no liquid in the wellbore. Since static gas gradient is very small the procedure will provide a quite acceptable result. The procedure will provide enormous result if there is liquid build up in the tubing[17].

4.2.4 Flowing Gas Material Balance

This method consists of a $\frac{P}{Z}$ plot of the flowing pressure (as opposed to the average shut in reservoir pressure) versus cumulative production. A straight line drawn through the initial reservoir pressure will give the original gas-in-place. The use of flowing material balance is based on the assumption that the well is produced long enough to reaches the pseudo-steady state condition. A closed reservoir reaches the pseudo-steady state condition when the

pressure transient reaches the outer boundary. In the Figure 4.3 the pressure transient reaches the outer boundary at time t_1. Thus the pseudo-steady state begins from time t_1 onwards[2, 18].

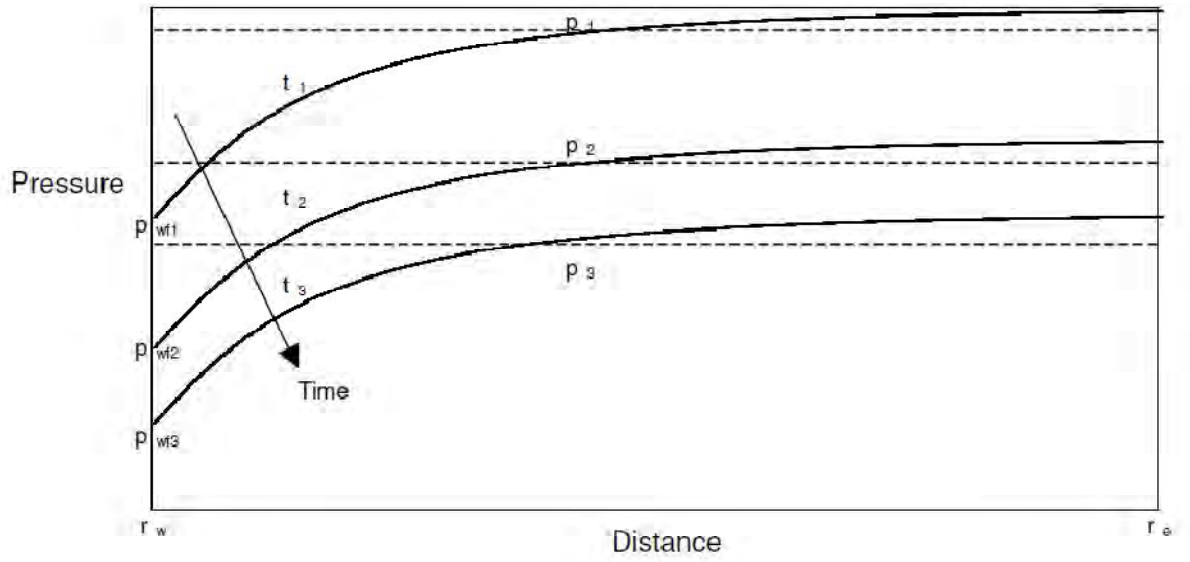

Figure 4.3: Reservoir pressure profile during the pseudo steady state condition.

During the pseudo-steady state, the rate change of pressure is constant at all points of the reservoir, i.e. pressure declines at the same rate at all point of the reservoir. Figure 4.3 shows the pressure profiles in the reservoir at three different times i.e. t_1, t_2 and t_3 during the pseudo-steady state period. Between time t_1, and t_2, pressure drop at all points of the reservoir is the same. That means pressure profile at time t_1 and t_2 are parallel. If P_1 and P_2 are the average reservoir pressures at time t_1 and t_2, respectively, the difference between P_1 and P_2 are also the same as that of the parallel lines at t_1 and t_2. This can be explained analytically in the following manner. For a liquid reservoir producing under pseudo-steady state, the inflow Equation is provided by

$$P_e - P_{wf} = \frac{q\mu}{2\pi kh}\left(ln\frac{r_e}{r_w} - \frac{1}{2} + s\right) \quad \text{(4.16)}$$

If the well produces at a constant flow rate, differentiating both side of the equation with respect to time, yields

$$\frac{dp_e}{dt} - \frac{dp_{wf}}{dt} = 0 \quad \text{(4.17)}$$

$$\text{i.e.} \frac{dp_e}{dt} = \frac{dp_{wf}}{dt} \quad \text{(4.18)}$$

Equation 4.18 shows that at pseudo-steady state condition and for a well producing at a constant flow rate, pressure falls at the same rate at the well bore and at the outer boundary of the reservoir. Writing Equation 4.16 for any radius r instead of r_e it can be easily shown that the pressure falls at the same rate throughout the whole reservoir. In terms of the average reservoir pressure inflow Equation at pseudo-steady state can be written as

$$p - p_{wf} = \frac{q\mu}{2\pi kh}\left(ln\frac{r_e}{r_w} - \frac{1}{2} + s\right) \quad \text{(4.19)}$$

Where, P is the average reservoir pressure. In similar way differentiating the both side s of the Equation 4.19 yields

$$\frac{dp}{dt} = \frac{dp_{wf}}{dt} \quad \text{(4.20)}$$

Equation 4.20 shows that the flowing wellbore pressure and the average reservoir pressure falls at the same rate for a well producing at a constant rate from a reservoir under pseudo-steady state condition. The same argument can be applied to the wells producing from a gas reservoir provided that the pressure drawdown is not very large. To account for the gas compressibility, p/z instead of pressure is used. For gas wells producing under pseudo steady state at large drawdown, real gas pseudo pressure instead of p/z has to be used.

From the above discussion, it can be said that during pseudo-steady state, the rate of change of p/z is also constant, and equal to the rate of change of p/z at any point of reservoir. For a closed reservoir a conventional material balance plot of p/z versus Gp yields a straight line between the point's pi/zi and the initial gas in place. Therefore a plot of flowing wellbore p/z vs. Gp will also yield straight line parallel to the conventional material balance line. Thus on a flowing wellbore p/z vs Gp graph, a parallel line through pi/zi corresponding to the initial reservoir pressure will yield the initial gas in place. Flowing wellhead p/z can also be used in a way similar to the flowing wellbore[2, 18].

4.2.5 Approximate Well Head Material Balance

It is not always recognized that the change in the compressibility factor, z in material balance calculation is often small (it can be the same order magnitude of the error of the data). If z is ignored, a material balance calculation (plot of flowing sand face pressure, Pwf versus cumulative gas production) can give a very reasonable approximation of the GIIP. The initial point $p = p_i$ and end point $p = 0$ are correct, but theoretically since z is ignored; the line joining them is not necessarily straight. If it is further recognized that wellhead pressure measurements are representative of bottom hole conditions (no fluid influx into the well-bore), a procedure similar to flowing well head pressure approach , but ignoring z, can be used to generate a reasonable wellhead material balance calculation. A line drawn through the data and then a line parallel through the initial static wellhead pressure will give an estimate of the original gas-in place[18].

4.3 Decline Curve Analysis

Decline curve analysis techniques offer an alternative to volumetric and material balance methods and history matching with reservoir simulation for estimating Gas Initially in Place (GIIP) and gas reserves. Application of decline curve techniques to gas reservoir is most appropriate when more conventional volumetric or material balance method are not accurate or when sufficient data are not available to justify complex reservoir simulation. For example material balance method require estimates of stabilized shut in bottom hole pressure (BHP's); however in low permeability reservoirs when long time is needed for stabilization accurate shut in bottom hole pressure often are not available[3].

Unlike volumetric methods that can be used early in the production life of a reservoir, decline curve analysis cannot be applied until some development has occurred and a production trend is established. An advantage of decline curve analysis is that this method estimates only the gas volume that is in pressure communication with and may ultimately be recovered by the producing wells. Volumetric estimates of gas in place and reserves, however, are based on the total gas volume in place, part of which may be unrecoverable with the existing wells because of unidentified reservoir discontinuities or heterogeneities.

The basics of decline curve analysis are to match past production performance histories or trends (i.e. actual production rate /time data) with a model. Assuming that future production

continues to follow the past trend, these models can be used to estimate original gas in place and to predict ultimate gas reserves at some future reservoir abandonment pressure or economic production rate. The remaining predicting life of a well or the entire field can be determined. In addition the individual well flowing characteristics can be estimated, such as formation permeability and skin factor, with decline-type-curve analysis techniques. Decline curve techniques are applicable to individual wells or an entire field.

4.3.1 Conventional Analysis Techniques

The rate of wells, or group of wells generally declines with time. An empirical formula can sometimes be found that fits the observed data so well that it seems rather safe to use the formula to estimate future relationships. The formula relating time, production rate, and cumulative production rate is usually derived by first plotting the observed data in such a way that a straight line relationship results. Some prediction can be made graphically by simply extrapolating the straight line plots or by the use of mathematical formulas. Most conventional decline curve analysis is based on Arps empirical rate/time decline equation[3]

$$q(t) = \frac{q_i}{(1+bD_i t)^{1/b}} \quad \text{..... (4.21)}$$

where $D_i = -dq(t)/dt/q(t)$ is the initial decline rate days^{-1}

Depending on the value of b there are three commonly recognized types of decline curves, each of this has the separate mathematical form that is related to the second factor, which characterizes a decline curves, that is the curvature. These types are referred as

1. Exponential decline
2. Harmonic decline
3. Hyperbolic decline

For constant percentage decline, rate versus time is straight line on semi log paper and rate versus cumulative production is a straight line on coordinate paper. Rate versus cumulative is a straight line on semi log paper for harmonic decline. All other has some curvature[8].

Exponential decline: exponential decline sometimes called constant-percentage decline[3], is characterized by a decrease in production rate per unit of time that is proportional to the

production rate. The exponential decline equation can be derived from the Equation 4.21 with a limiting process as b→0

$$q(t) = \frac{q_i}{e^{D_i t}} = q_i e^{-D_i t} \quad \text{..... (4.22)}$$

Taking the natural logarithm (ln) of both sides of Equation 4.22 gives

$$ln[q(t)] = ln(q_i) + ln e^{-D_i t} \quad \text{..... (4.23)}$$

which after rearranging gives $ln[q(t)] = ln(q_i) - D_i t$.....(4.24) because the natural logarithm

to the base 10 (log) by $ln(x) = 2.303 log(x)$, we can write Equation 4.24 in terms of the log function as

$log[q(t)] = log(qi) - \frac{D_i t}{2.303}$.....(4.25) the form of Equation 4.25 suggests that a plot of log flow rate $q(t)$ versus t will be a straight line with a slope $-\frac{D_i t}{2.303}$ and an intercept $log(q_i)$ if the production data exhibit linear behavior on semi log plot , we can use the Equation 4.25 to calculate Di from the slope and q_i from the intercept. After calculating the initial decline rate and initial flow rate we can use Equation 4.22 to extrapolate the production trend into the future to some economic limit. From this extrapolation, we can estimate gas reserve and the time at which the economic limit will be reached.

The curve of rate vs. cumulative production for exponential decline will be linear on a Cartesian graph, as the following derivation indicates, if we integrate Equation 4.22 from the initial time to time t, we obtain

$$Q(t) = \int_0^t q(t) dt = \int_0^t q_i e^{-D_i t} dt \quad \text{..... (4.26)}$$

The cumulative gas production is

$$Gp(t) = \left(-\frac{qi}{Di} e^{-D_i t}\right) \quad \text{..... (4.27)}$$

Rearranging yields $Gp(t) = -\frac{1}{D_i}(q_i e^{-D_i t}) + \frac{q_i}{D_i}$..... (4.28)

Combining Equation 4.22 and 4.28 we can write the cumulative production relation in terms of rate,

$$Gp(t) = -\frac{1}{D_i}q(t) + \frac{q_i}{Di} \quad \text{(4.29)}$$

Rearranging and solving for production rate $q(t)$, gives

$$q(t) = -D_i Gp(t) + q_i \quad \text{(4.30)}$$

Equation 4.30 suggests that a plot of $q(t)$ vs. $G(p)$ will yield a straight line of slope $-Di$ and intercept q_{i}

Harmonic decline: when $b = 1$, the decline is said to be harmonic[3], and the general equation 4.21 reduce to $q(t) = q_i/(1 + D_i t)$……(4.31) taking logarithms to the base 10 of both sides of Equation 4.31 yields $log\ q(t) = log(q_i) - log(i + D_i t)$……(4.32) the form of Equation 4.32 suggests that $q(t)$ is a linear function $(1 + D_i t)$ on log graph paper and will exhibit a straight line with a slope -1 and an intercept of $log(q_i)$. To predict future performance of wells exhibiting harmonic decline behavior we must assume of Di until a plot of $log[q(t)]$ vs. $log(1 + D_i t)$ is a straight line with a slope of -1. To use the rate/cumulative production plot for harmonic decline, we must integrate Equation 4.31 with respect to time to obtain a relationship for cumulative production

$$Gp(t) = \int_0^t q(t)dt = \int_0^t \frac{q_i}{1+D_i t}dt \quad \text{(4.33)}$$

or

$$Gp(t) = \frac{q_i}{Di}\ln(1 + D_i t) = 2.303\frac{q_i}{Di}\log(1 + D_i t) \quad \text{(4.34)}$$

Substituting the rate from Equation 4.32 into Equation 4.34, we obtain the rate /cumulative production relationship for harmonic decline,

$$Gp(t) = 2.303\frac{q_i}{D_i}[log q_i - log q(t)] \quad \text{(4.35)}$$

or in terms of production rate

$$\log q(t) = log q_i D_i \left(\frac{Di}{2.303 q_i}\right) Gp(t) \quad \text{(4.36)}$$

the form of Equation 4.36 suggests that a plot of $logq(t)\ vs.\ Gp(t)$ will be linear with a slope of $-(D_i/2.303q_i)$ and an intercept of $\log(q_i)$.

Hyperbolic decline:

When 0<b<1, the decline is hyperbolic[3], and the rate behavior is described by

$$q(t) = \frac{q_i}{(1+bD_it)^{1/b}} \quad \text{(4.37)}$$

Taking the logarithm of both sides of the Equation 4.37 and rearranging yields

$$logq(t) = \log(q_i) - \frac{1}{b}\log(1 + bD_it) \quad \text{(4.38)}$$

The form of the Equation 4.38 suggests that if rate time data can be modeled with the hyperbolic equation, then a log log plot of $q(t)$ vs. $(1 + bD_it)$ will exhibit a straight line with the slope of $1/b$ and an intercept of $log(q_i)$. The cumulative production/time relationship is obtained by integrating Equation 4.37

$$Gp(t) = \int_0^t q(t)dt \int_0^t \frac{q_i}{(1+bD_it)^{1/b}} dt \quad \text{(4.39)}$$

After integrating and rearranging

$$Gp(t) = \frac{q_i}{Di(b-1)}[(1 + bD_it)^{\frac{(1-b)}{-b}} - 1] \quad \text{(4.40)}$$

if we substitute $q_i = {q_i}^b {q_i}^{1-b}$ into Equation 4.40 and rearrange , we can write

$$Gp(t) = \frac{{q_i}^b}{Di(b-1)}\{[q_i(1 + bD_it)^{-1/b}](1\text{-}b)\text{-}{q_i}^{1-b}\} \quad \text{(4.41)}$$

Substituting Equation 4.37 into Equation 4.41 yields an expression for calculating cumulative gas production in terms of gas flow rate during hyperbolic decline

$$Gp(t)\frac{{q_i}^b}{Di(b-1)}[q(t)^{1-b}{q_i}^{1-b}] \quad \text{(4.42)}$$

4.3.2 Fetkovitch Decline Type Curve

The Fetkovitch decline type curves are based on analytical solutions to the flow equations for production at a constant bottom hole pressure from a well centered in a circular reservoir or reservoir area with no flow boundaries. The Fetkovitch type curve includes both transient and infinite acting and boundary dominated flow regimes. Both the transient rate/time and cumulative production/time type curves are characterized by a correlating parameter defined

as the ratio of the outer drainage radius to the apparent well bore radius, while the pseudo-steady state flow regimes are characterized by the Arps decline constant b. Again, $b = 0$ corresponds to exponential decline behavior, while b=1 represents harmonic decline. Values in the range $0 < b < 1$ suggests hyperbolic decline characteristics[3].

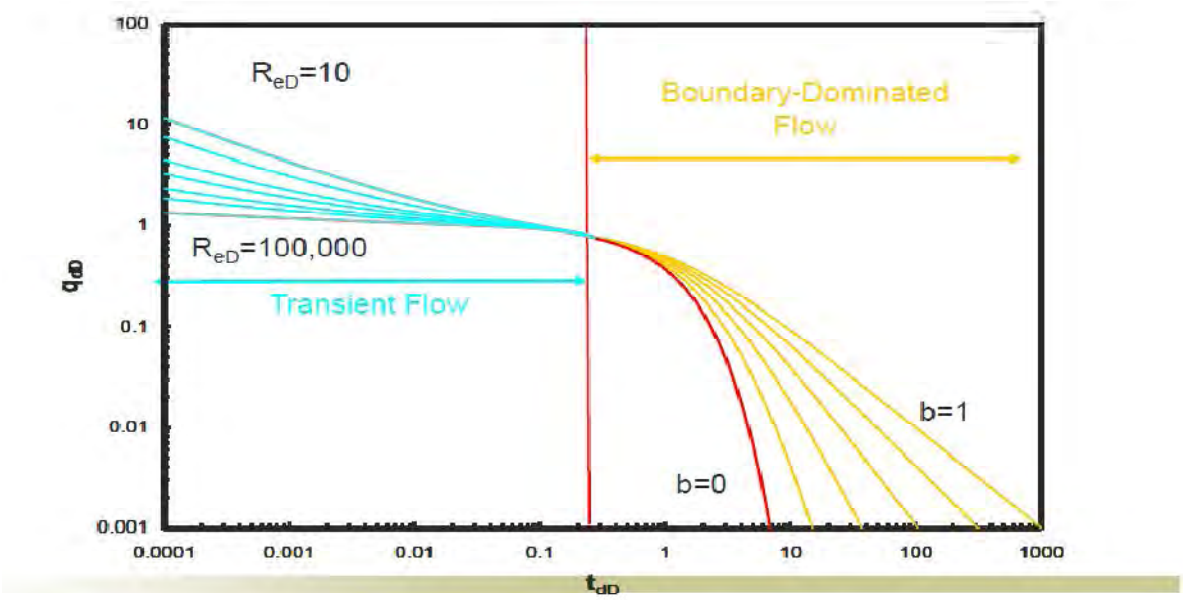

Figure 4.4: Fetkovitch type curve

Fetkovitch type curves are plotted in terms of dimensionless variable, dimensionless rate

$$q_{Dd} = \frac{50300q(t)P_{sc}T[ln\frac{r_e}{r_w}-\frac{1}{2}]}{T_{sc}kh[Pp(Pi)-Pp(Pwf)]}$$ vs. dimensionless time

$$t_{Dd}= \frac{\frac{0.00633kt}{\phi\mu_g c_t r_{wa}}}{1/2[\left(\frac{r_e}{r_{wa}}^2\right)-1][ln\frac{r_e}{r_{wa}}-\frac{1}{2}]}$$ similarly the cumulative production/time type curves are plots of dimensionless cumulative production defined by

$$Q_{Dd} = \frac{637.8P_{sc}TGp(t)}{T_{sc}\, h\phi c_t(r_e{}^2-r_w{}^2[Pp(pi)-Pp(Pwf)]}$$

The Fetkovitch type curve can be used to calculate permeability, skin and reservoir radius

Permeability, $k = [\frac{q(t)}{qDd}]_{mp} \frac{50300P_{sc}T[ln\frac{r_e}{r_w}-\frac{1}{2}]}{T_{sc}h[Pp(pi)-Pp(Pwf)]}$

Skin factor, $S = \ln\left[\frac{r_w \frac{r_e}{r_{wa}}}{\sqrt{\frac{A}{\pi}}}\right] = ln\left[\frac{r_w}{r_e}\left(\frac{r_e}{r_{wa}}\right)\right]$ where $r_e = \sqrt{\frac{Vp}{\pi h \phi}}$ and $A = \pi r^2$

$$Vp = \frac{2000 P_{sc} T}{\left(\mu_g c_t\right)_i T[P_p(p_i) - P_p(P_{wf})]}\left(\frac{t}{td}\right)_{mp}\left[\frac{q(t)}{q_{Dd}}\right]_{mp}$$

Analysis

Boundary-Dominated Match

To obtain information about reserves and drainage areas, it is recommend that to focus on the boundary-dominated (depletion) stems of the typecurves. These are located to the right of where the Rate vs. Time and the Cumulative Production vs. Time typecurves intersect. Each of the depletion stems represents a different b value, identical to the b values used in the hyperbolic Arps analysis. Once a b value has been selected, Harmony calculates recoverable reserves and expected ultimate recovery. If a sandface flowing pressure is specified on the Analysis tab, Harmony also calculates drainage area and original gas-in-place[19].

Transient Match

To obtain information about permeability and skin, it is recommended that to focus on the transient stems of the typecurves. These are located to the left of where the Rate vs. Time and the Cumulative Production vs. Time typecurves intersect. Each of the transient stems represents a different r_{eD} value. Once a r_{eD} value has been selected and a sandface flowing pressure is specified, Harmony calculates permeability and skin[19].

4.3.3 Blasingame Type Curve Analysis

Blasingame type curve has the identical format to those of Fetkovitch[20]; however there are three important differences in presentation 1. Models are based on constant Rate solution instead of constant pressure 2. Exponential and Hyperbolic stems are absent, only Harmonic stem is plotted. 3. Rate integral and rate integral derivative type curve are used (simultaneous type curve match). Data used on Blasingame type curve makes use of modern decline curve analysis

-Normalized Rate $(q/\Delta p)$
-Material Balance Time/ Pseudo Time

Blasingame type curve analysis parameters are shown in Table 4.1

Table 4.1 Blasingame Type Curve Analysis Definitions:

Method	Type curve	Data-gas
Normalized Rate	$q_{Dd} = \frac{141.2qB\mu}{kh\Delta p}[\ln\frac{r_e}{r_w} - \frac{1}{2}]$	$\frac{q}{\Delta p}$
Rate Integral	$q_{Ddi} = \frac{1}{t_{DA}}\int_0^{t_{DA}} q\,Dd(t)dt$	$(\frac{q}{\Delta p_p})_i = \frac{1}{t_{ca}}\int_0^{t_{ca}} \frac{q}{\Delta p_p}dt$
Rate-integral-derivative	$q_{Ddid} = t_{DA}\frac{\Delta q_{Ddi}}{dt_{DA}}$	$(\frac{q}{\Delta p_p})_{id} = \frac{t_{ca}\mathrm{d}(\frac{q}{\Delta p_p})_i}{dt_{ca}}$

Rate integral $(\frac{q}{\Delta p})_i = \frac{1}{t_c}\int_0^{t_c}\frac{q}{\Delta p}dt$

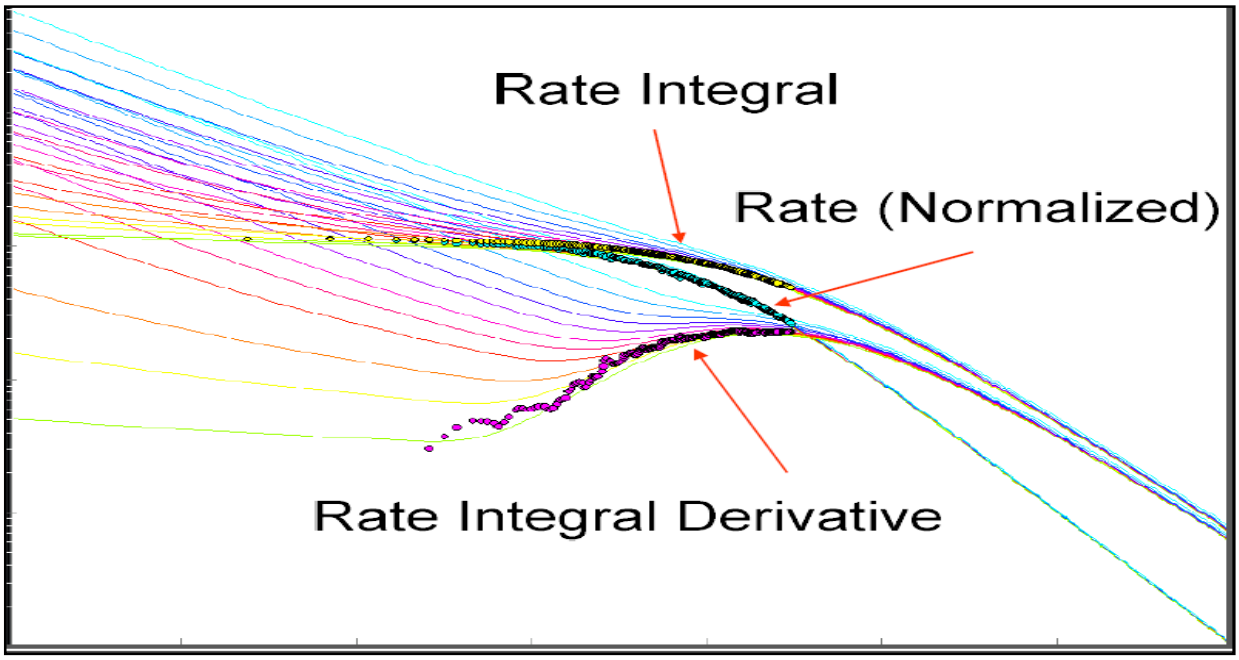

Figure 4.5: Blasingame type curve plot

Blasingame Type curve Analysis Transient Calculations:

For oil permeability K is obtained from rearranging the dimension of

$$q_{Dd} = \frac{q}{\Delta p}\left(\frac{141.2B\mu}{kh}\right)\left(\left(ln\frac{r_e}{r_w}\right)_{match} - \frac{1}{2}\right)$$

$$k = \left(\frac{\frac{q}{\Delta p}}{q_{Dd}}\right)_{match}\left(\frac{141.2B\mu}{kh}\right)\left(\left(ln\frac{r_e}{r_w}\right)_{match} - \frac{1}{2}\right)$$

Solve for rwa from the dimension of

$$t_{Dd} = \frac{0.006328kt_e}{\frac{1}{2}\phi\mu c_t r_{wa}{}^2\left(\left(\frac{r_e}{r_{wa}}\right)^2_{match} - 1\right)\left(\left(ln\frac{r_e}{r_{wa}}\right)_{match} - \frac{1}{2}\right)}$$

$$r_{wa} = \sqrt{\left(\frac{t_e}{t_{Dd}}\right)_{match}\frac{0.006328k}{\phi\mu c_t\frac{1}{2}\left(\left(\frac{r_e}{r_{wa}}\right)^2_{match} - 1\right)\left(\left(ln\frac{r_e}{r_{wa}}\right)_{match} - \frac{1}{2}\right)}}, \qquad s = ln\frac{r_w}{r_{wa}}$$

Blasingame Type curve Analysis Boundary Dominated Calculations:

Oil-in-place calculation is based on the harmonic stem of Fetkovitch type curves. In Blasingame type curve analysis, $q_{Dd} = \frac{q/\Delta p}{(q/\Delta p)_i}$ and $t_{Dd} = D_i t_c$

The Fetkovitch definition for the harmonic type curve and the PSS equation for oil in harmonic form $q_{Dd} = \frac{1}{1+t_{Dd}}$ and using material

From the above equations balance time $\frac{q}{\Delta p} = \frac{\frac{1}{b}}{\frac{1}{c_t N b t_c}+1}$

$\frac{q}{\Delta p} = \frac{\left(\frac{q}{\Delta p}\right)_i}{1+D_i t_v}$ where $\left(\frac{q}{\Delta p}\right)_i = \frac{1}{b}$ and $D_i = \frac{1}{CtNb}$ Oil in place calculation as follows rearranging the equation for Di, $N = \frac{1}{C_{tD_i}b}$ now substituting the definitions of q_{Dd} and t_{Dd}back into the above equation

$$N = \frac{1}{C_t\left[\frac{t_{Dd}}{t_c}\right]\left[\frac{q_{Dd}}{q/\Delta p}\right]} = \frac{1}{C_t}\left[\frac{t_c}{t_{Dd}}\right]_{match\ point}\left[\frac{(q/\Delta p)}{q_{Dd}}\right]_{match\ point}$$

Gas in place calculations:

Gas in place calculation is same as that of oil, with the additional complications of pseudo-time and pseudo-pressure, in Blasingame type curve analysis, q_{Dd} and t_{Dd} are defined as follows

$q_{Dd} = \frac{q/\Delta p_p}{(q/\Delta p_p)_i}$ and $t_{Dd} = D_i t_{ca}$ Fetkovitch definition for the harmonic type curve and the PSS equation for gas in harmonic form:

$q_{Dd} = \frac{1}{1+t_{Dd}}$ and using material balance pseudo time $\frac{q}{\Delta p_p} = \frac{\frac{1}{b}}{\frac{2p_i}{(Z\mu c_t)_i G_i b} t_{ca}+1}$ from these equation $\frac{q}{\Delta p} = \frac{(\frac{q}{\Delta p})_i}{1+D_i t_c}$ where $(\frac{q}{\Delta p})_i = \frac{1}{b}$ and $D_i = \frac{2p_i}{(Z\mu C_t) G_i b}$ rearranging the equation as follows gas in place $G_i = \frac{2p_i}{D_i (Z\mu C_{t)_i} b}$ now substitute the definitions of q_{Dd} and t_{Dd} back into the above equation:

$$G_i = \frac{2p_i}{\frac{t_{Dd}}{t_{ca}}(Z\mu C_t)_i [\frac{q_{Dd}}{(\frac{q}{\Delta p_p})}]} = \frac{2p_i}{(Z\mu c_t)_i} \left[(\frac{t_{ca}}{t_{Dd}})_{match\ point}\right] [(\frac{\frac{q}{\Delta p_p}}{t_{Dd}})_{match\ point}]$$

Analysis procedure:

Boundary-Dominated Match

To obtain information about reserves and drainage area, it is recommended to focus on the boundary-dominated (depletion) stems of the typecurves. These are located on the right-side of the plot, where each set of typecurves converges to a single line. The Blasingame type curve analysis does not require hyperbolic exponent values. Instead, the data is matched on the single depletion stem. As the data is moved about the plot, the GIIP is continuously updated. [19]

Transient Match

To obtain information about permeability and skin needs to focus on the transient stems of the typecurves. On the Blasingame typecurve plot, these appear on the left-side of the plot as a "fan" of different r_{eD} values for the radial and water-drive models. These values are used to calculate permeability and skin.[19]

4.3.4 Agarwal –Gardner Type Curve Analysis

Agarwal and Gardner have developed several different diagnostic methods, each based on modern decline theory[20]. The AG type curve is all derived using the well testing definition of dimensionless rate and time (as opposed to the Fetkovitch definitions). The models are all based on constant rate solution. The methods they present are as follows

1. Rate vs. time type curves (t_D and t_{DA}format)
2. Cumulative production vs. time type curves (t_D and t_{DA} format)
3. Rate vs. cumulative Production type curves (t_{DA} format), linear format and logarithmic format

Agarwal and Gardner rate vs. Time typecurves are the same as conventional drawdown typecurves, but are inverted and plotted in t_{DA} (time based area format), q_D vs. $t_{DA.}$ The AG derivative plot is not a rate derivative (as per Blasingame), Rather it is an Inverse Pressure Derivative.

$$P_D(der) = t(dpD/dt)\ and\ 1/\ P_D(der) = (t(dpD/dt)) - 1$$

Agarwal-Gardner rate vs. Cumulative type curves are different from conventional type curves because they are plotted on linear coordinates. They are designed to analyze boundary dominated data only, thus they do not yield estimate of permeability and skin only fluid in place.

Plot: $q_D\ (1/pD)$ vs. Q_{DA} for gas

$$q_D = \frac{1.417e6*T}{kh}\frac{q(t)}{\Psi_i - \Psi_{wf}(t)}\ \ , Q_{DA} = q_D * t_{DA} = \frac{1}{2\pi}\frac{2q_{tca}}{(c_t \mu Z)_i G_i(\Psi_i - \Psi_{wf})}$$

or alternatively $\frac{1}{2\pi}\frac{\Psi_i - \Psi}{\Psi_i - \Psi_{wf}}$

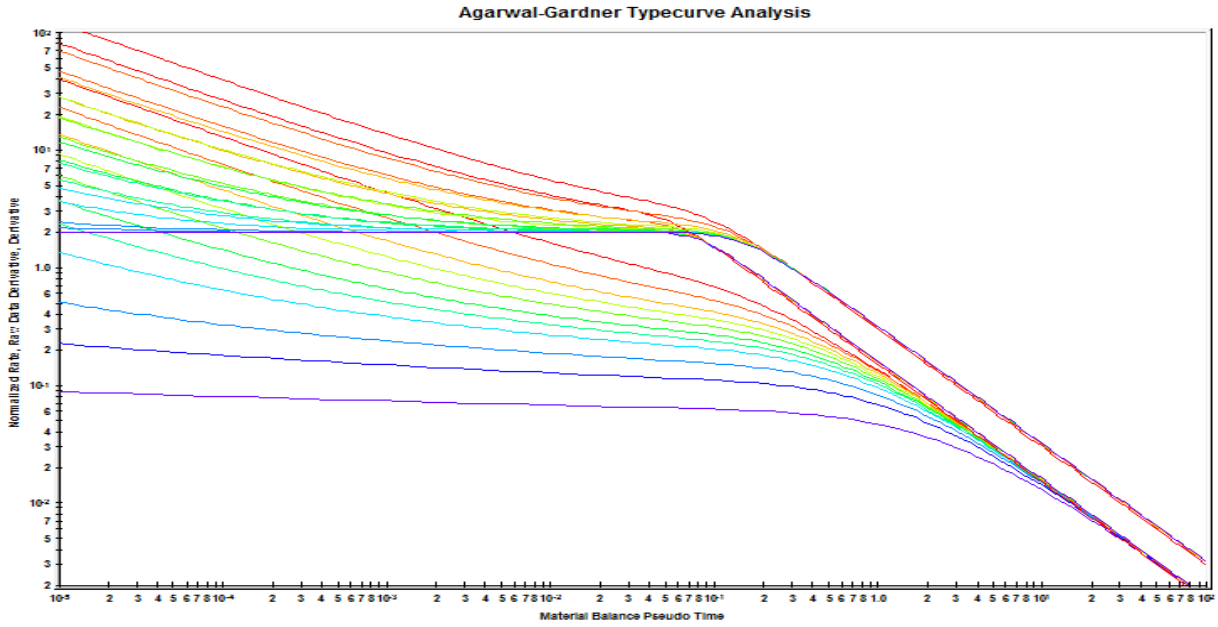

Figure 4.6: Agarwal-Gardner type curve.

Analysis

The normalized rate and inverse semi-log derivative data are plotted against material balance time on a log-log scale of the same size as the typecurves. This plot is called the "data plot". Any convenient units can be used for normalized rate or time because a change in units simply causes a uniform shift of the raw data on a logarithmic scale. It is recommended that daily operated-rates be plotted, and not the monthly rates; especially when transient data sets are analyzed.

The data plot is moved over the type curve plot, while the axes of the two plots are kept parallel, until a good match is obtained. Several different typecurves should be tried to obtain the best fit of all the data. The type curve that best fits the data is selected and its r_e/r_{wa} value is noted.

Type curve analysis is done by selecting a match point, and reading its coordinates off the data plot $(q/\Delta p \; and \; tc) \; match$, and the type curve plot $(q_D \; and \; t_{DA}) \; match$. At the same time the stem value r_e/r_{wa} of the matching curve is noted.

Boundary-Dominated Match

To obtain information about reserves and drainage areas needs to focus on the boundary-dominated (depletion) stems of the typecurves. These are located on the right-side of the plot, where each set of typecurves converges to a single line[19].

Transient Match

To obtain information about permeability and skin, it is needed to focus on the transient stems of the typecurves. On the Agarwal-Gardner type curve plot, these appear on the left-side of the plot as a "fan" of different r_{eD} values for the radial and water-drive models. Select the type curve that best matches the data; this provides an associated r_{eD} value. From the selection, permeability and skin is calculated[19].

4.3.5 NPI (Normalized Pressure Integral) Analysis

Normalized pressure integral (NPI) typecurves are the inverse of Agarwal-Gardner typecurves[20]. NPI analysis plots of a normalized pressure rather than normalized Rate. The analysis consists of three sets of type curve.

1. Normalized pressure vs. tc (material balance time)
2. Pressure integral vs. tc
3. pressure integral- derivative vs. tc

Pressure integral methodology was developed by Tom Blasingame; originally used to interpret drawdown data with a lot of noise (i.e. conventional pressure derivative contains far too much scatter) NPI utilizes a pressure that is normalized using the current Rate. it also utilize the concept of material balance time and pseudo time.

NPI type curve analysis definitions are shown in Table 4.2

Table 4.2 NPI definitions:

Method	Dimensionless form of Type curve	Data for Gas
Normalized pressure	$P_D = \frac{kh\Delta p}{141.2q\beta\mu}$	$\frac{\Delta p_p}{q}$
Conventional pressure derivative	$P_{Dd} = \frac{dp_D}{d(ln\ t_{DA})}$	$(\frac{\Delta p_p}{q})_i = \frac{\frac{d(\Delta p_p)}{q}}{d(\ln t_{ca})}$
Pressure Integral	$P_{Di} = \frac{1}{t_{DA}}\int_0^{t_{DA}} P_p(t)dt$	$(\frac{\Delta p_p}{q})_i = \frac{1}{t_{CA}}\int_0^{t_{DA}} \frac{\Delta p_p}{q} dt$
Pressure integral Derivative	$P_{Did} = t_{DA}\frac{\Delta p_{Di}}{dt_{DA}}$	$(\frac{\Delta p}{q})_{id} = \frac{t_{ca} d(\frac{\Delta p_p}{q})_i}{dt_{ca}}$

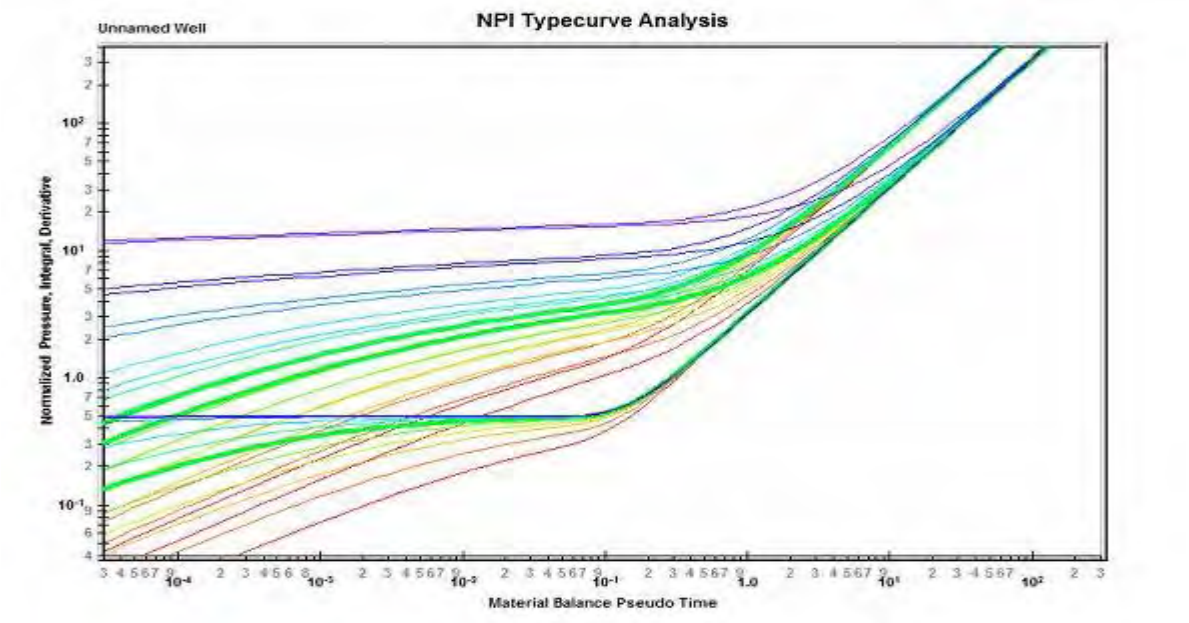

Figure 4.7: NPI type curve analysis.

Analysis:

Boundary-Dominated Match

To obtain information about reserves and drainage areas, it is recommended that to focus on the boundary-dominated (depletion) stems of typecurves. These are located on the right-side of the plot, where each set of type curve converges to a single line. The NPI type curve analysis does not require hyperbolic exponent values. Instead, the data is matched on the single depletion stem[21].

Transient Match

To obtain information about permeability and skin, needs to focus on the transient stems of the typecurves. On the NPI typecurve plot, these appear on the left-side of the plot as a "fan" of different r_{eD} values for the radial and water-drive models. The best matching typecurve, which provides an associated r_{eD} value, is used to calculate permeability and skin[19]

.

Calculation of parameters for gas wells:

$$p_D = \frac{kh\Delta p_p}{1.417*10^6 Tq}, \quad t_{DA} = \frac{0.0063kt_{ca}}{\pi\phi\mu_i c_{ti} re^2}$$

$$\text{Permeability} k = \frac{1.417*10^6 T}{h}\left(\frac{p_D}{\frac{\Delta p_p}{q}}\right)match, \quad r_e = \sqrt{\frac{0.00633k}{\phi\pi\mu_i c_{ti}}\left(\frac{p_D}{\frac{\Delta p_p}{q}}\right)match}$$

$$r_{wa} = \left(\frac{r_e}{\frac{r_e}{r_{wa}}}\right)_{match} \qquad \text{Skin } s = \ln\left(\frac{r_w}{r_{wa}}\right)$$

$$G = \frac{0.00633*1.417*10^6 s_g p_i T_{sc}}{\mu_i C_{ti} z_i p_{sc}}\left(\frac{t_{ca}}{t_{DA}}\right)match\left(\frac{p_D}{\frac{\Delta p_p}{q}}\right)\text{match}*10^9 \text{ BCF}$$

4.4 Reservoir Simulation

Simulation of petroleum reservoir performance refers to the construction and operation of a model whose behavior assumes the appearance of actual reservoir behavior. A model itself is either physical or mathematical. A mathematical model is a set of equations that, subject to certain assumptions, describes the physical processes active in the reservoir. Although the model itself obviously lacks the reality of the reservoir, the behavior of a valid model simulates assumes the appearance of the actual reservoir.

The major goal of reservoir simulation is to predict future performance of the reservoir and find ways and means of optimizing the recovery of the hydrocarbons under various operating condition. Whereas the field can be produced only once, at considerable expense, a model can be produced or run many times at low expense over a short period of time. Observation of model results that represent different producing conditions aids selection of an optimal set of producing conditions for the reservoir.

4.4.1 Steps of the Reservoir Simulation

Set simulation study objectives: The first step in reservoir simulation study is to set clear objectives. These objectives must be achievable and compatible with reservoir and production data.

Gather and validate reservoir data: After the simulation objectives have been set, reservoir and production data are gathered. The data meeting the objectives are incorporated into the simulator.

Design the reservoir simulator: Once the data are gathered and validated, the simulator is designed. This step involves construction of a conceptual physical model, development of mathematical and numerical model and design of computer codes.

History match the reservoir simulator: after the reservoir simulator is constructed, it must be turned or history matched, with available reservoir and production data since much of the data in a typical simulator needs to be verified.

Make prediction: In final application step various development and production plans are evaluated, and a sensitivity analysis of various reservoir and production parameter is carried out[21].

4.4.2 History Matching Overview

History matching is the process of adjusting the reservoir geological model to match the model from field production data. Reservoir production performance greatly determines the economic feasibility of oil and gas recovery and also the future sustenance of production operations. Thus, for efficient reservoir management, a thorough analysis of past, present and future reservoir performance is required, and history matching is a very handy tool for this.

4.4.3 Objectives of History Matching

History matching aids in updating the current reservoir model, matching it with past production, and optimized future prediction. Rwechungura et al.[22], asserts that the main reason for history matching is not just to match historical data, but to enable the prediction of future performance of the reservoir and thus production optimization with regards to economy and oil and gas recovery by improved or enhanced methods. According to Olumide[23] the actual geometry of a reservoir is largely unknown, thus productivity forecasts made with such a model would be laden with errors. For this reason the model has to be adjusted by history matching to obtain the suitable model with which prediction of future reservoir performance can be competently carried out.

4.4.4 Benefits of History Matching

Aside from giving a good match and providing a model for future predictions, history matching process provides some other benefits. Nan Cheng[24] stated that the other benefits of history matching include:

- Model calibration, which helps to improve and validate reservoir description;
- Prediction of future performance with higher degree of confidence;
- Enhancing the understanding of the reservoir; and
- Detecting operational issues during the process of reservoir management.

Olumide[23] adds that history matching improves the quality of the simulation model, helps to locate weakness in available data and provides in-depth understanding of the processes taking place in the reservoir.

4.4.5 Methods of History Matching

Many methods of history matching have been developed over the years with many researchers trying to find new ways of faster, efficient, accurate and less time-consuming methods. Earliest history matches were performed by trial and error with the hope that manually adjusting the value of some parameters might help give the desired match. Rwechungura et al.[22] stated that the quality of such history matching would largely depend on the engineer's experience and the budget allocated for the process. This is due to the fact that petroleum reservoirs are usually very complex and heterogeneous having hundreds of thousands (and in very large reservoirs, millions) of grid blocks in the simulation model required for high resolution evaluation of reservoir parameters. Due to these afore mentioned complexities and the fact that many uncertainties abound in determination of the absolute values and effects of reservoir parameters, manual history matching is not readily considered and is not reliable when the project period is long. For this reason computerized (or automatic) history matching methods have been developed and utilized by many researchers. However, if the field or segment under consideration is small, accurately delineated, and the reservoir parameters and characteristics well defined, then manual history matching can be applied with some degree of comfort. Manual history matching basically involves manual perturbation of pre-selected parameters based on sensitivity studies carried out to pre-determine which parameters affect production the most. According to Rwechungura et al.[22], the mathematical model required for the estimation of unknown parameters in history matching consists of two components namely:

- A reservoir simulator to model the flow through porous media, and
- A rock physics model to enable computation of seismic responses.

Olumide[23] states that the objective function is a function of the difference between the observed reservoir performance and the response calculated by the simulation model using the available parameters and can contain many terms representing various constraints.
Reservoir simulation models are widely employed in practical multiphase fluid-flow studies that forecast future performance and make crucial decisions on managing hydrocarbon reservoirs. For such studies to lead to reliable conclusions, a key requirement is to ensure that the reservoir model is consistent with all the available data. Constructing reservoir models that are consistent with the available geophysical and geological static data is possible and

relatively well understood. The main challenge is to condition such models to the available production dynamic data through the process of history-matching.

Modification of grid block properties, such as porosity and permeability is typically achieved by using box multipliers. Applying a multiplier to a given domain, in effect, collapses a large number of parameters (the property value at every grid block in a box) into a single parameter. While this kind of simplification allows more control for the engineer, the concept of box multipliers itself is in conflict with any geological sense. Moreover, capturing the optimal location and the size of the box involves a trial-and-error exercise that is well-known to be both tedious and challenging. The above challenges, as well as the trial-and-error nature, make history-matching the most expensive and time/resource consuming step in the reservoir modeling process.

Interest in computer aided history-matching tools has been increasing recently. Commercial tools are now available that are meant to reduce the manual work conducted by the reservoir engineer. A common feature in these packages, however, is that they require the user to specify upfront the parameters that are to be evaluated and tuned. Moreover, the number of such parameters has to be kept small, since the computational costs increase rapidly as more parameters are included. The requirement to specify a small set of parameters in advance is an awkward first step [25].

4.4.6 Eclipse 100

The ECLIPSE 100 is fully implicit, three phase, three dimensional, general purpose Black-Oil simulator. This means ECLIPSE solves the Black-Oil equations using IMPES (Implicit Pressure Explicit Saturation) method. The program is written by FORTAN77 and can be used on any computer with an appropriate complaier having sufficient memory available. ECLIPSE 100 can be used to simulate 1, 2 or 3 phase systems. Two phase options (oil/water, oil/gas, and gas/water) are solved as two component systems saving both computer storage and computer time. In addition to gas dissolving in oil (variable bubble point pressure or gas/oil ratio), ECLIPSE 100 may also be used to model oil vaporizing in gas (variable dew point pressure or oil/gas ratio. Both corner-point and conventional block-center geometry options are available in ECLIPSE. Radial and Cartesian block-center options are available in 1, 2 or 3 dimensions. A 3D radial option completes the circle allowing flow to take place across the 0/360 degree interface. To run simulation you need an input file with all data concerning reservoir and process of its exploitation. Input data for ECLIPSE is prepared in free format using a keyword system. Any standard editor may be used to prepare the input file. Alternatively ECLIPSE Office may be used to prepare data interactively through panels, and submit runs. The name of input file has to be in the following format: FILENAME.DATA

An ECLIPSE data input file is split into sections, each of which is introduced by a section-header keyword. A list of all section-header keywords is given in following, together with a brief description of the contents of each section and examples of keywords using in file code.

The keywords in the input data file (including section-header keywords) are each of up to 8 characters in length and must start in column 1. All characters up to column 8 are significant. Any characters on the same line as a keyword from column 9 onwards will be treated as a comment[26, 27].

Section-header keywords[26,27]

The list of section-header keywords in proper order:

1. RUNSPEC

2. GRID

3. EDIT

4. PROPS

5. REGIONS

6. SOLUTION

7. SUMMARY

8. SCHEDULE

1. RUNSPEC: Title, problem dimensions, switches, phases present, components etc.

2. GRID: The GRID section determines the basic geometry of the simulation grid and various rock properties (porosity, absolute permeability, net-to-gross ratios) in each grid cell. From this information, the program calculates the grid block pore volumes, mid-point depths and inter-block transmissibility's

3. EDIT: Modifications to calculated pore volumes, grid block centre depths and transmissibility's.

4. PROPS: Tables of properties of reservoir rock and fluids as functions of fluid pressures, saturations and compositions (density, viscosity, relative permeability, capillary pressure etc.).

5. REGIONS: Splits computational grid into regions for calculation of:

-PVT properties (fluid densities and viscosities),-saturation properties (relative permeability's and capillary pressures)

-Initial conditions, (equilibrium pressures and saturations)

- Fluids in place (fluid in place and inter-region flows) If this section is omitted, all grid blocks are put in region 1.

6. SOLUTION: Specification of initial conditions in reservoir - may be:

-calculated using specified fluid contact depths to give potential equilibrium

-read from a restart file set up by an earlier run- specified by the user for every grid block (not recommended for general use)

This section contains sufficient data to define the initial state (pressure, saturations, and compositions) of every grid block in the reservoir.

7. SUMMARY: Specification of data to be written to the Summary file after each time step. Necessary if certain types of graphical output (for example water-cut as a function of time) are to be generated after the run has finished. If this section is omitted no Summary files are created.

8. SCHEDULE: Specifies the operations to be simulated (production and injection controls and constraints) and the times at which output reports are required. Vertical flow performance curves and simulator tuning parameters may also be specified in the SCHEDULE Section.

CHAPTER 5

VOLUMETRIC ANALYSIS USING MONTE CARLO SIMULATION APPROACH

5.1 Monte Carlo Simulation of Lower Gas Sand of Narshingdi Gas Field using MBAL (IPM) Software

The following input parameter was used to calculate probabilistic GIIP for the LGS of Narshingdi gas field.

Number Histogram Steps: 20

Number of Cases: 5000

Reservoir Temperature: 205 (deg F)

Reservoir Pressure: 4575 (psig)

Here the number of cases defines the number of segments of equal probability the distribution will be divided into and the histogram steps defines the number of steps that will be plotted on the histogram. Table 5.1 shows the input parameters for Monte Carlo Simulation

Table 5.1: Input parameters for Monte Carlo Simulation[5]

Parameter	Distribution	Minimum	Maximum	Mode	Unit
Area	Triangular	5159	12898	7739	(acres)
Thickness	Triangular	25	34	30	(feet)
Porosity	Triangular	0.16	0.18	0.17	(fraction)
Gas Saturation	Triangular	0.57	0.6	0.59	(fraction)
CGR	Triangular	1.9	3.1	2.4	(STB/MMscf)
Oil Gravity	Fixed Value	40			(API)
Gas Gravity	Triangular	0.596	0.618	0.6	(sp. gravity)

Probabilistic reserves calculated using the parameter of Table 5.1 is shown graphically in the Figure 5.1 and the results are summarized in Table 5.2

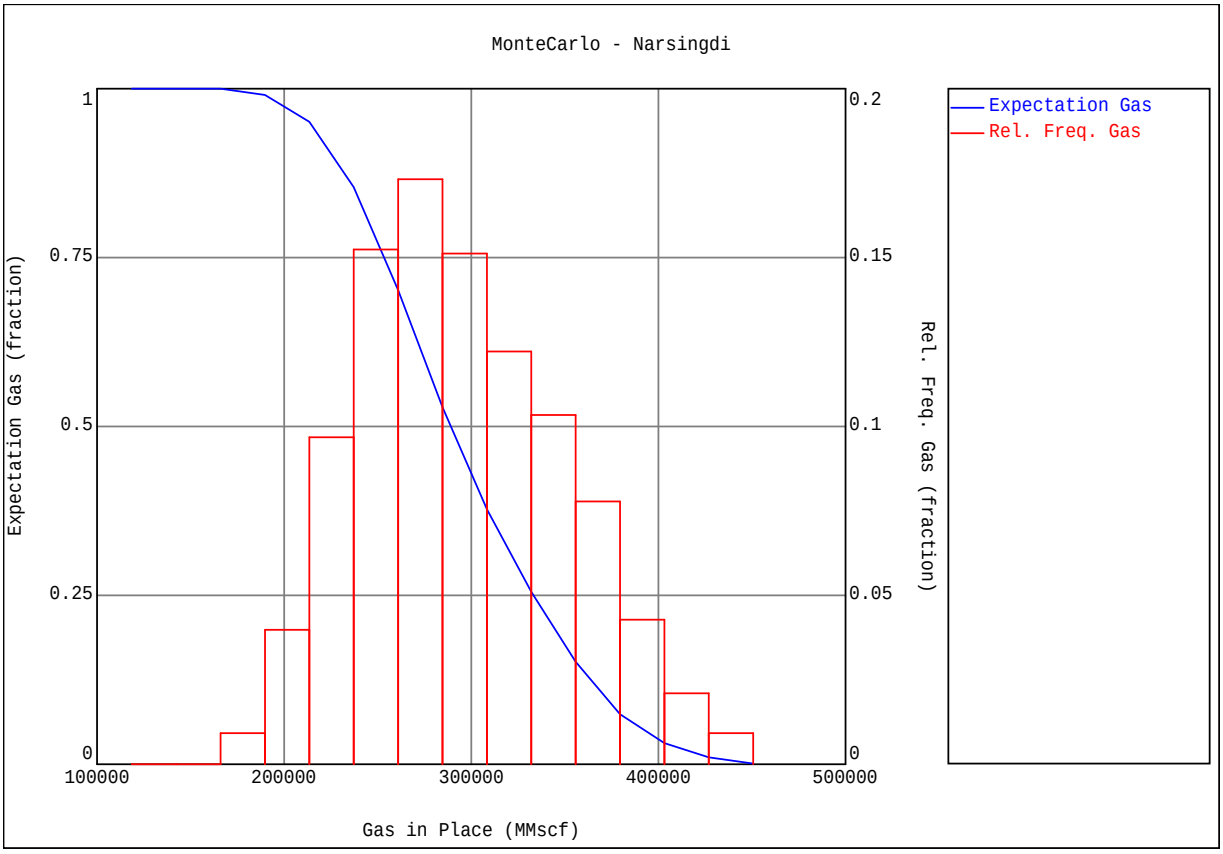

Figure 5.1: Expectation curve of Monte Carlo Simulation of LGS.

Table 5.2 Monte Carlo Simulation Results for LGS

	GIIP (BCF)
Mean Reward	294.742
Standard Deviation	56.0831
$P_{90,}$ Proved Reserve	225.953
$P_{50,}$ Proved + Probable Reserve	289.096
$P_{10,}$ Proved +Probable + Possible Reserve	371.553

The expectation curve Figure 5.1 of the Lower Gas Sand shows that, the P_{90} value of GIIP is 225.953 BCF, the P_{50} value is 289.096 BCF, and the P_{10} value is 371.553 BCF. So the difference between proved reserve and possible reserve is 145.6 BCF, the amount of difference is high so the expectation curve tells us the reserve distribution and risk level.

5.2 Monte Carlo Simulation Using Excel for LGS

The same calculation was performed using the Excel for the LGS and UGS of this gas field. Here the number of simulation run was 6000. The input parameters are shown in Table 5.3

Table 5.3 Input parameters for Monte Carlo Simulation[5]

	Area (acre)	Thickness (ft)	Porosity (fraction)	Gas Saturation Sg=(1-Swc) (fraction)	Formation volume factor (1/Bg) (scf/ft^3)
Min, a	5.16E+03	25	0.16	0.57	245
Mode, c	7.74E+03	30	0.17	0.59	247
Max, b	1.29+04	34	0.18	0.60	250
F(c)	0.3	0.56	0.5	0.7	0.4

Triangular-distributed random variate was used to calculate GIIP creating the random variable applying the following triangular rule.

$$X = a + \sqrt{U(b-a)(c-a)} \quad \text{for } 0<U<F(c)$$

$$X = b - \sqrt{(1-U)(b-a)(b-c)} \quad \text{for } F(c)\leq U<1$$

Where $F(c) = \frac{(c-a)}{(b-a)}$

Here a is the Minimum value, b is the Maximum value and c is the most likely or most common value of area, thickness, porosity, gas saturation and gas formation values.

The random variables for GIIP calculation are shown in Table 5.4. The expectation curve for LGS is shown in Figure 5.2. The result summary from the expectation curve is shown in Table 5.5

Table 5.4 Random variables for GIIP calculation

Iteration No.	Random Variable	Area (Acre)	Random Variable	Thickness (ft)	Random Variable	Porosity (%)	Random Variable	Saturation (%)	Random Variable	1/Bg (Scf/ft^3)	GIIP (BCF)
1	0.841	10382	0.163	27.71	0.26	0.167	0.510	0.587	0.822	248.3	306.01
2	0.728	9601	0.055	26.57	0.33	0.168	0.677	0.590	0.267	246.6	272.13
.....	.....	.....	.....	.....	....	.....	.....	.....	.....	.....	.....
5999	0.172	7013	0.726	30.86	0.78	0.173	0.244	0.582	0.743	248.0	236.10
6000	0.519	8516	0.434	29.42	0.11	0.164	0.575	0.585	0.437	247.0	261.71

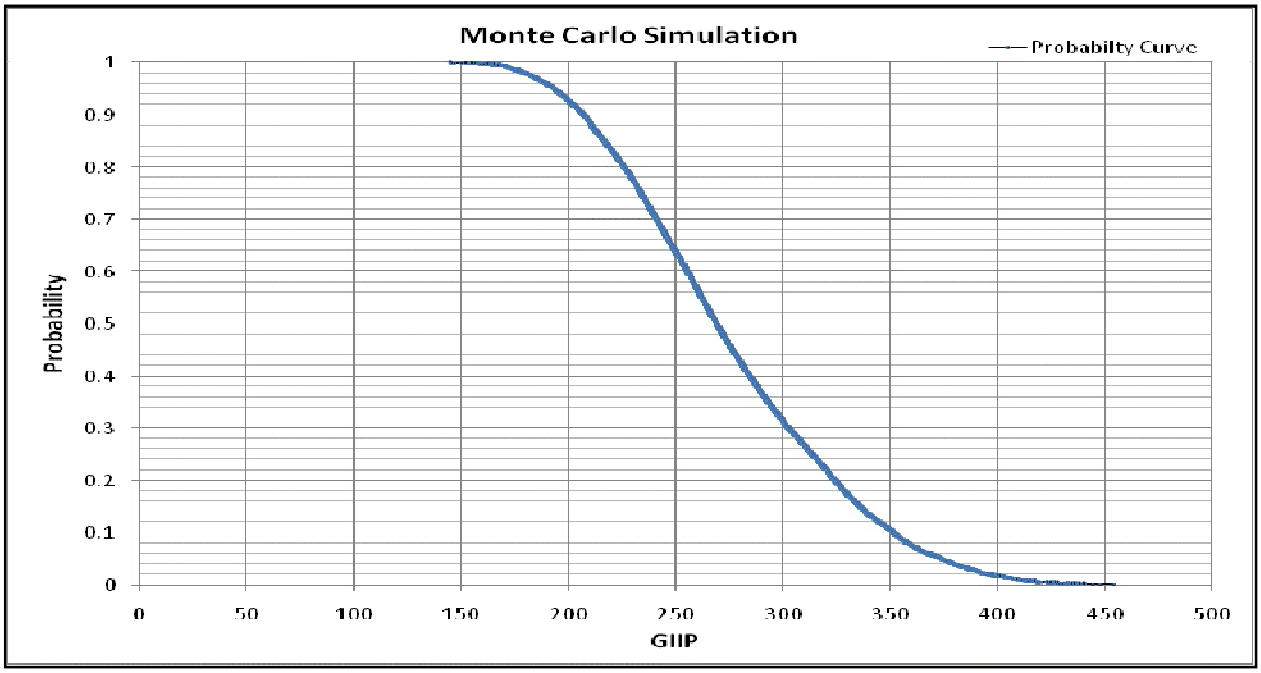

Figure 5.2: Expectation curve of Monte Carlo Simulation LGS.

Table 5.5 Result for LGS

Probability	GIIP (BCF)
P_{90}	204.6289
P_{50}	268.53
P_{10}	351.278

The result that is found from the software and using the excel sheet approach is almost similar.

5.3 Monte Carlo Simulation using Excel for UGS

Table 5.6 Input parameters of Monte Carlo Simulation for UGS[5]

	Area (acre)	Thickness (ft)	Porosity (fraction)	Gas Saturation Sg=(1-Swc) (fraction)	Formation Volume Factor (1/Bg) (scf/ft^3)
Min, a	2890	10	0.20	0.58	241
Mode, c	4330	16	0.21	0.59	244
Max, b	7220	20	0.22	0.60	248
F(c)	0.33	0. 60	0.50	0.50	0.43

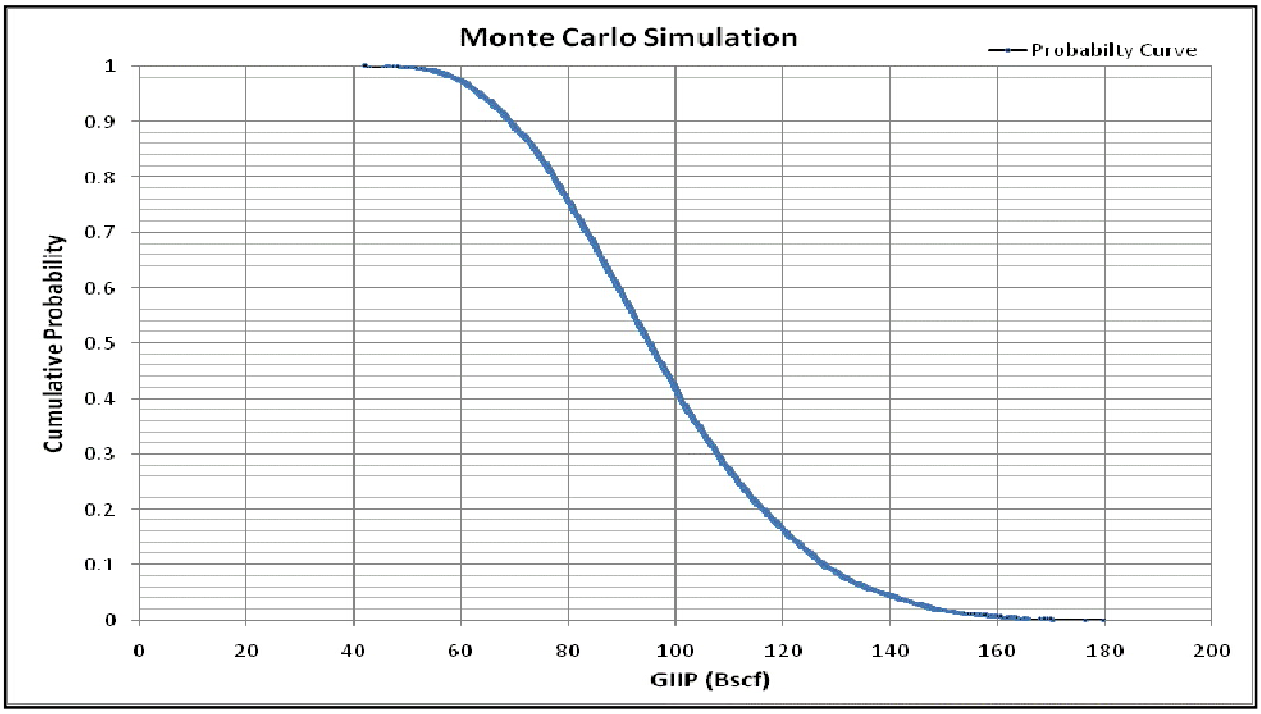

Figure 5.3: Expectation curve of Monte Carlo Simulation UGS

Table 5.7 Result for UGS

Probability	GIIP (BCF)
P_{90}	69.24548
P_{50}	95.21098
P_{10}	127.5092

The expectation curve of upper gas sand shows that the P_{90} value or the proved reserve is 69.24548 BCF, the P_{50} value is 95.21098 BCF, and the P_{10} value or the maximum amount of GIIP value is 127.5092 BCF. Now the production is coming from only the lower gas sand, so the upper gas sand can also contribute to the total gas production from the field.

CHAPTER 6

MATERIAL BALANCE ANALYSIS

6.1: Material Balance using the software MBAL

The recorded shut in well head pressure data was taken from the monthly record of Narshingdi gas field, and corresponding static bottom hole pressure were calculated using Average Temperature and Z-Factor Method (Appendix1). Static bottom hole pressure data was used to calculate the reserve and GIIP using the software MBAL.

MBAL provides a better understanding of the reservoir behavior and it has the capabilities of history matching to determine hydrocarbon in place and main drive mechanism of the reservoir. This software can be used for single tank model and multiple tank models which offer the possibility of connecting tanks through transmissibility. As the Narshingdi gas field is producing only from the lower gas sand single tank model was used to understand the reservoir behavior and drive mechanism. The data required for the modeling of tank includes:
Initial reservoir pressure (4575 psia),
Temperature (205^{o}F),
Porosity (21.4%),
Connate water saturation (22%),
Formation compressibility (3e-6 1/psi),
Relative permeability function and production history.

Drive mechanism of the reservoir is shown in Figure 6.1

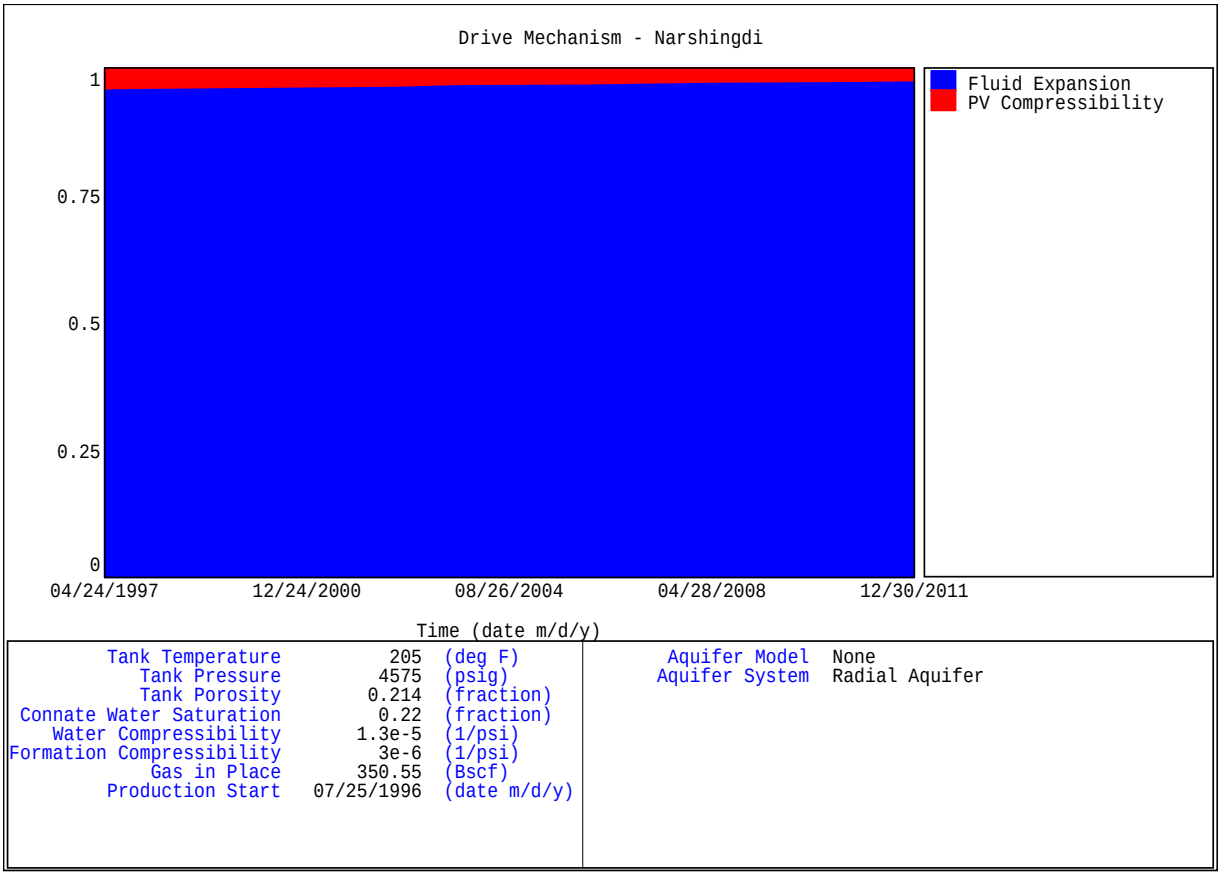

Figure 6.1: Drive mechanism of the reservoir

The energy plot derived from the MBAL shows the relative contribution of the main energy source in the reservoir. Here in the Figure 6.1 the blue and red color represent relative energy supplied by compaction drive and depletion drive mechanism respectively. It is clear from the plot that fluid expansion is the main source of energy for the reservoir providing 95% of the total energy. Rock compaction provided 5% of the energy.

Figure 6.2 shows the P/Z plot for LGS.

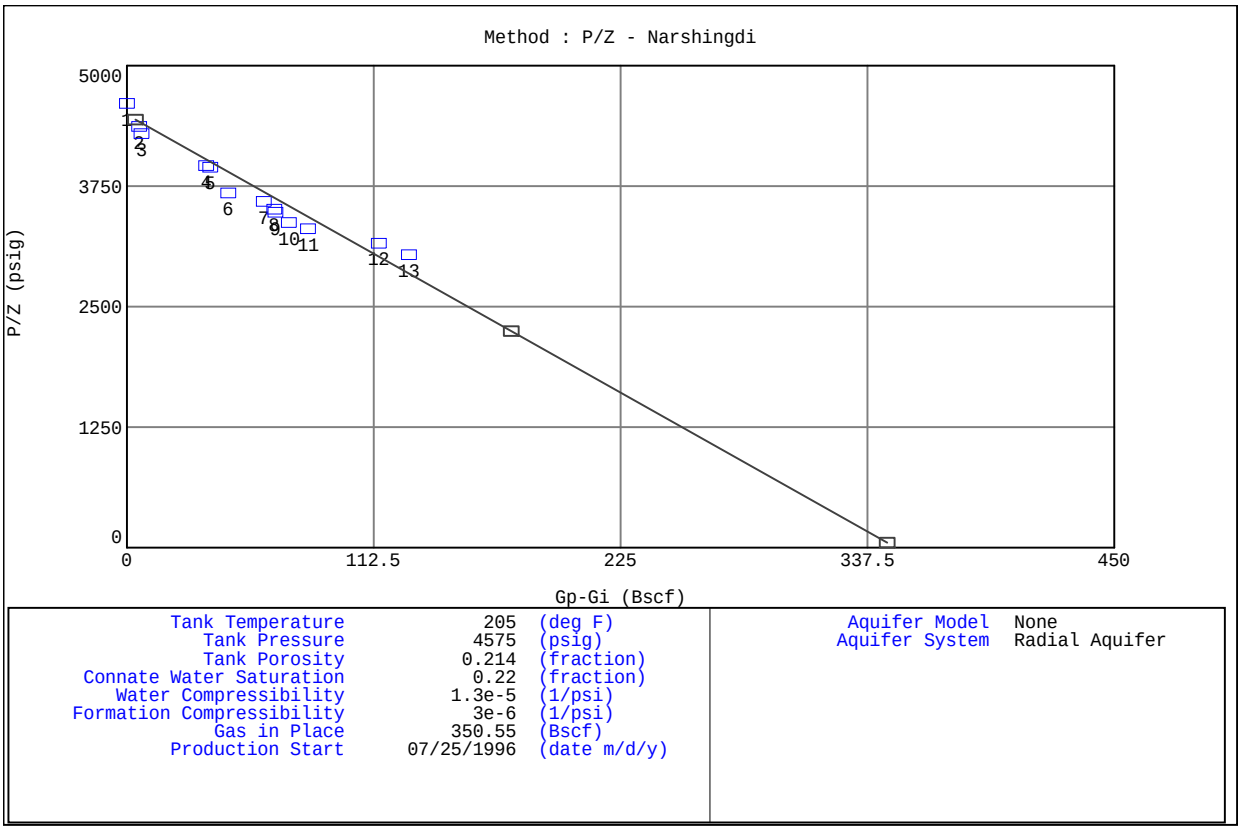

Figure 6.2: P/Z plot

Gas Initially in Place (GIIP) in lower gas sand value calculated from the P/Z plot is 350 BCF. The P/Z plot also shows that the reservoir is volumetrically close here so the reservoir pressure is decling.

6.2: Material Balance Using the Shut in Well Head Pressure

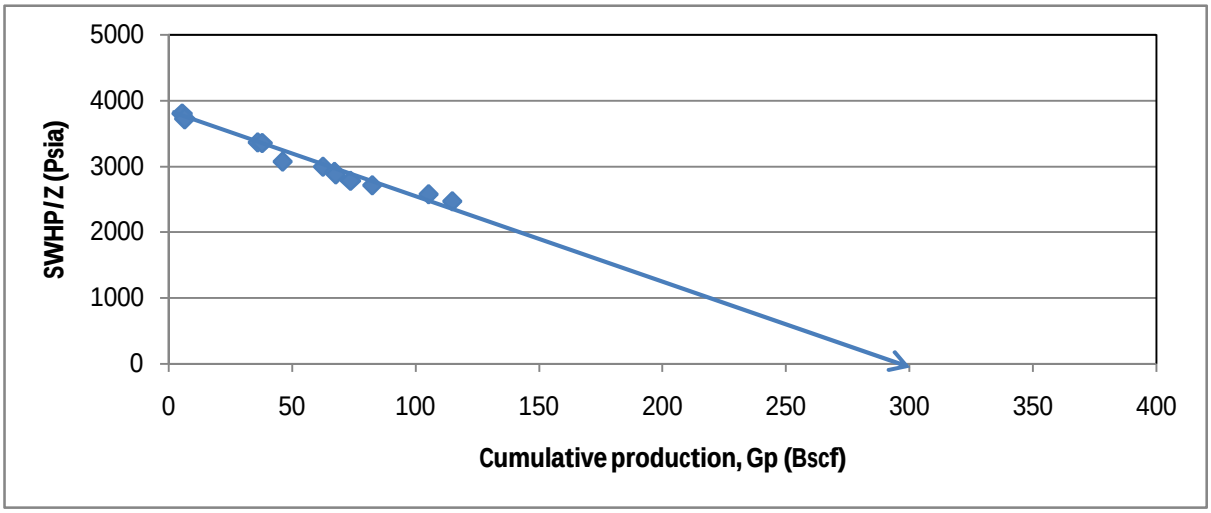

Figure 6.3: Shut in well head pressure vs. Cumulative production

Figure 6.3 shows the material balance using the shut in well head pressure approach. This approach shows the GIIP value is 300 BCF and it is 50 BCF lower than the shut in bottom hole pressure approach.

6.3: Material Balance Using the Flowing Bottom Hole Pressure

The flowing bottom hole pressure used here is calculated using the software PROSPER from the monthly representative well head pressure. The recorded flowing well head pressure was taken from monthly records of Narshingdi gas field.

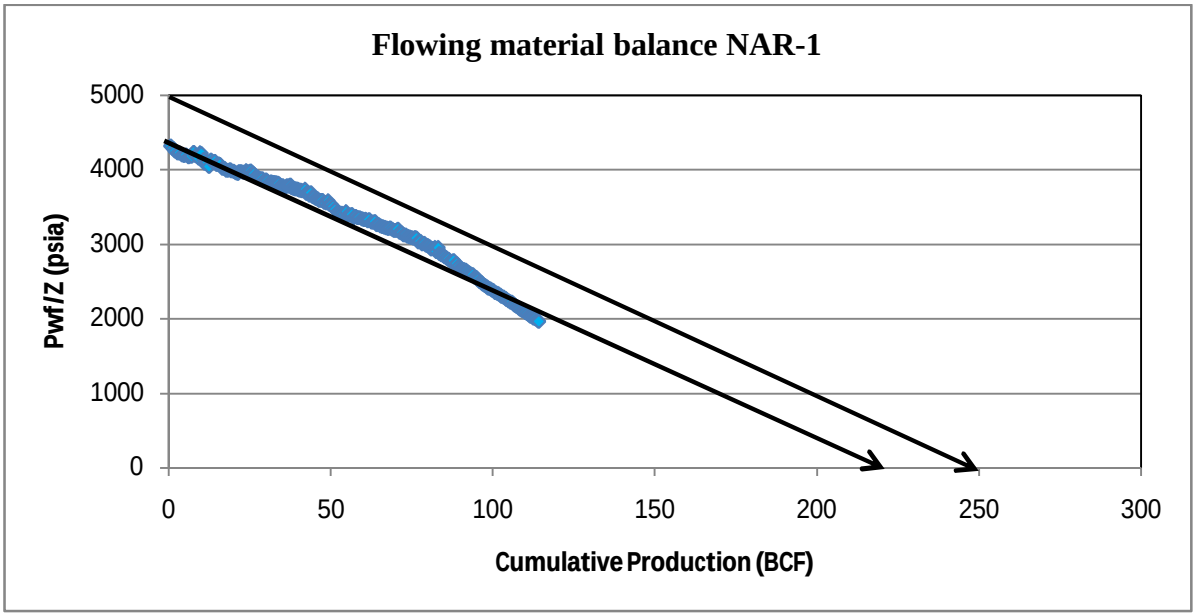

Figure 6.4: Flowing bottom hole pressure vs. cumulative production for NAR-1

Here in the Figure 6.4 a straight line from the initial reservoir pressure parallel to the flowing bottom hole pressure data was drawn to calculate the GIIP. In the Narshingdi gas field the initial reservoir pressure was 4575 psia and the corresponding z factor was calculated 0.962 so the parallel line was drawn from the 4752 psia.

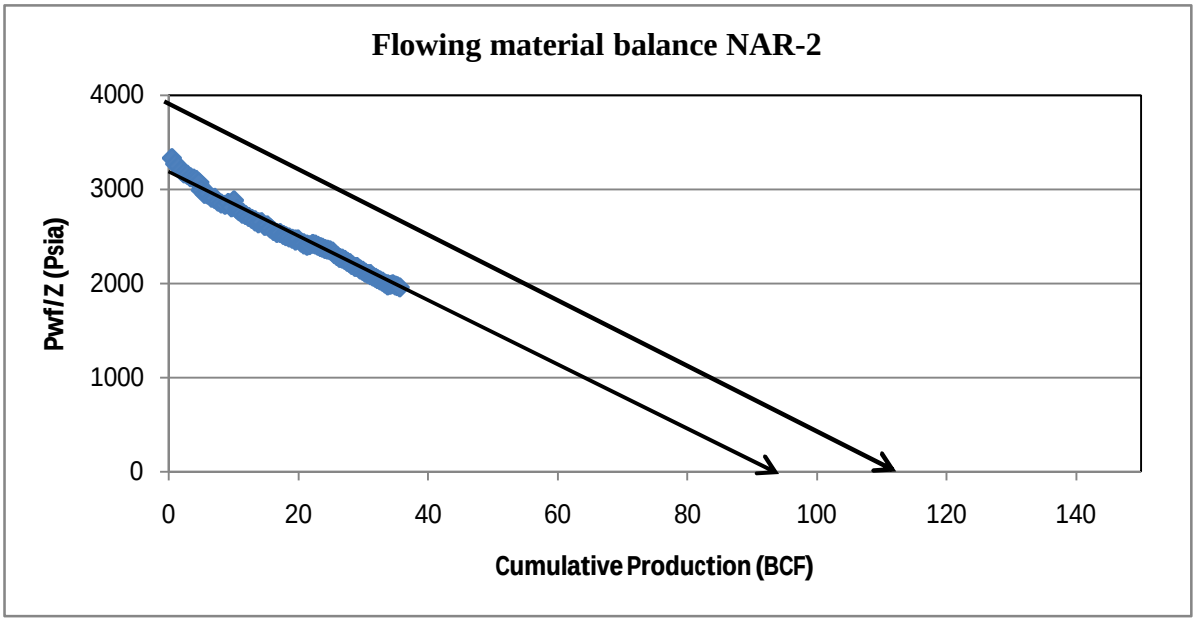

Figure 6.5: Flowing bottom hole pressure vs. cumulative production for NAR-2

For the well NAR-2 same calculation was performed to calculate the GIIP. Here initial reservoir pressure for this well was 3550 psia and the corresponding z factor was calculated as 0.92 so the parallel line was drawn from the 3867 psia.

6.4: Material Balance Using the Flowing Well Head Pressure

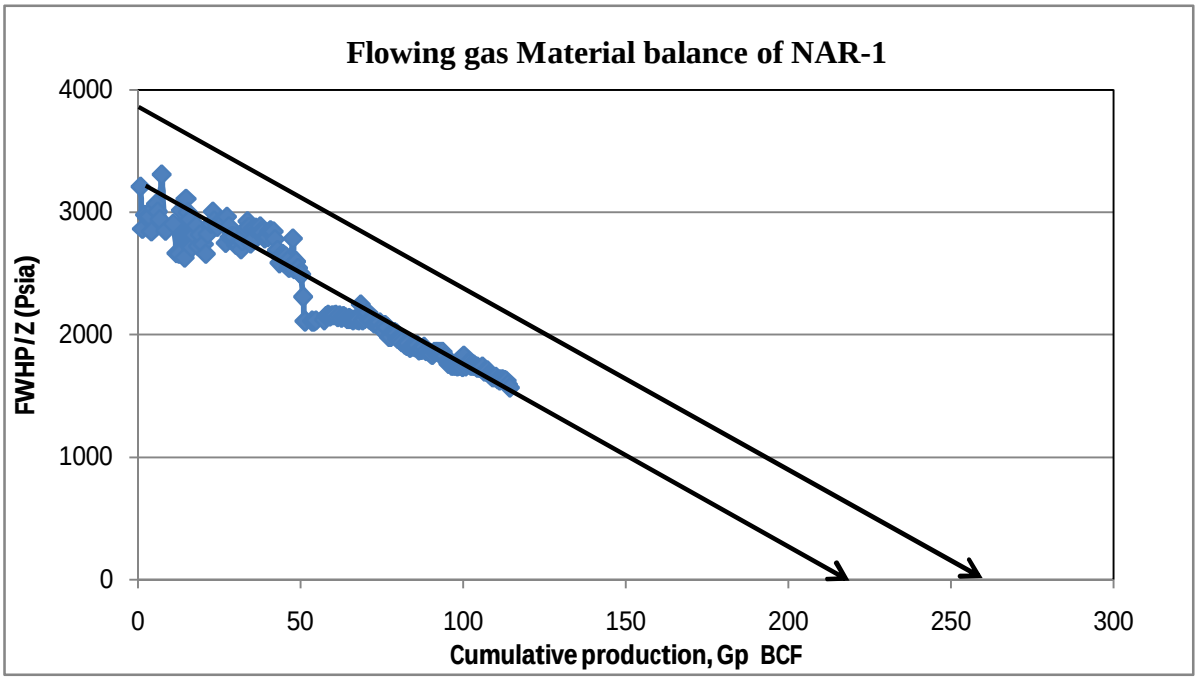

Figure 6.6: Flowing well head pressure vs. cumulative production for NAR-1

In case of the flowing well head pressure approach a straight line was drawn parallel to the flowing well head pressure data, from the initial well head pressure to calculate the GIIP. In the Narshingdi gas field the initial well head pressure was 3480 psia for NAR-1 and the corresponding z factor was 0.92 so the parallel line was drawn from the 3800 psia (Figure 6.6)

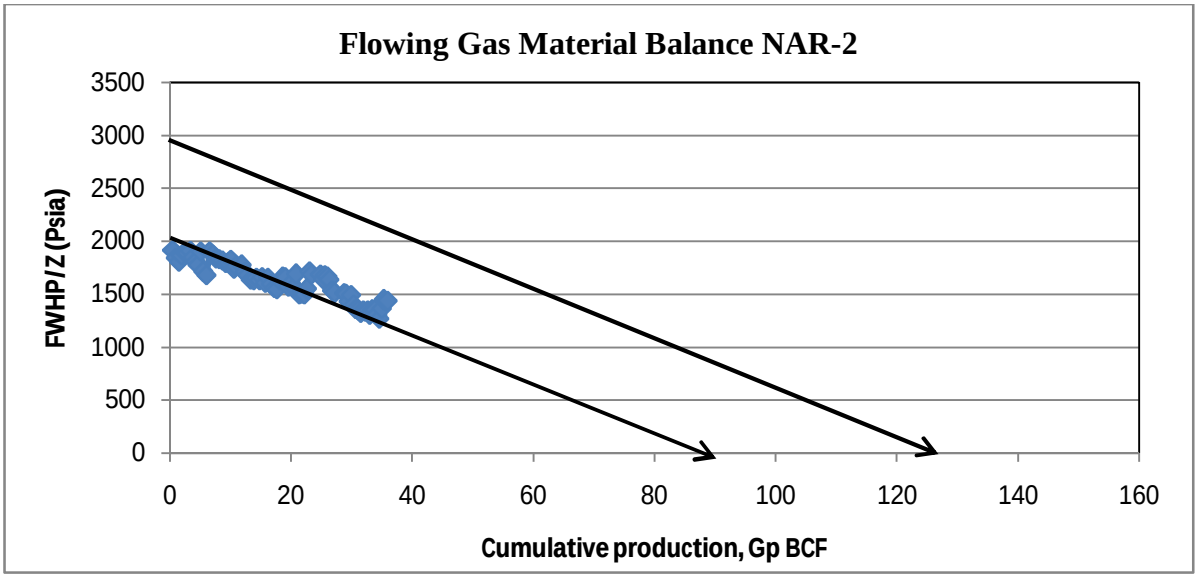

Figure 6.7: Flowing well head pressure vs. cumulative production for NAR-2

For the well NAR-2 same calculation was performed to calculate the GIIP. Figure 6.7 shows that the GIIP for NAR-2 is128 BCF.

6.5: Approximate Well Head Material Balance (AWMB)

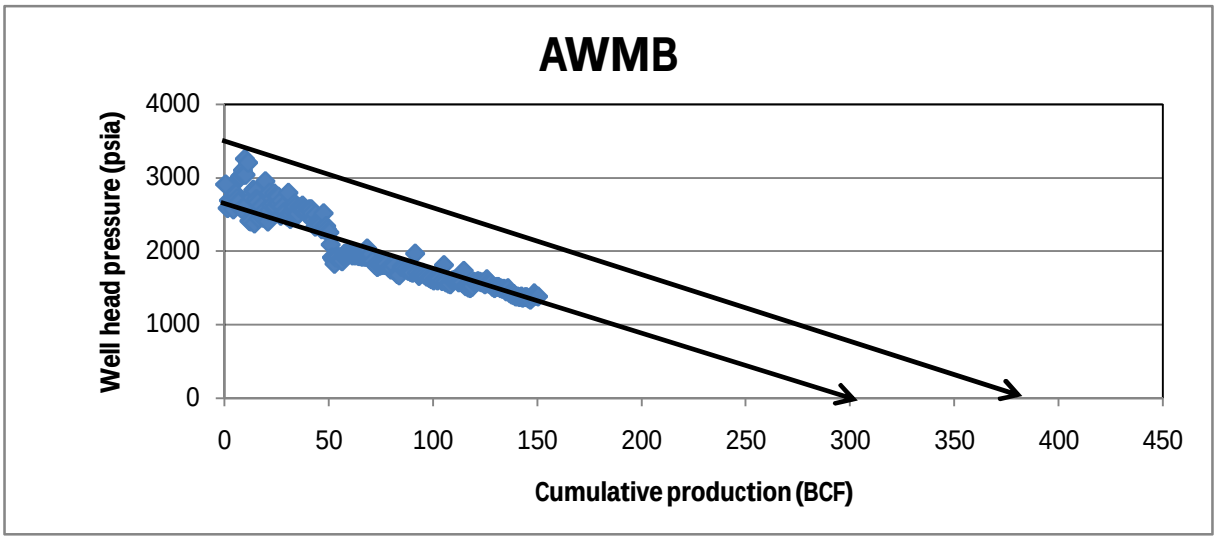

Figure 6.8: Approximate well head pressure vs. cumulative production

In Figure 6.8, approximate well head material balance shows that the GIIP for LGS is 390 BCF.

The results of material balance analysis are summarized in Table 6.1 and 6.2

Table-6.1: Results of Material Balance:

Method	Well No.	GIIP (BCF)	GIIP total (BCF)
Flowing gas material balance (using flowing bottom hole pressure)	NAR-1	250	366
	NAR-2	116	
Flowing gas material balance (using flowing well head pressure)	NAR-1	255	382
	NAR-2	127	
Approximate well head material balance			390
Material balance using static well head pressure			300
Material balance using static bottom hole pressure			350

Table-6.2: Reserve and recovery factor for P/Z plot (SBHP Method):

GIIP (BCF)	Recoverable reserve at P/Z of 1000 psia	Gp up to December 2013 (BCF)	Remaining Reserve (BCF)	Recovery factor
350	275	150	125	79 %

CHAPTER 7

ADVANCED DECLINE CURVE ANALYSIS

7.1 Result From Fekete (FAST R.T.A)

FAST.RTA™ is a decline analysis tool that analyses production rates and flowing pressures. Methods include traditional decline analysis, Fetkovitch, Blasingame, Agarwal-Gardner, NPI, Transient and Wattenbarger type curves, specialized analysis and flowing material balance. Reservoir models include volumetric and water drive types. Well models include horizontal, vertical, and hydraulically fractured well types. FAST.RTA™ analyses production data, yielding hydrocarbons in place (GIIP), expected ultimate recovery (EUR), drainage area, permeability, skin and fractures half length and aquifer strength. It allows the evaluation of infill potential, characterization of the reservoir, and estimation of reserves with ease and efficiency. There are a number of conventional analysis techniques incorporated within the FAST.RTA™ and are used for production data analysis, including: 1) Arp decline analysis (exponential, hyperbolic and harmonic); 2) Fetkovich type curve analysis; 3) Blasingame type curve analysis; 4) Agarwal-Gardner type curve analysis; 5) Normalized Pressure Integral (NPI) type curves; 6) Flowing Material Balance; 7) Wattenbarger; 8) Analytical & Numerical Modelling.

Advanced decline curve (rate transient) analysis was performed using the Fekete software to determine the reservoir volume and ultimate recovery at abandonment tubing head pressure 1000 psi for the two well of lower gas sand of the Narshingdi gas field. The results found from the Blasingame type curve, Agarwal-Gardner Type curve and from the Normalized Pressure Integral (NPI) are shown graphically in the following figure and the outputs are also summarized in the following table. For the calculation vertical model was used.

NAR-1

7.2 Blasingame Type Curve Plot

The data plotted in the Blasingame plot uses Normalized rate integral and a derivative function to reduce the noise level. From the Blasingame it is obvious that the production response consists of two distinct flow periods, a transient production followed by a pseudo-steady state (boundary dominated). The transient flow period was used to calculate

permeability thickness product of the well's drainage volume, skin factor, and drainage radius. The pseudo-steady state period was used to identify remaining reserves. The data plotted in Blasingame type curve was moved vertically and horizontally until a match is obtained with one set of curves. After the proper type curve matching a match point was used to calculate original gas in place and other parameters.

The plot is shown in Figure 7.1

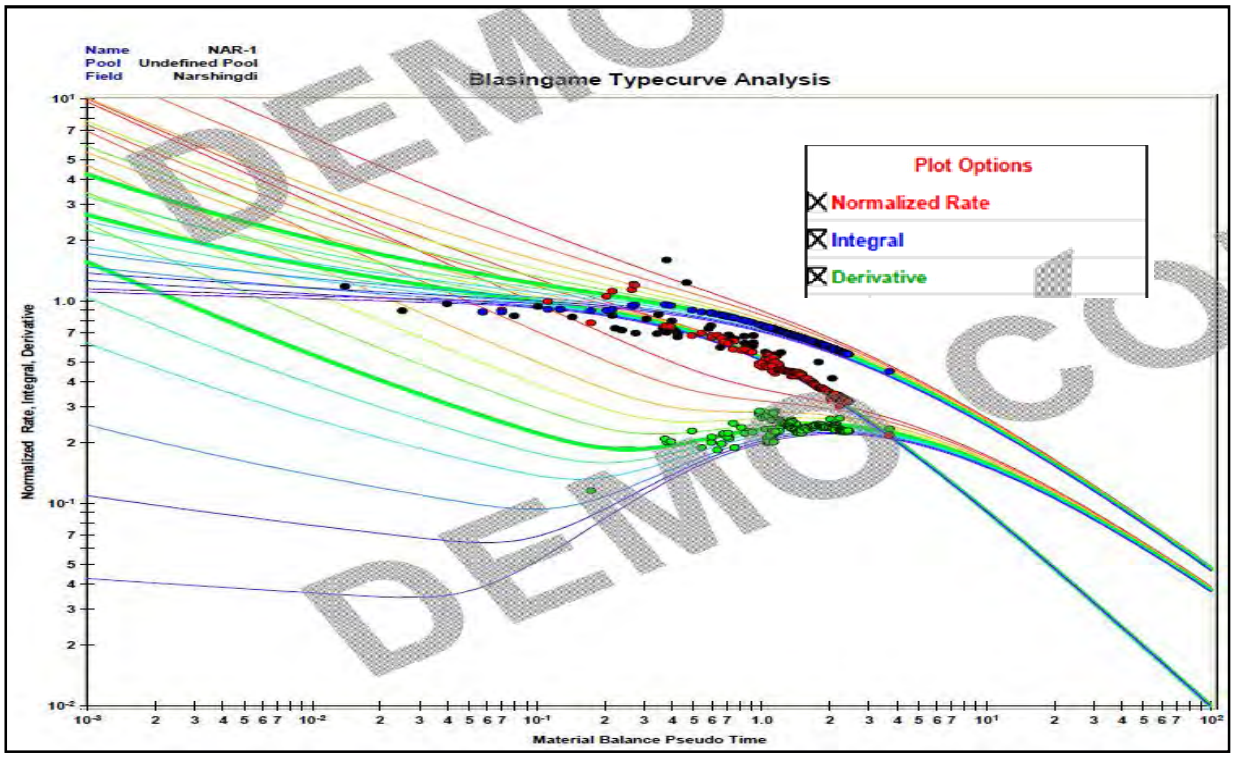

Figure 7.1: Blasingame Type curve analysis for NAR-1

The results of Blasingame type curve analysis are summarized in Table 7.1

Table 7.1 Results for Blasingame Type Curve Analysis:

Parameter	Result
Well type	Vertical well
GIIP	282 (BCF)
Reservoir Area	9852 (Acre)
Pab (abandonment pressure)	1000 (psia)
RF	72.41 %
EUR	204 (BCF)

7.3 Agarwal-Gardner Type Curve Analysis

Agarwal-Gardner type curve analysis represent advancement over Blasingame type curves as a clear distinction can be made between transient and boundary dominated flow periods. Agarwal-Gardner type curve includes raw and smoothed data derivative plots and normalized rate to estimate GIIP, RF, EUR and reservoir drainage area. Figure 7.2 shows the Agarwal-Gardener type curve analysis plot. To obtain information about the reserve and drainage area boundary dominated (depletion) stems of the type curve was used, it is located on the right side of the plot where each set of type curves converges to a single line.

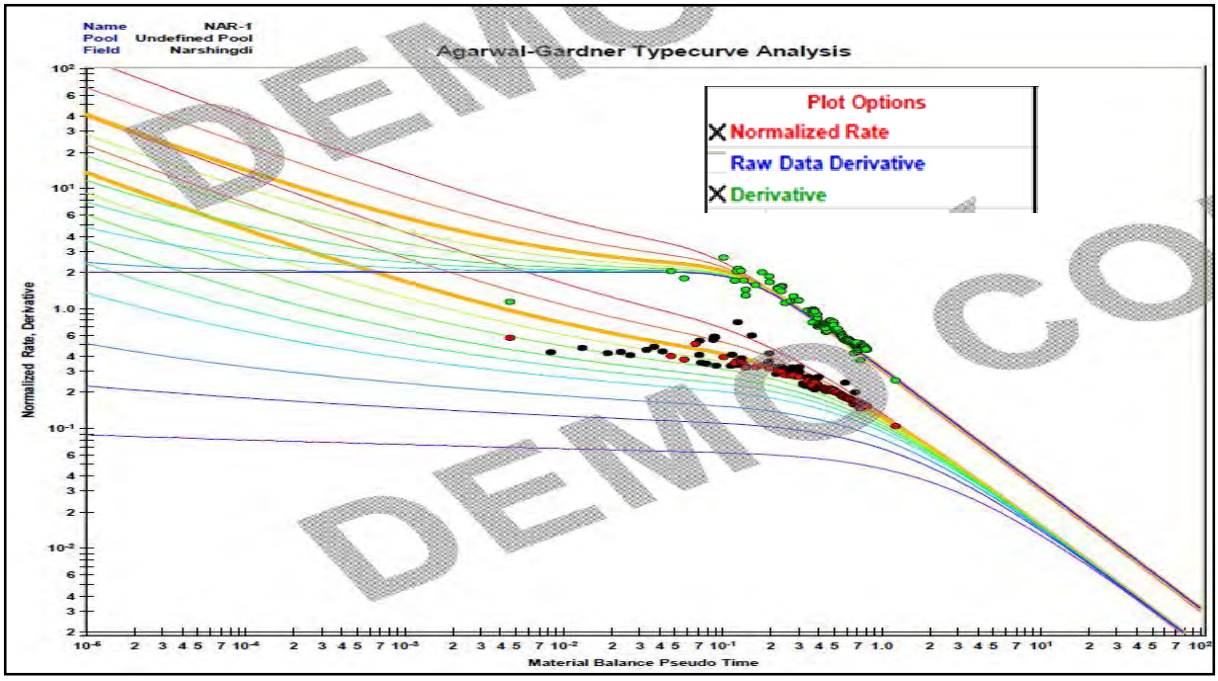

Figure 7.2: Agarwal-Gardner Type curve analysis for NAR-1

The results of Agarwal-Gardner type curve analysis are summarized in Table 7.2

Table 7.2 Results of the Agarwal type curve analysis

Parameter	Result
GIIP	284.241 (BCF)
Reservoir Area	9932 (Acre)
Pab (abandonment pressure)	1000 (psia)
RF	72.41 %
EUR	205.814 (BCF)

In this Agarwal-Gardener type curve analysis Figure 7.2 normalized rate and derivative was used to calculate GIIP, reservoir drainage area, ultimate recovery and recovery factor.

7.4 NPI Type Curve Analysis

Normalized pressure integrals (NPI) are well test style type curve analysis with integration for data smoothing. In NPI type curve analysis the normalized pressure, pressure integral and pressure integral derivative are plotted vs. material balance time data on log-log scale of the same size as the type curves. This data plot was moved over the type curve plot, while the axes of the two plots were kept parallel until a good match was obtained. The boundary dominated stem that is located at the right side of the plot was used to calculate GIIP, reservoir drainage area, RF and EUR. The plot is shown in Figure 7.3

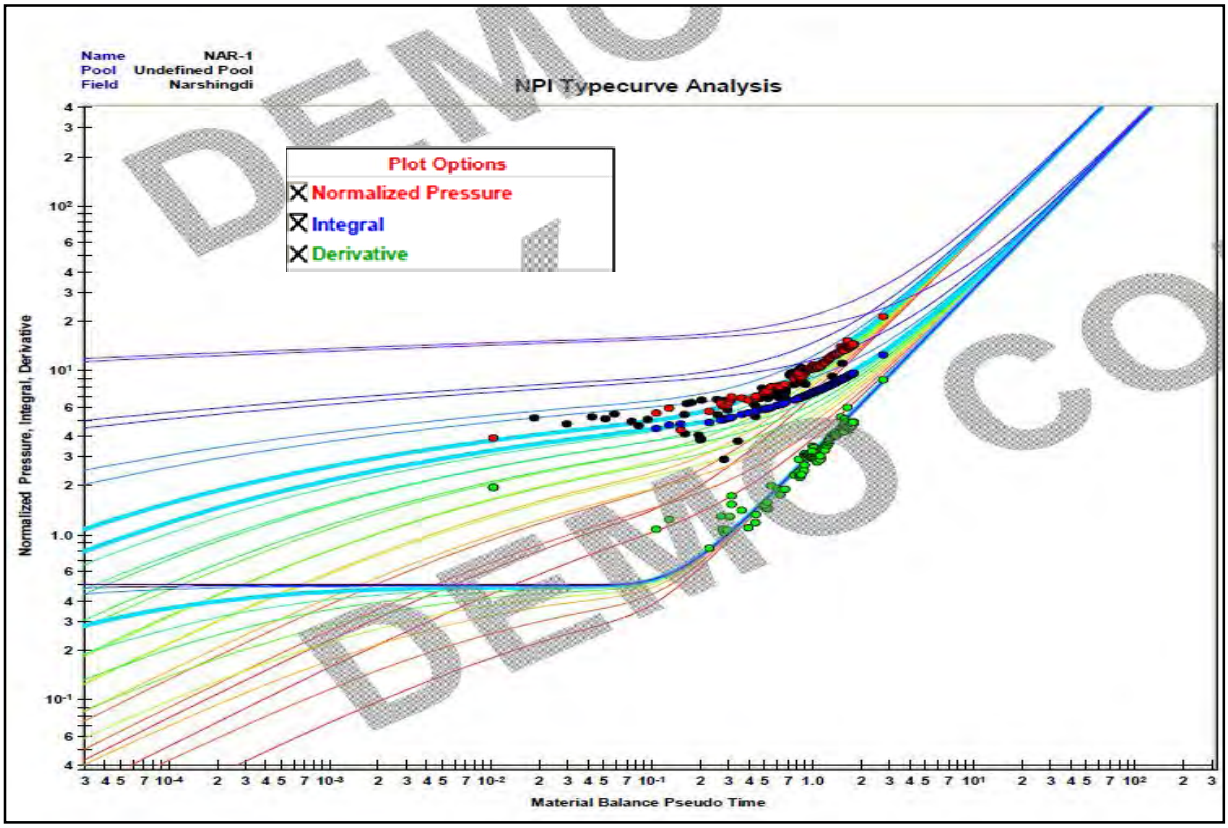

Figure 7.3: NPI Type curve analysis for NAR-1

The results of NPI type curve analysis are summarized in Table 7.3

Table 7.3 Result of the NPI type curve analysis

Parameter	Result
GIIP	280 (BCF)
Reservoir Area	9782 (Acre)
Pab (abandonment pressure)	1000 (psia)
RF	72.41 %
EUR	202 (BCF)

The estimated parameters from various type curves are almost similar. The small variations in the result were due to decline curve analysis and the fact that type curve matching of gas well decline curves requires observed data from the wellbore (bottom hole pressure) whereas the available pressure data was flowing tubing head pressures. For well no NAR-1, the three different techniques of R.T.A analysis shows that the Gas Initially in Place is around 280 BCF and the ultimate recovery of gas is about 200 BCF at a recovery factor of 72.41% for the abandonment tubing head pressure 1000 psia. The ultimate recovery factor will increase if we can lower the abandonment pressure. The drainage area calculated using the type curve analysis is within in the range of drainage area used in volumetric method for Monte Carlo simulation.

NAR-2

7.5 Blasingame Type Curve Plot

In case of NAR-2 same procedure was followed that was followed in NAR-1. The type curve analysis plot is shown in Figure 7.4

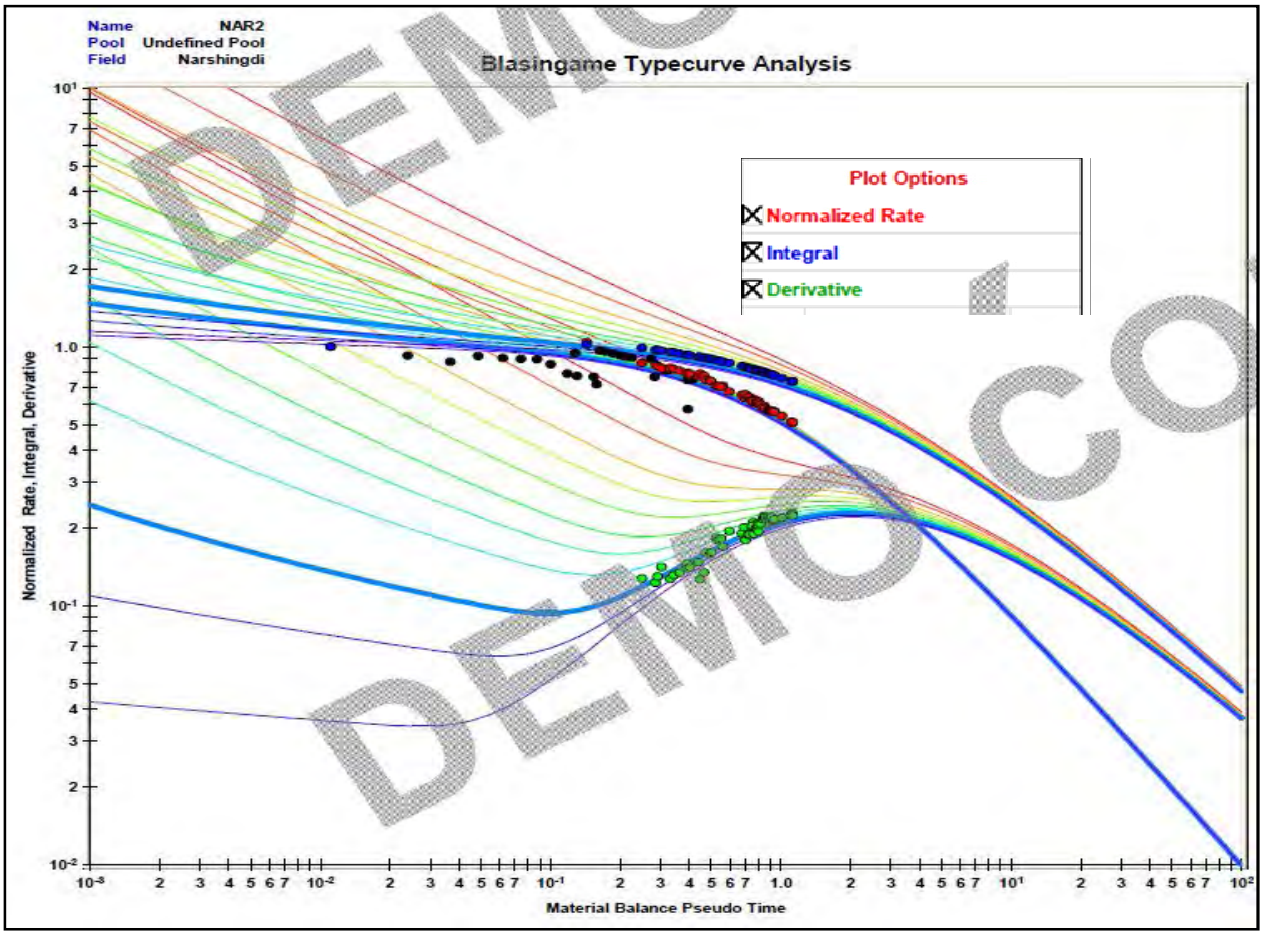

Figure 7.4: Blasingame Type curve analysis for NAR-2

The results are summarized in Table 7.4

Table 7.4 Results of the Blasingame type curve analysis for NAR-2:

Parameter	Result
Well type	Vertical well
GIIP	131 (BCF)
Reservoir Area	4942 (Acre)
Pab (abandonment pressure)	1000 (psia)
RF	67.34 %
EUR	88(BCF)

7.6 Agarwal-Gardner Type Curve

The Agarwal-Gardener type curve analysis plot is shown in Figure 7.5

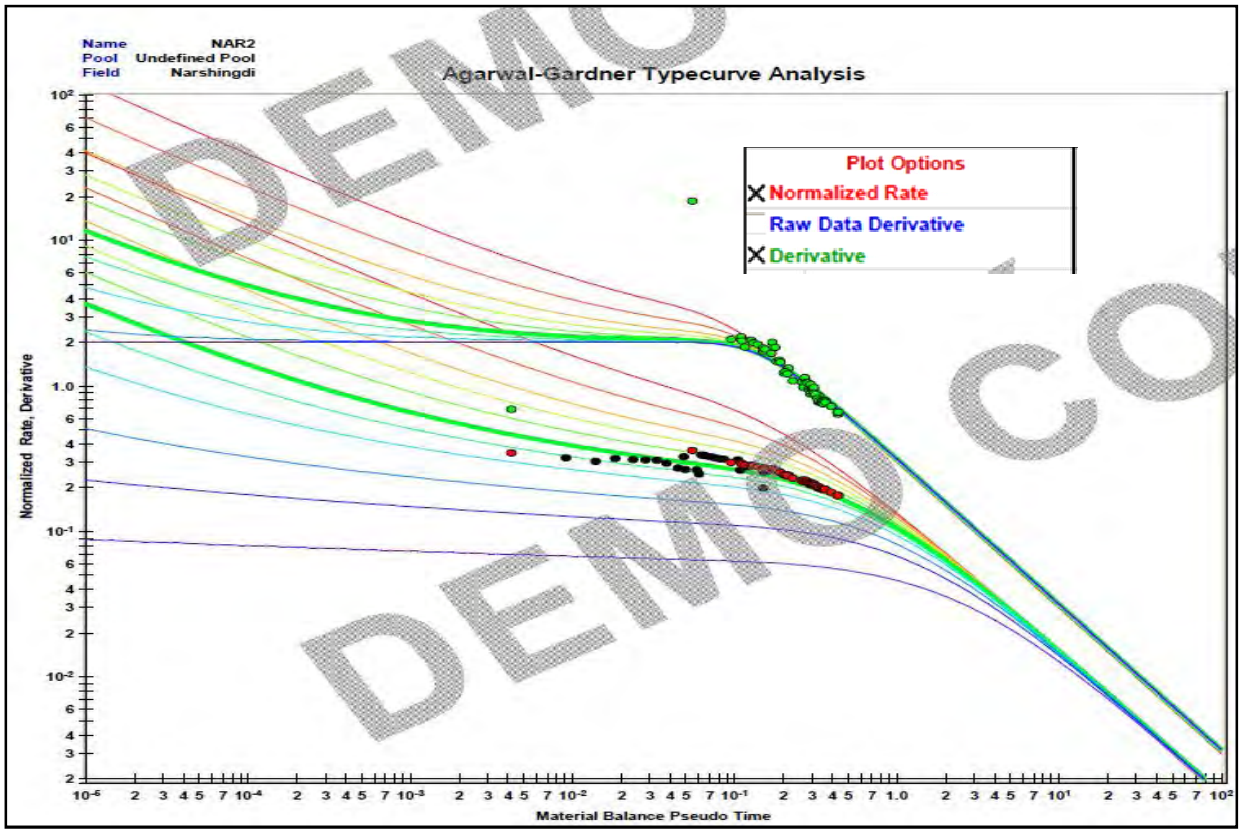

Figure 7.5: Agarwal-Gardner Type curve analysis for NAR-2

The results are summarized in Table 7.5

Table 7.5 Results of the Agarwal-Gardner type curve analysis for NAR-2:

Parameter	Result
GIIP	137 (BCF)
Reservoir Area	5174 (Acre)
Pab (abandonment pressure)	1000 (psia)
RF	67.34 %
EUR	92.638 (BCF)

7.7 NPI Type Curve

NPI type curve analysis plot is shown in Figure 7.6

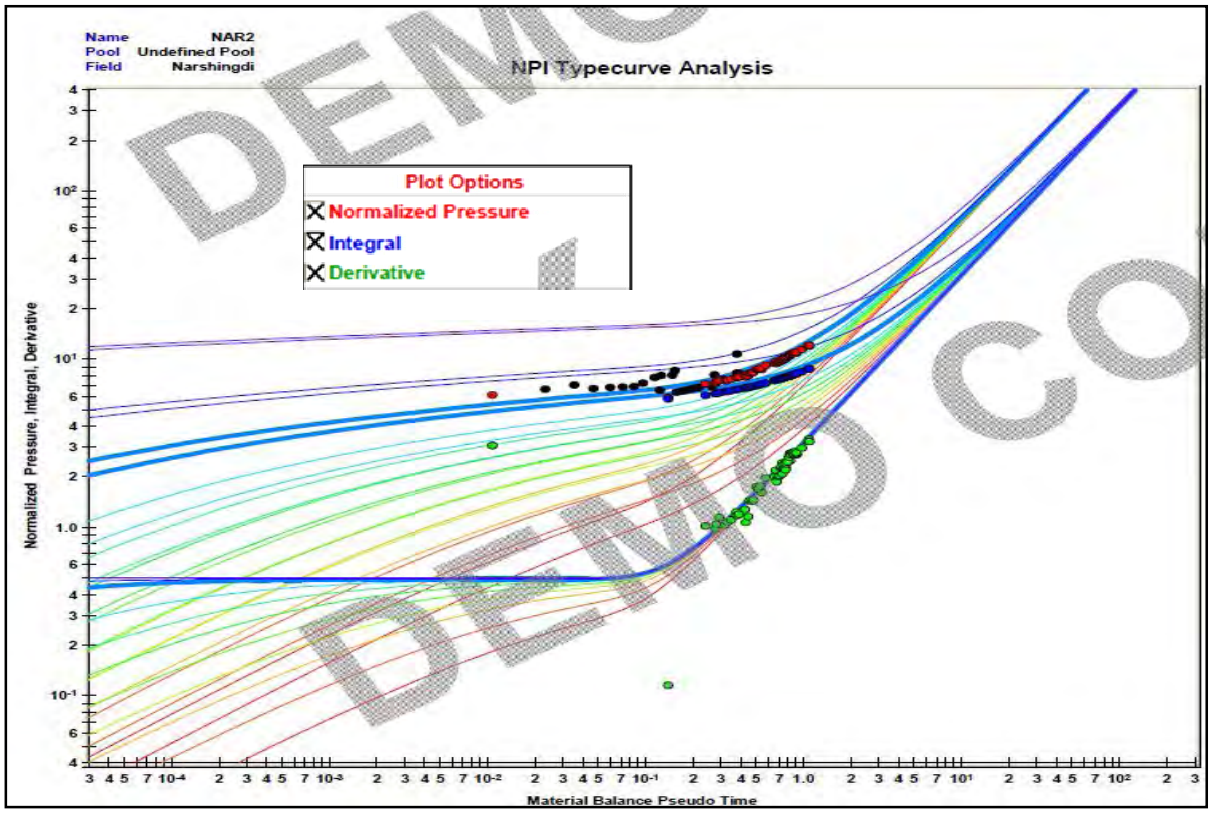

Figure 7.6: NPI Type curve analysis for NAR-2

The results of NPI type curve analysis are summarized in Table 7.6

Table 7.6 Results of the NPI type curve analysis for NAR-2:

Parameter	Result
GIIP	133 (BCF)
Reservoir Area	5018 (Acre)
Pab	1000 (psia)
RF	67.34 %
EUR	89.85 (BCF)

For NAR-2, the three different techniques of advanced decline curve analysis shows that the Gas Initially in Place is around 130 BCF and the ultimate recovery of gas is about 90 Bscf at a recovery factor of 67.34% for the abandonment tubing head pressure 1000 psia. The ultimate recovery factor will increase if we can lower the abandonment pressure.

Result from Topaze Software: Software Topaze (Kappa, Ecrin V4.12.04) was also used for advanced decline curve analysis. The type curves analyses are summarized here.

NAR-1

7.8 Blasingame Type Curve

The plot is shown in Figure 7.7

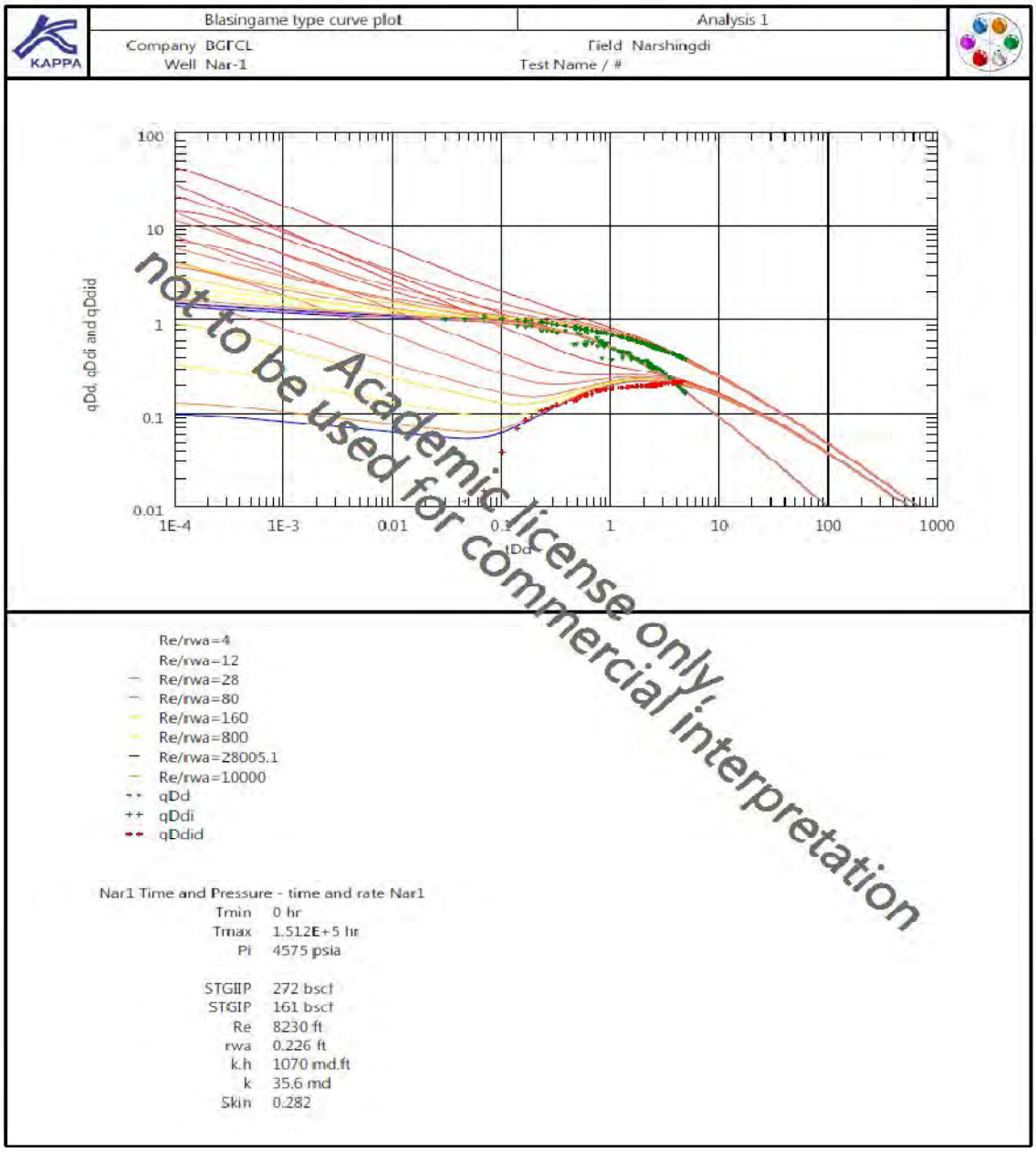

Figure 7.7: Blasingame type curve plot.

The Blasingame type curve analysis shows that the average permeability of the reservoir is 35.6 md and this value of permeability is well agreed with the value that was found from the

reservoir simulation study. The analysis also shows that the skin factor for NAR-1 is 0.282 and the value is not higher and suggests that it may not cause extra pressure drop in the well bore.

7.9 Blasingame Plot

The x axis of the Blasingame type curve (Figure 7.8) is an equivalent time and the plotted channels are triangle in green is an instantaneous productivity index, with plus sigh in green is the integral of the previous function divided by the time and with plus sign in red, the derivative of pressure integral with respect to the log of equivalent time.

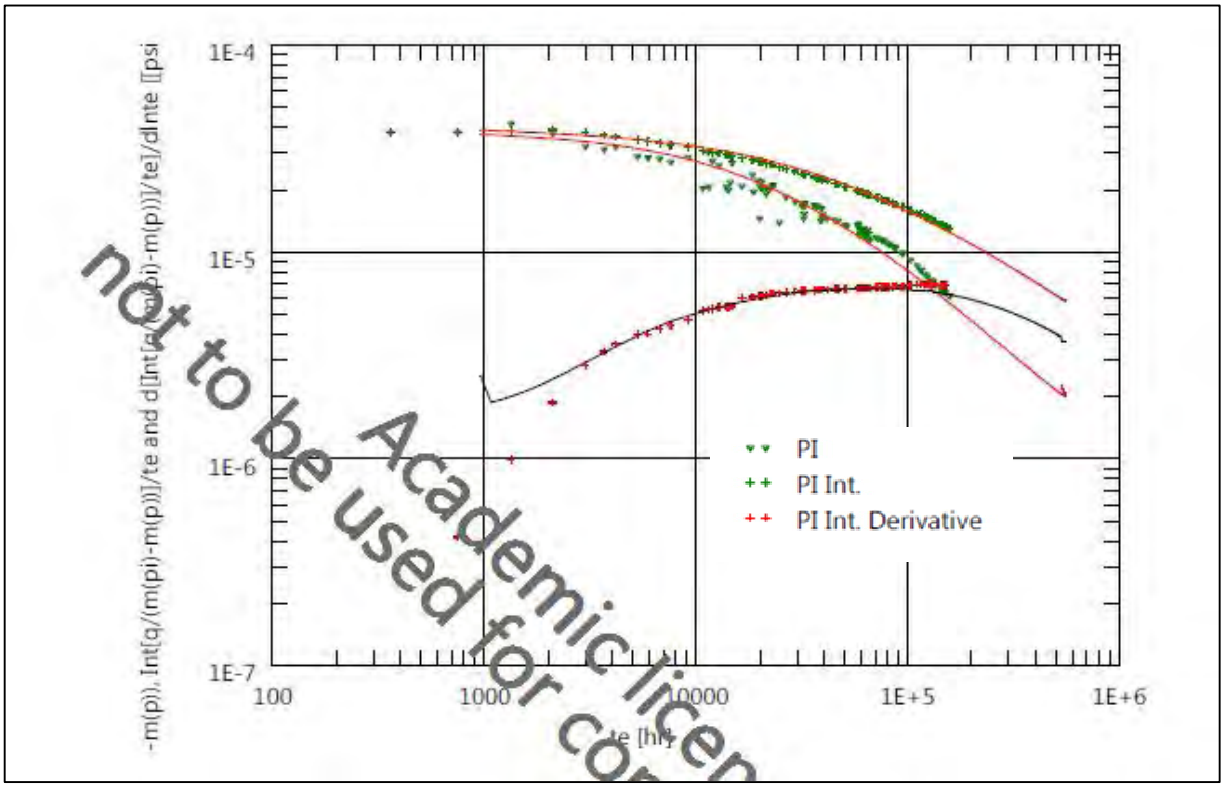

Figure 7.8: Blasingame plot.

Table 7.7 Main model parameters for Blasingame plot from Topaze:

Selected model Standard model, Material Balance	Well Vertical	Reservoir Homogenous	Boundary Circle, no flow
pi, initial pressure	4575 psia		
GIIP	292 BCF		
GIP	179 BCF		
K, average permeability	32 md		
S, skin factor	0.247		
Re-no flow	8520 ft		

7.10 Fetkovitch Type Curve Plot

In the Fetkovitch plot (Figure7.9), there are two sets of curves that converge in the centre. Matching data on the left side provides information about the transient behavior of the system while the right side provides information about the boundary dominated behavior of the reservoir (reserves, area). Fetkovitch methodology was designed to analyze transient and boundary dominated flow at a constant bottom hole pressure but in case of this analysis the pressure was variable so the matching obtained here was not so good.

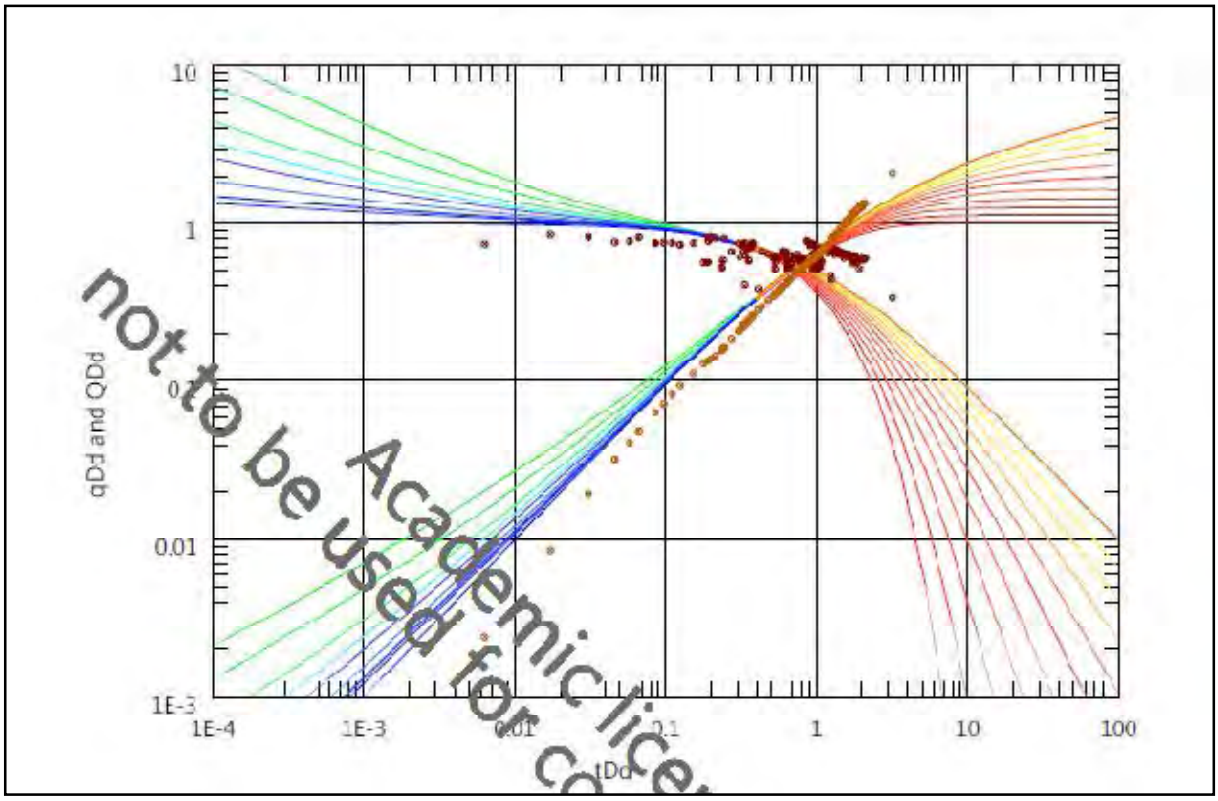

Figure 7.9: Fetkovitch type curve plot for NAR-1.

The main model parameters are summarized in Table 7.8

Table 7.8 Main model parameters for Fetkovitch Type Curve plot from Topaze

Selected model Standard model, Material Balance	Well Vertical	Reservoir Homogenous	Boundary Circle, no flow
b, decline exponent	1		
GIIP	282 BCF		
GIP	172 BCF		
pi, initial pressure	4575 psia		
Re-no flow	8390 ft		
S, skin factor	0.123		

7.11 Log-Log Plot

The log- log plot is almost an inverted Blasingame plot. The x-axis is the equivalent time (Figure 7.10), and in the y axis with plus sign in green is the integral of a rate normalized pressure, divided by time. With plus sign in red is the derivative of the previous function with respect to the log of equivalent time.

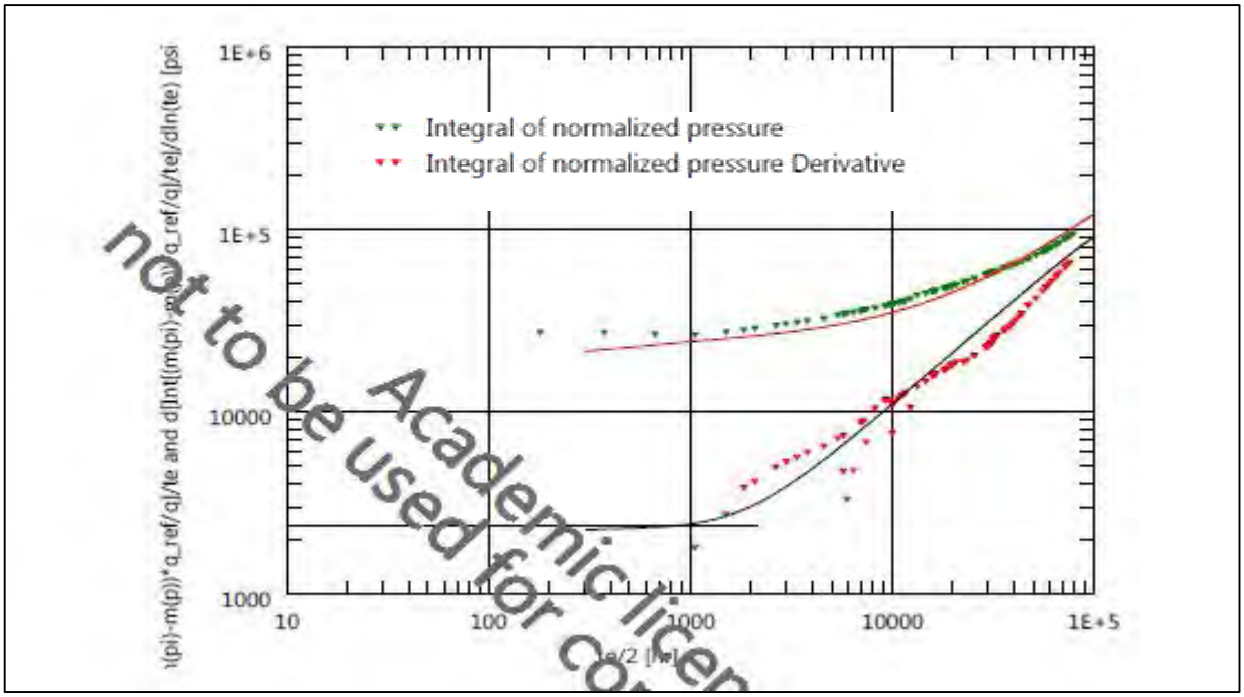

Figure7.10: Log-Log plot.

The main model parameters are summarized in Table 7.9

Table 7.9 Main model parameters for Log-log plot from Topaze software:

Log log plot	Well	Reservoir	Boundary
	Vertical	Homogenous	Circle, no flow
pi, initial pressure	4575 psia		
GIIP	282 BCF		
GIP	170 BCF		
Re-no flow	8380 ft		

Different procedure like Blasingame plot, Blasingame type curve plot, Fetkovitch type curve plot, Log-Log plot were used to calculate the same parameters calculated from the Fekete R.T.A. The different technique shows that the Gas Initially in Place is about 280 BCF and it varied here ±10 BCF. The Blasingame type curve plot shows that the average permeability is 35.6md and the skin factor is 0.282.

NAR-2

7.12 Arps Decline

The formulas of Arps decline curve provide a powerful and practical tool for production forecast. Depending on the value of b (decline exponent) there are three commonly recognized types of decline curves, each of this has the separate mathematical form that is related to the second factor, which characterizes a decline curves, that is the curvature. These types are referred as Exponential decline, Harmonic decline and Hyperbolic decline. Arps decline plot is shown in Figure 7.11

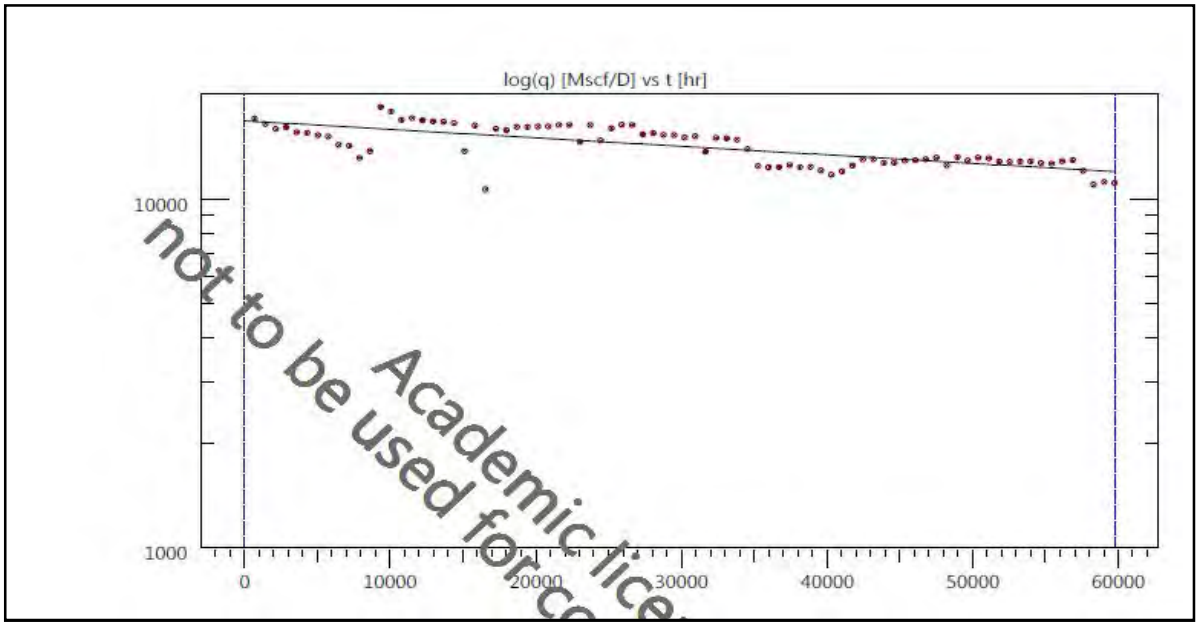

Figure 7.11: Arps plot for NAR-2

Table 7.10 Main model parameters for Arps decline curve

Model name	Arps model
b, decline exponent	0
Q(ta)	124 BCF
Reserve at maximum time	88.9 BCF
qi, initial rate	16.7 MMscf/d
Di, decline rate	1.35E-4 $[Day]^{-1}$

The decline exponent b=0 suggests that the decline type for NAR-2 is exponential decline/constant percentage decline.

7.13 Blasingame Type Curve Plot:

Blasingame Type curve analysis plot is shown in Figure 7.12

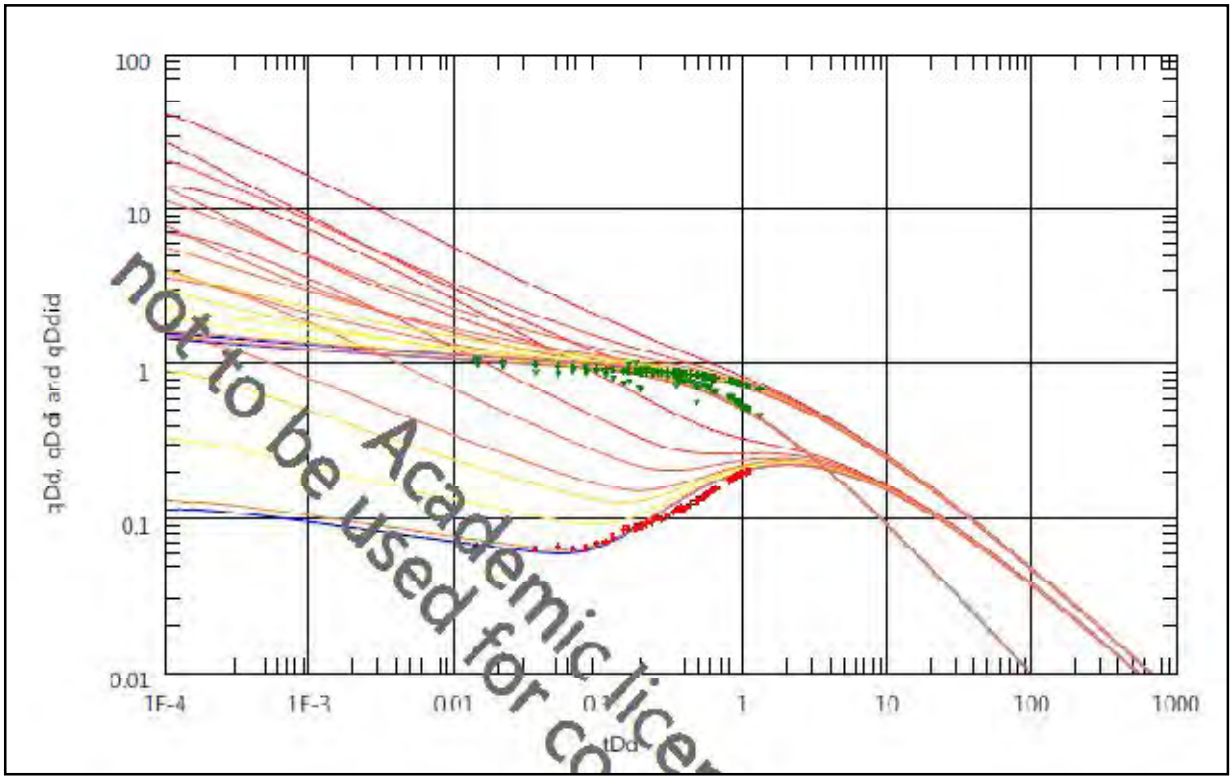

Figure 7.12: Blasingame type curve plot for NAR-2

Table 7.11 Main model parameters of Blasingame type curve plot from Topaze software for NAR-2

Model name	Blasingame type curve plot
b, decline exponent	0
GIIP	133 BCF
GIP	98.5 BCF
qi, initial rate	16.7 MMscf/d

The decline exponent of the Blasingame type curve analysis also suggests that the decline type is constant percentage decline for NAR-2. The Blasingame type curve plot shows that the GIIP for NAR-2 is 133 BCF that is 9 BCF higher than the GIIP 124 BCF calculated from Arps decline curve.

7.14 Fetkovitch Type Curve

The Fetkovitch type curve plot is shown in Figure 7.13

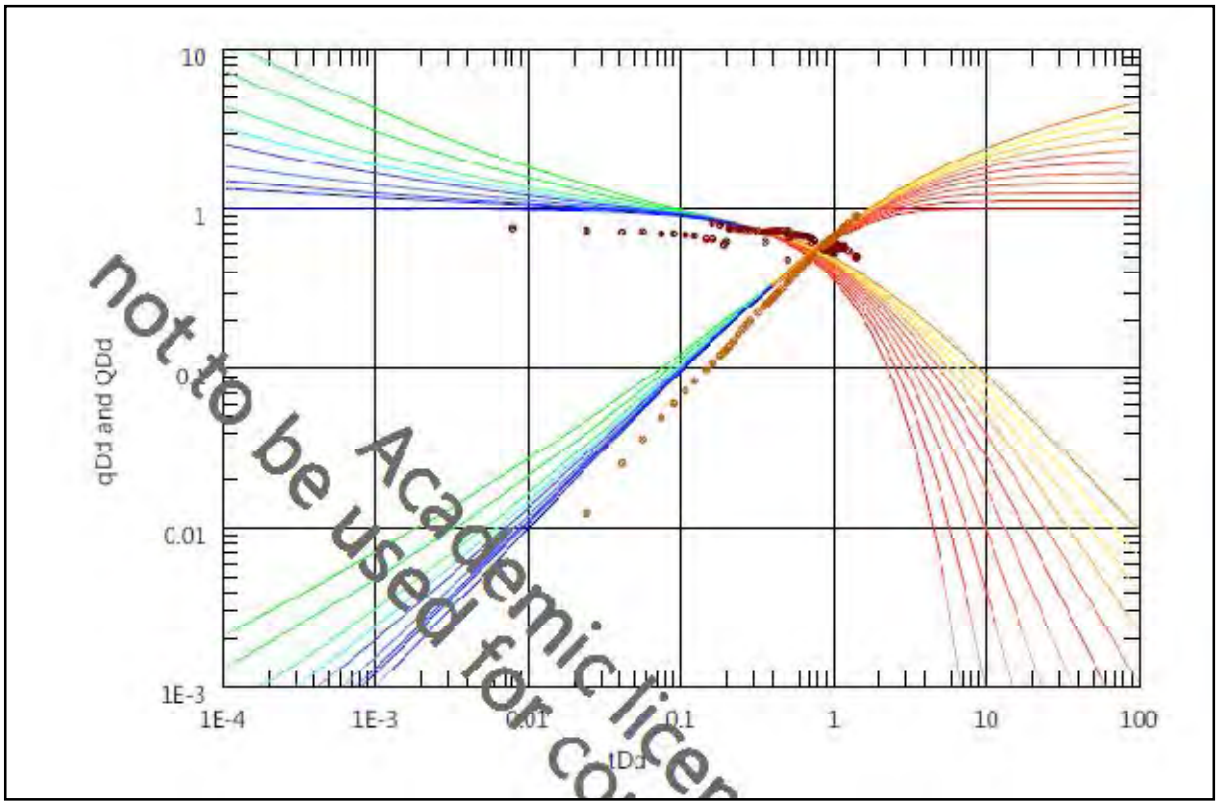

Figure 7.13: Fetkovitch type curve plot for NAR-2

Table 7.12 Main model parameters of Fetkovitch Type curve plot for NAR-2 from Topaze software

Model name	Fetkovitch type curve plot
b	0.5
GIIP	129 BCF
GIP	94.4 BCF
pi, initial pressure	3552.11 psia

The above graphical representation of different techniques for the well NAR- 2 shows that the Gas Initially in Place is about 130 BCF. So the result has a good match with the result that is found from the Fekete software.

CHAPTER 8

RESERVOIR SIMULATION

History matching is the process of adjusting the reservoir geological model to match the model from field production data. Reservoir production performance greatly determines the economic feasibility of oil and gas recovery and also the future sustenance of production operations. Thus, for efficient reservoir management, a thorough analysis of past, present and future reservoir performance is required, and history matching is a very handy tool for this.

Objectives of simulation study

- History matching of the reservoir pressure and well tubing head pressure
- Estimating the GIIP for UGS, LGS and field total
- Estimating the recoverable reserve at an abandonment tubing head pressure 1000 psia
- Analyzing the percentage increase of recoverable reserve and recovery factor at an abandonment tubing head pressure 500 and 100 psia using the compressor
- Analyzing the effect of adding one more vertical well in the LGS

Simulation Assumptions

- The wells NAR-1 and NAR-2 are producing from the LGS and both of the wells are vertical.
- There is no production yet from the UGS
- The production history of NAR-1, July 1996 to December 2013 and NAR-2, February 2008 to December 2013 was used as an input data
- Prediction of gas production was made from January 2014 to July 2030 for both wells for different abandonment tubing head pressure and economic rate

8.1 Geological Model

The geological model of Narshingdi gas field was collected from Petrobangla. The model was built using PETREL^{TM}. The input data to build the geological model involves integrating seismic interpretation, geological correlation of the wells and petrophysical data. In order to create the structural model both the top and base of the reservoir units were modeled in the make horizons process. Petrophysical properties modeled across the field were net to gross, as a binary property, effective porosity, permeability and water saturation. These were

modeled using the Sequential Gaussian Simulation (SGS) algorithm within PETREL™. Shales were given a porosity and permeability value of zero and water saturation of one. The model grid consists of 101, 147, 29 blocks to represent four sand layer of the field. The dimension of each block is 328×328 ft grid blocks. The gas zone is divided into two layers, upper gas sand (UGS) and lower gas sand (LGS). The zones are separated by middle gas sand-1 and middle gas sand-2. The 3D view of Narshingdi gas field is shown in Figure 8.1

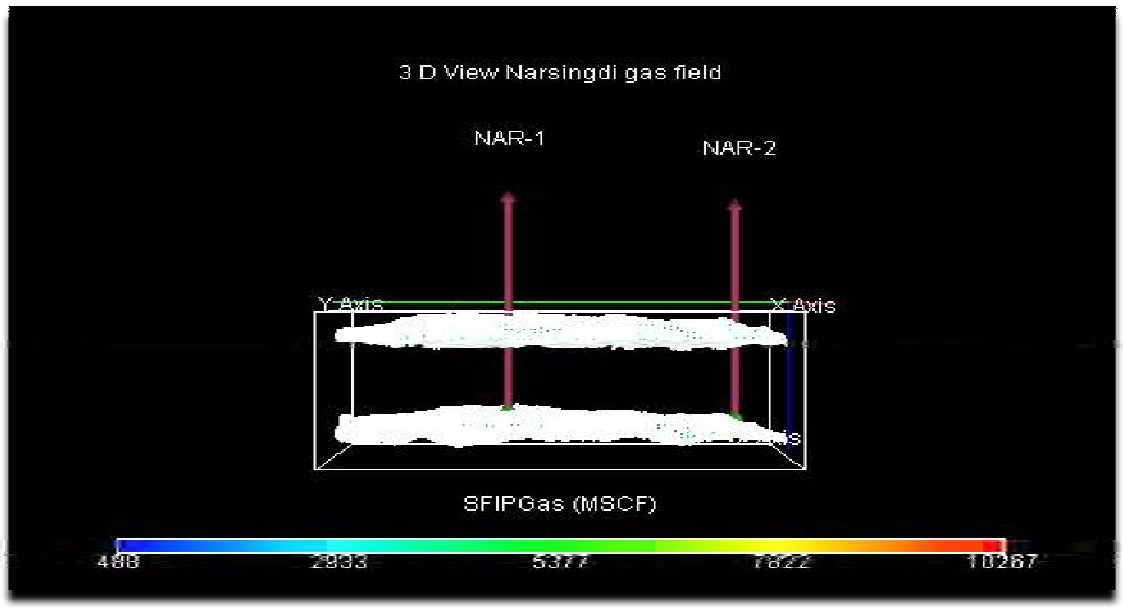

Figure 8.1: 3D view of Narshingdi gas field

Properties of the simulation layer are shown in the Table 8.1.

Table 8.1 Properties of Simulation Layer

Sand layers	Simulation layers	Porosity (%)	Active/Inactive
Upper gas sand	1-4	0.15-0.22	Active
Middle gas sand-1	5-15	-	Inactive
Middle gas sand-2	16-24	-	Inactive
Lower gas sand	25-29	0.07-0.22	Active

The porosity distribution in the LGS in the grid blocks is shown in the Figure 8.2

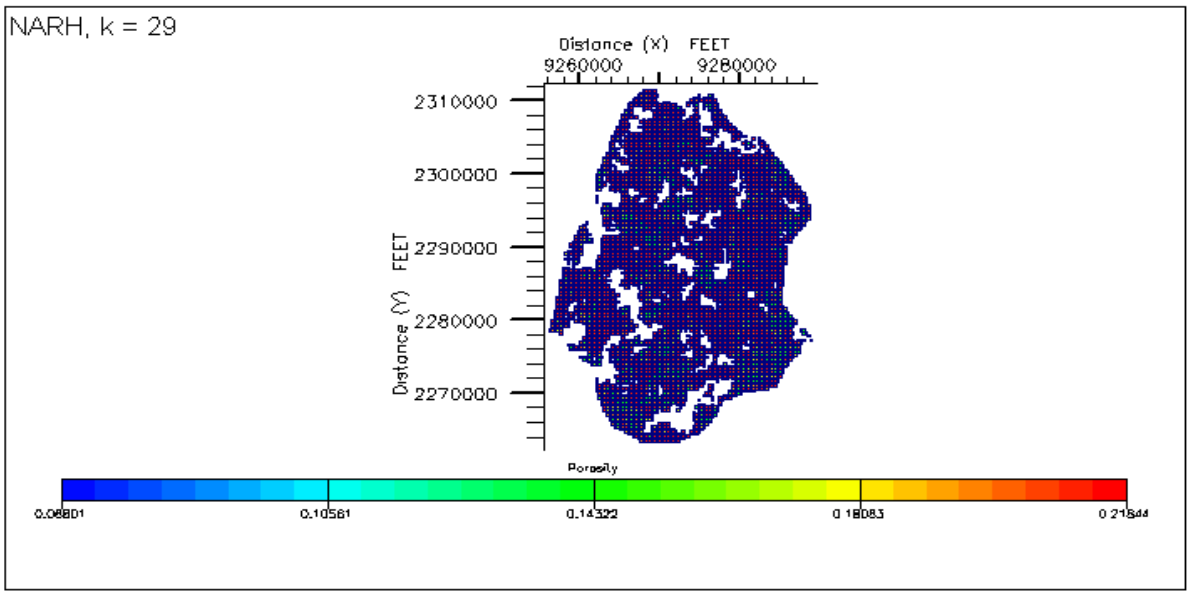

Figure 8.2: Porosity distribution in the lower gas sand

Permeability: The permeability distribution of the lower gas sand show that the range of permeability is 1-100 md and the permeability of upper gas sand is homogenous 77 md. The permeability distribution is shown in Figure 8.3

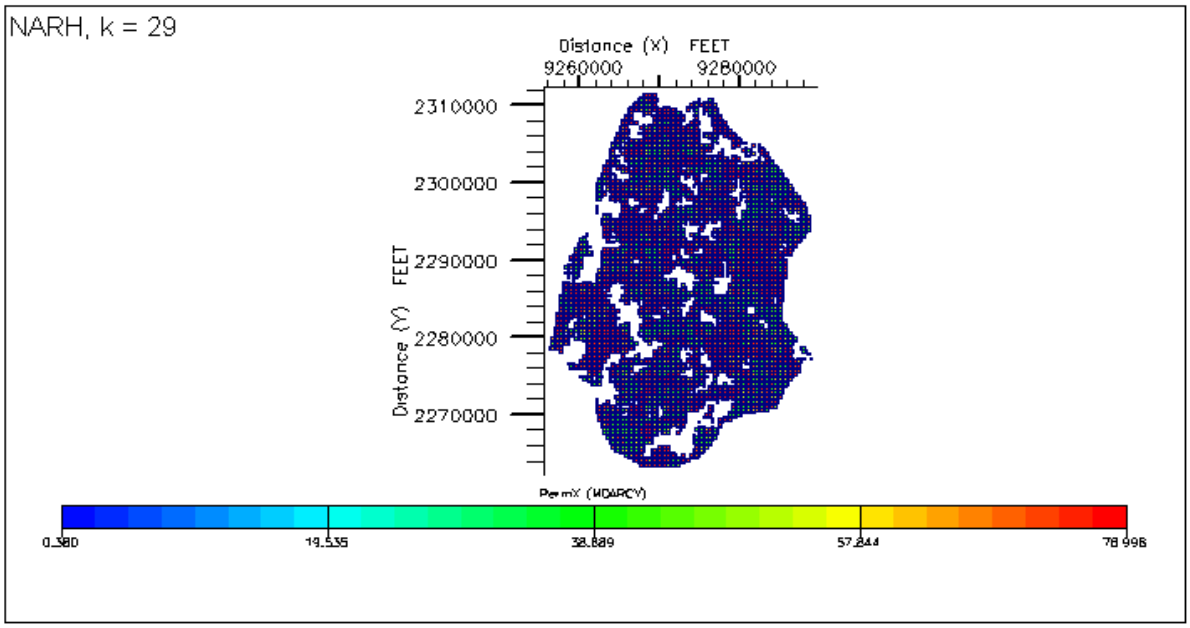

Figure 8.3: Permeability distribution in the X direction

8.2 Flowing and Shut in Pressure

Few shut in well head pressure data were measured during the period when production from the wells were suspended for encountering some production related problems. No shut in BHP (Bottom Hole Pressure) was measured. Available THP's were matched with historical data.

8.3 PVT

PVT properties are based on gas composition from production test-1 (NAR-1) in lower gas sand. The properties are shown in Table 8.2 and 8.3

Table 8.2 PVT properties of LGS

Property	Value	Unit
Initial reservoir temperature	205.8	^oF
Initial pressure of LGS	4274	Psia
Initial pressure of UGS	4054	Psia
Specific gravity	0.6	
Gas FVF at surface condition	228.84691	RB/MSCF
Gas viscosity at surface condition	0.0135	Cp
Gas density at surface condition	0.04645	Lb/ft^3

Table 8.3: Water PVT Properties

Property	Value	Unit
Density at surface condition	62.37	Lb/ft^3
Viscosity at surface condition	0.30123	Cp
Compressibility at surface condition	3.0749e-6	$Psia^{-1}$
FVF at surface condition	1.02736	Rb/stb

Rock compressibility: Rock compressibility was taken 3e-6 at pressure 3804 psia

Table 8.4: Gas composition for lower gas sand

Component	Molecular weight (lbm/lb mol)	Mol (%)
N_2	28.02	0.0034
H_2S	34.08	0
CO_2	44.01	0.0060
C_1	16.04	0.9479
C_2	30.07	0.0249
C_3	44.09	0.0060
iC_4	58.12	0.0020
nC_4	58.12	0.0015
iC_5	72.15	0.0007
nC_5	72.15	0.0006
C_6	86.17	0.0005
C_{7+}	109	0.0065
		Σ 1.0000

The variation in the value of gas formation value factor and viscosity with pressure are shown in the Figure 8.4

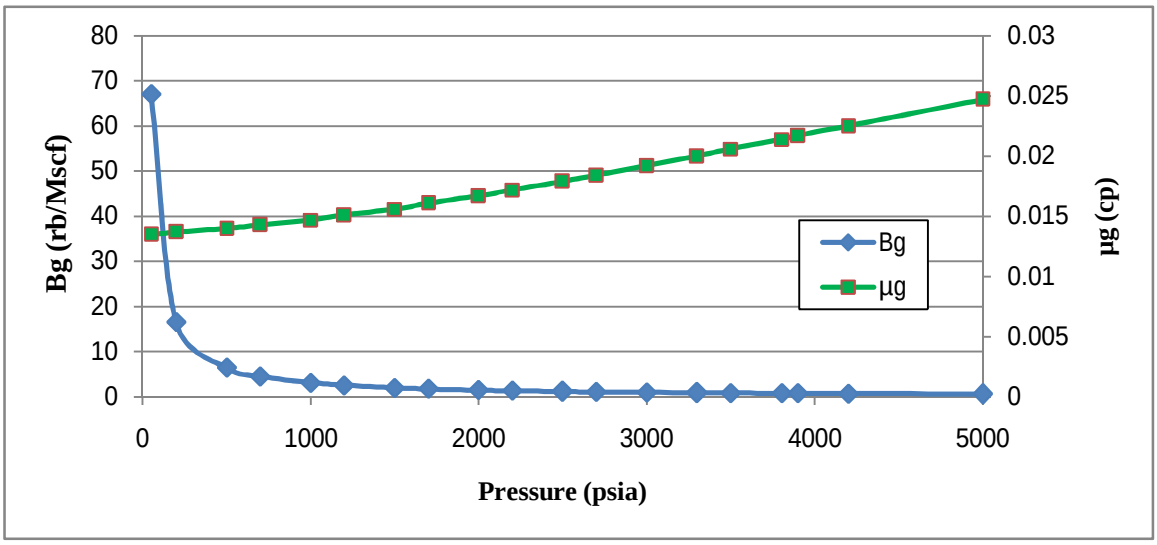

Figure 8.4: Properties of gas (Bg & μ_g) in the lower gas sand.

The relationship of compressibility factor and reservoir pressure is shown in the Figure 8.5

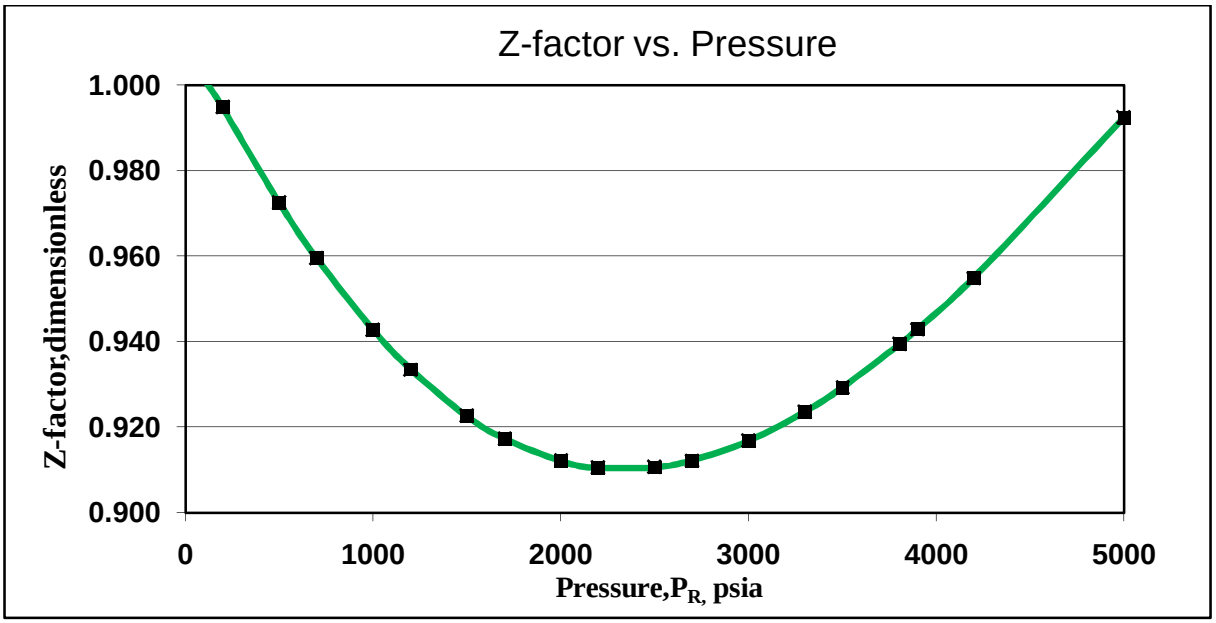

Figure 8.5: Z factor correlation in the lower gas sand

8.4 Relative Permeability and Saturation Data

No special core analysis (SCAL) has been performed on Narshingdi gas reservoir. Therefore no relative permeability saturation relationship data were available. The Figure 8.6 shows the variation of permeability with gas saturation. The data used here was generated using the Brooks-Corey's equation for two phase flow. It was assumed that the fluid is neither segregated nor evenly distributed by using a pore size distribution index of 2. This gives Corey exponent of 4 for water and 2 for the gas while calculating relative permeability. The endpoint saturation was based on the value of minimum water saturation in the model. The relationship is shown Figure 8.6

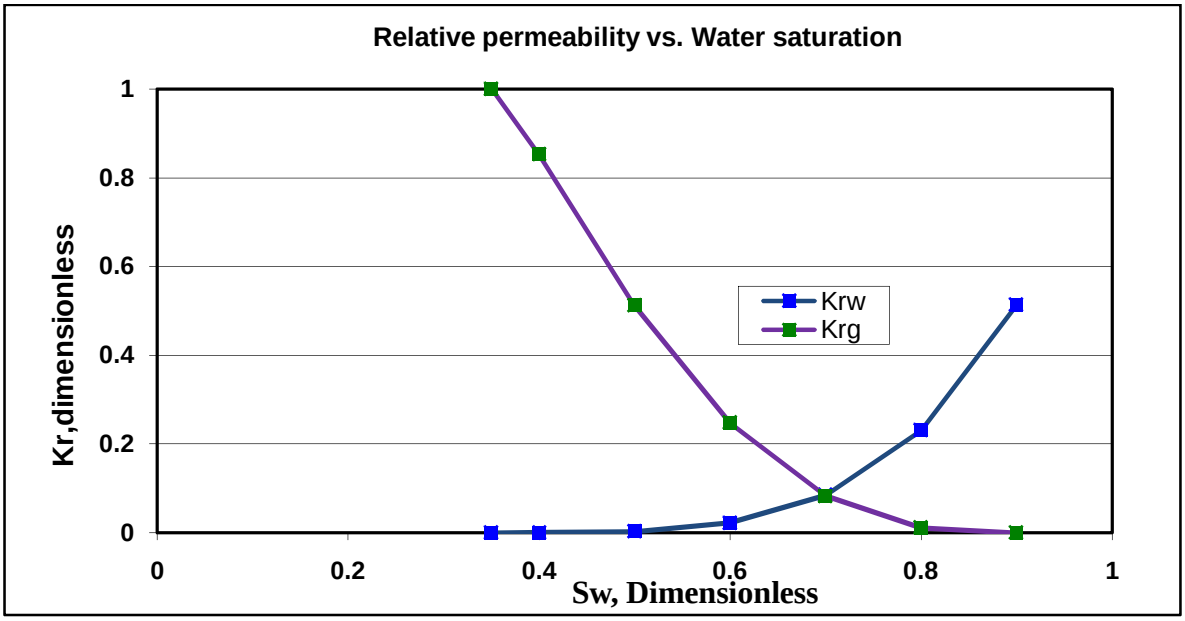

Figure 8.6: Relative permeability vs. Saturation curve.

8.5 Volumetric

The model has a minimum saturation of 0.35 based on the initial water saturation distribution, but there are many grid cells mostly isolated with higher initial water saturation above free water level. The net-to-gross ratio has been reviewed and modified by RPS to define each grid cells in the model as either sand or shale i.e. a two facieses model.

8.6 Well Performance

To calculate well head pressure for history match and production forecast vertical lift performance (VLP) curve has been generated using the software PROSPER for different flow rate and tubing head pressure. The minimum gas flow rate for continuous removal of liquid is approximately 4MMSCFD and 5MMSCFD for NAR-1 and NAR-2 respectively. This means that there will be well liquid loading at flow rates lower than the minimum. These minimum values have been used as the economic gas rates to forecast simulation runs.

8.7 Model Initialization and Stability

There is no Modular Formation Tester/ Repeat Formation Tester (MDT/RFT) pressure data for either the upper and lower gas sand to provide information on initial reservoir conditions, the initial condition for lower gas sand has been based on the November 2001 pressure build up analysis while the gas gradient of 0.08 psi/ft is assumed to estimate the initial reservoir

pressure for UGS. The lower gas sand has a snappy contact with shales and shows no indication of a gas water contact (GWC) based on Narshingdi log data. There is a gas down to (GDT) based at 10376 ftss which appears to be inconsistent with a GDT at 10531ftss. There remains uncertainty over the fluid contract in the lower gas sand. It has been estimated as 10396 ftss for history matching purposes using the deeper closing contour from the structure surface map which is between the GDT in NAR-1 and spill point.

8.8 History Match

The aim of history matching is to find a model which displays a minimal difference between the performance of the model and the production history of a reservoir. The history match process is iterative and validates the hydrocarbon volume present in the reservoir. The following parameters were history matched

- Average Reservoir Pressure (or static bottom hole pressure)
- Tubing head pressure for each well

History matching parameters:

- Pore volume: The initial simulation run showed a good pressure match for NAR-1 but a large deviation for NAR-2. A change in pore volume was considered to get a better history match for both NAR-1 and NAR-2. The pore volume was changed several times; finally a 7% increase in the pore volume of the LGS produced a better pressure match for the both wells.
- Permeability: Values of permeability was adjusted to improve the pressure history of the wells (NAR-1 and NAR-2). The vertical to horizontal permeability ratio 0.1 was used for the better match.
- Fluid contact: Several modifications were made in the fluid contact level. Finally the contact was lowered 20 ft. to match the production behavior.

8.9 Average Reservoir Pressure Match

The recorded shut in well head pressure was converted to shut in bottom hole pressure using the average temperature and Z factor method (Appendix 1) and these data were matched to the simulated reservoir pressure, and match is reasonably good. The match is shown in Figure 8.7

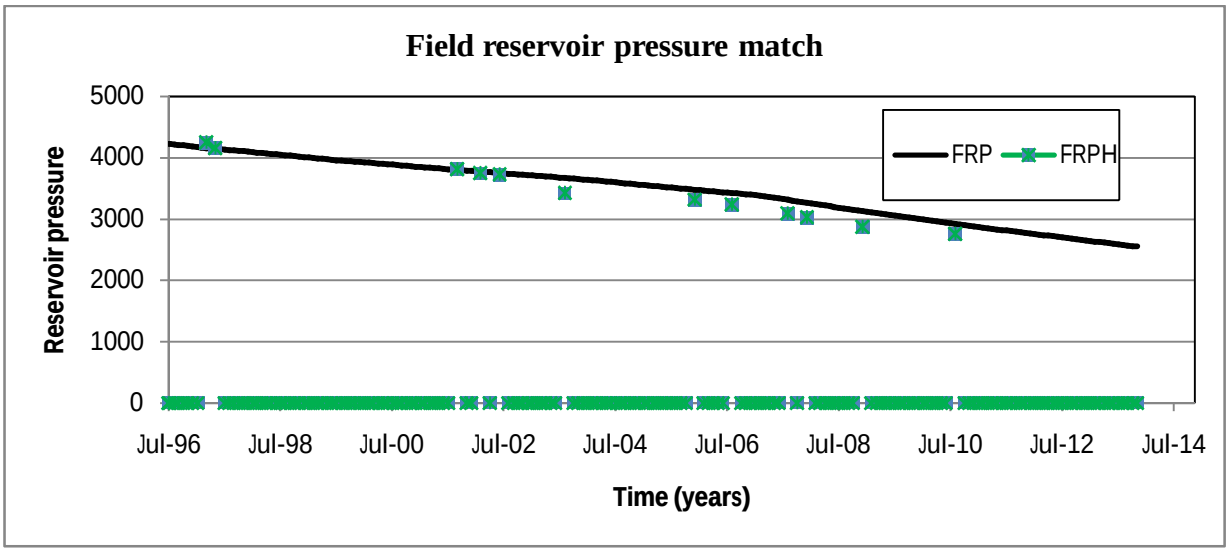

Figure 8.7: Field reservoir pressure match

8.10 Tubing Head Pressure Match

The historical tubing head pressure data was matched with the simulated tubing head pressure data for the both well NAR-1 and NAR-2. The match result is shown in Figure 8.8 and 8.9.

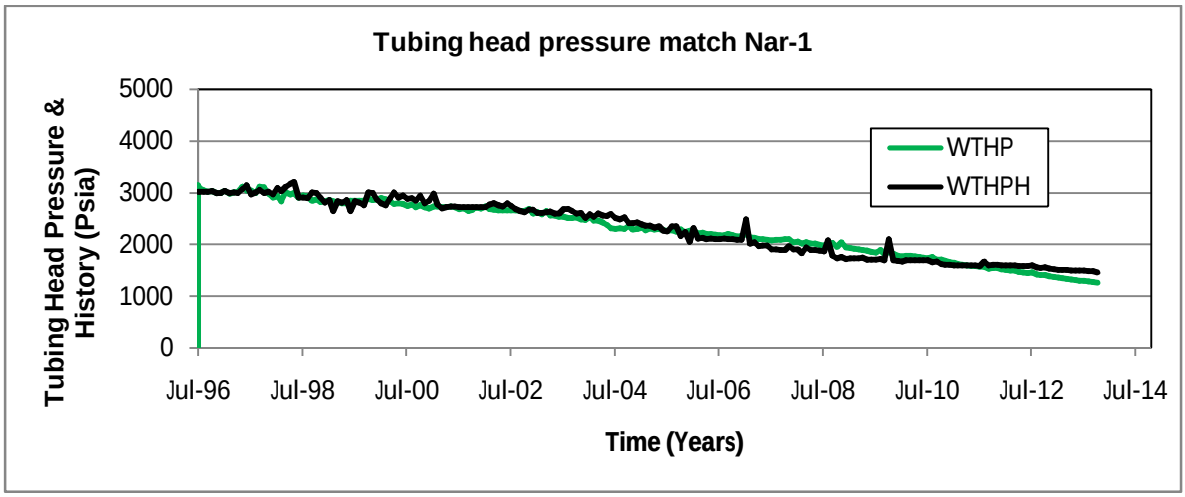

Figure 8.8: Tubing Head Pressure Match NAR-1

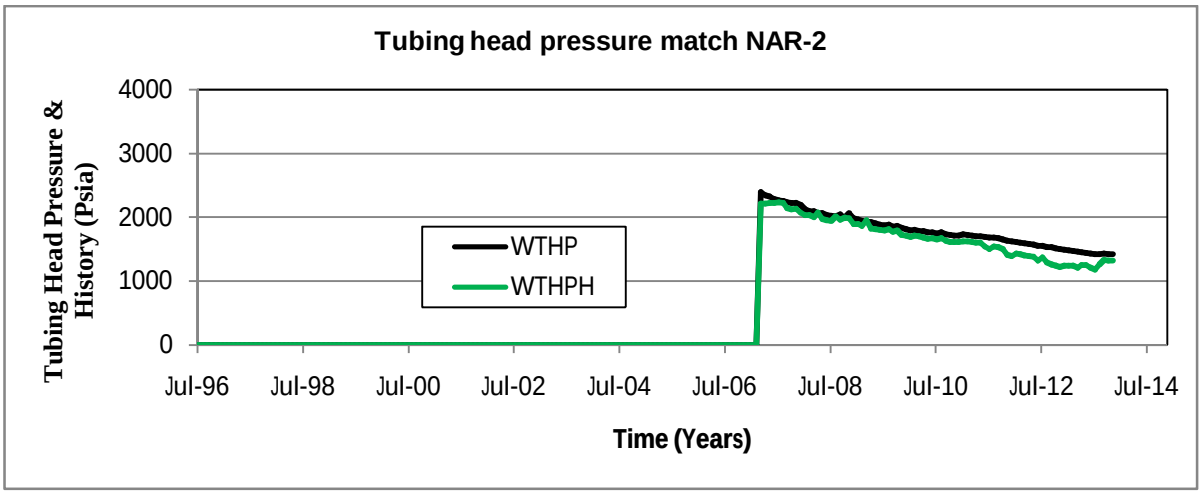

Figure 8.9: Tubing Head Pressure Match NAR-2

The tubing head pressure match for NAR-1 (Figure 8.8) is good. The peaks in well tubing head pressure history are due to the noise and not the original response of the reservoir. The tubing head pressure match for NAR-2 (Figure-8.9) shows that, the simulated tubing head pressure match is slightly higher than the history of tubing head pressure but the overall match is reasonably satisfactory.

8.11 Simulation Result

The GIIP calculated from the simulation for upper gas sand, lower gas sand and field total is shown in Figure 8.10. The Figure 8.10 shows that the GIP at zero time (GIIP) for UGS and LGS are 83.53 BCF and 302.72 BCF respectively. So the field total GIIP is 386.24 BCF. The Figure 8.10 also shows that field gas in place and the gas in place in the lower gas sand is decreasing as the two wells NAR-1 and NAR-2 are producing from the LGS. As the UGS is not producing so the GIP of UGS sand is unchanged. Up to December 2013, LGS produced 149 BCF gas so the GIP of LGS and field total are 153 and 233 BCF respectively.

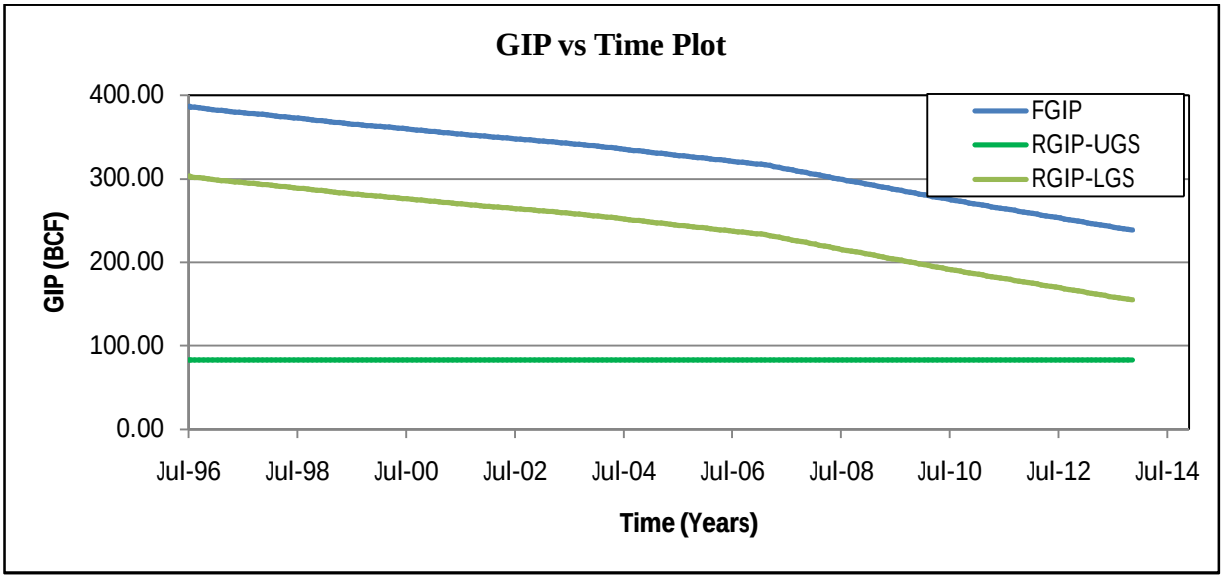

Figure 8.10: GIP vs Time plot for Field, LGS and UGS.

8.12 Forecasting

Two forecasting cases are considered to forecast the future performance of the LGS. These are

Case-1, Forecast do nothing:

The do nothing scenario is predicting future performance with the existing wells until the economic rates of the wells are reached. The economic limits for the two wells are NAR-1: 4 MMSCFD, NAR-2: 5 MMSCFD, and the tubing head pressure limit is 1000 psia.

Case-2, Impact of Additional Vertical Well:

In this prediction case, drilling of a new vertical well was considered to the lower gas sand to produce at a rate of 10 MMSCFD from the January 2015 with the two other wells (NAR-1 and NAR-2) peoducing at a rate of 18 and 15 MMSCFD. The economic limits for the three wells are NAR-1: 4 MMSCFD, NAR-2: 5 MMSCFD, NAR-3: 4 MMSCFD and the abandonment tubing head pressure limit is 1000 psia.

Effect of using compressor:

As the general abandonment tubing head pressure limit is 1000 psia, when the THP decreases than 1000 psia it requires associated pressure boosting to keep the flowing and to keep the sells line pressure requirements.

For both of the cases (Case1 and Case2) abandonment tubing head pressure was lowered to 500 psia and 100 psia to show the effect of using compressor on ultimate recovery.

Forecasting Case-1 Result: Figure 8.11 shows the production rates and field production total over the predicting years up to July 2030. Field gas production rate forecast shows that NAR-2 will shut in October 2019 due to minimum economic rate and the filed production rate will fall sharply. NAR-1 will produce up to January 2022, and at that time field gas production total will be 204.022 BCF.

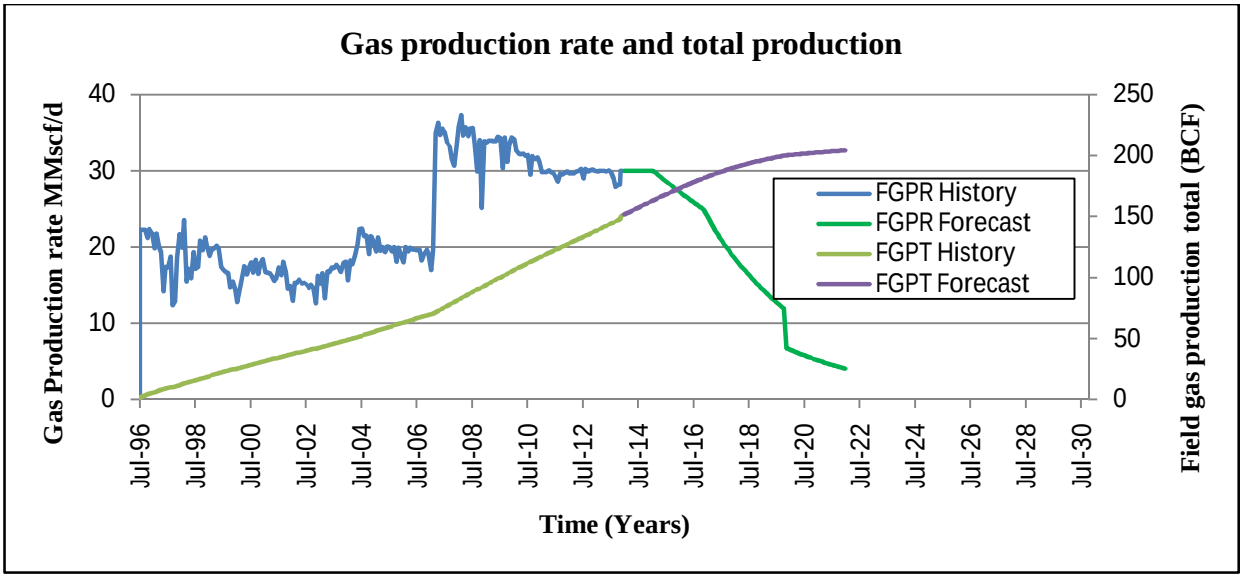

Figure 8.11: Forecasting do nothing production profile for THP 1000 psia

The Figure 8.12 shows the pressure behavior of the lower gas sand with respect to time. The figure confirms that the tubing head, bottom hole and reservoir pressure will decline as there is no pressure support in the lower gas sand.

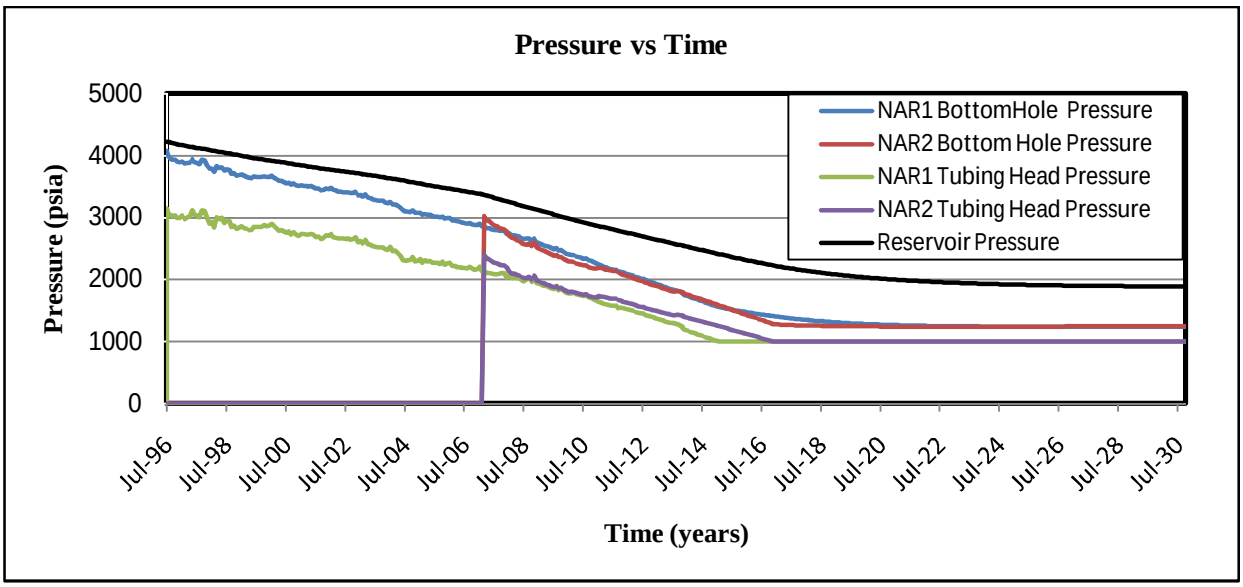

Figure 8.12: Forecasting do nothing pressure profile

8.13 Impact of Gas Compression for Case-1

The tubing head pressure limit was lowered to 500 psia to show the impact of gas compression on overall production. The Figure 8.13 shows that the overall production of lower gas sand will increase up to 38.573 BCF and then total production will be 242.595 BCF. In this case NAR-2 and NAR-1 will produce up to September 2023 and November 2026 to reach the economic rate limit.

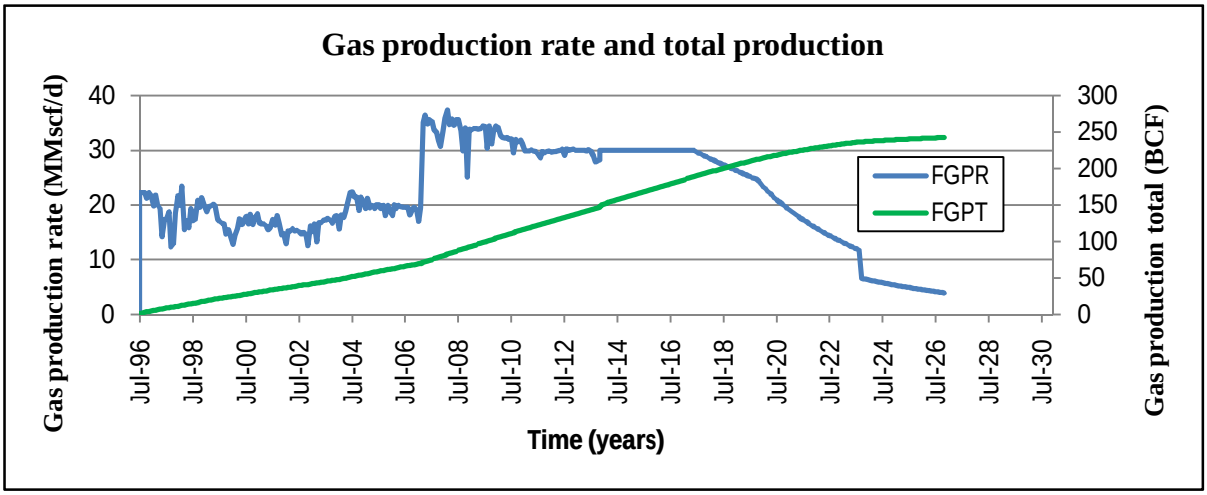

Figure 8.13: Field gas production rate and gas production total for THP 500 psia

The well head pressure was further lowered to 100 psia (Figure 8.14) and in this case the field gas production total for lower gas sand become 260.472 BCF and it means 56.45 BCF more gas will be produced than the do nothing scenarios. The Figure also shows that NAR- 2 and NAR-1 will produce up to August 2025 and 2029 respectively; the total production rate will fall sharply after August 2025 as NAR-2 will reach to the economic limit.

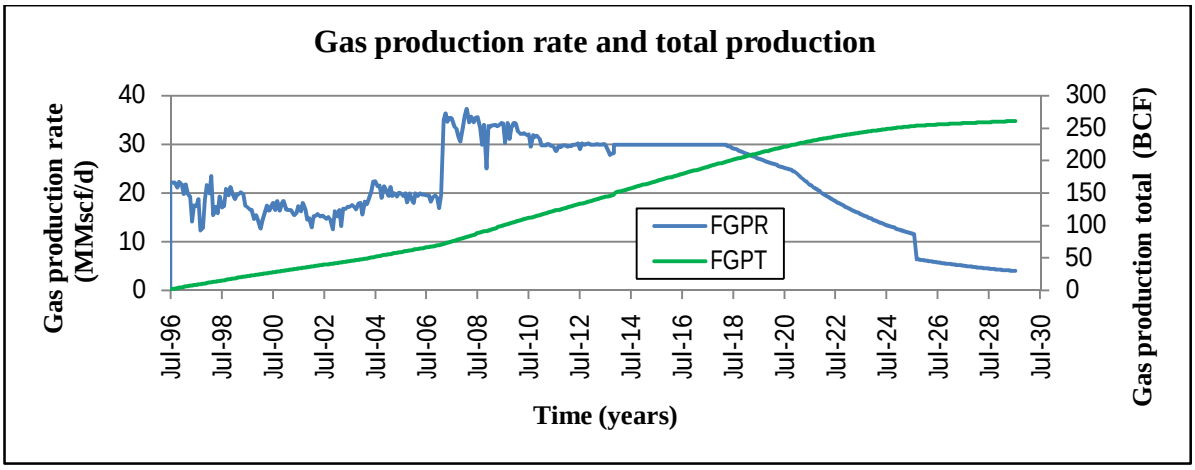

Figure 8.14: Field gas production rate and gas production total for THP 100 psia

The Figure 8.15 shows the field gas production rate for 1000 psia, 500 psia and 100 psia. The field life will increase if the pressure limit is lowered.

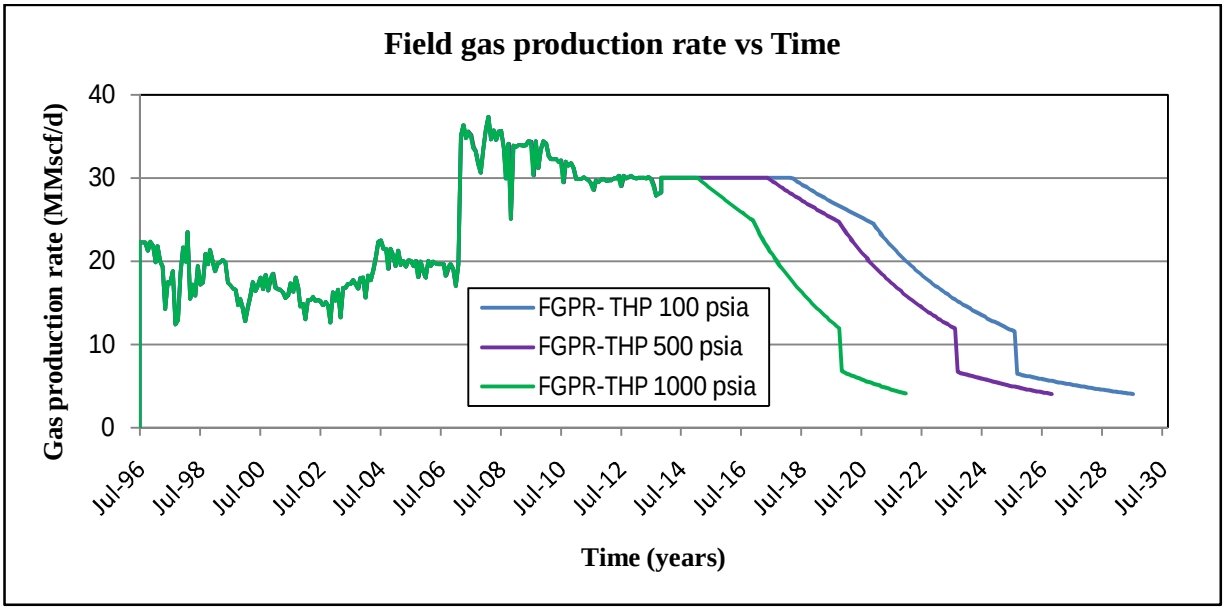

Figure 8.15: Field production rate for different tubing head pressure

Figure 8.16 shows that field gas production total is 204.02, 242.59 and 260.47 BCF for tubing head pressure limit 1000, 500, 100 psia respectively.

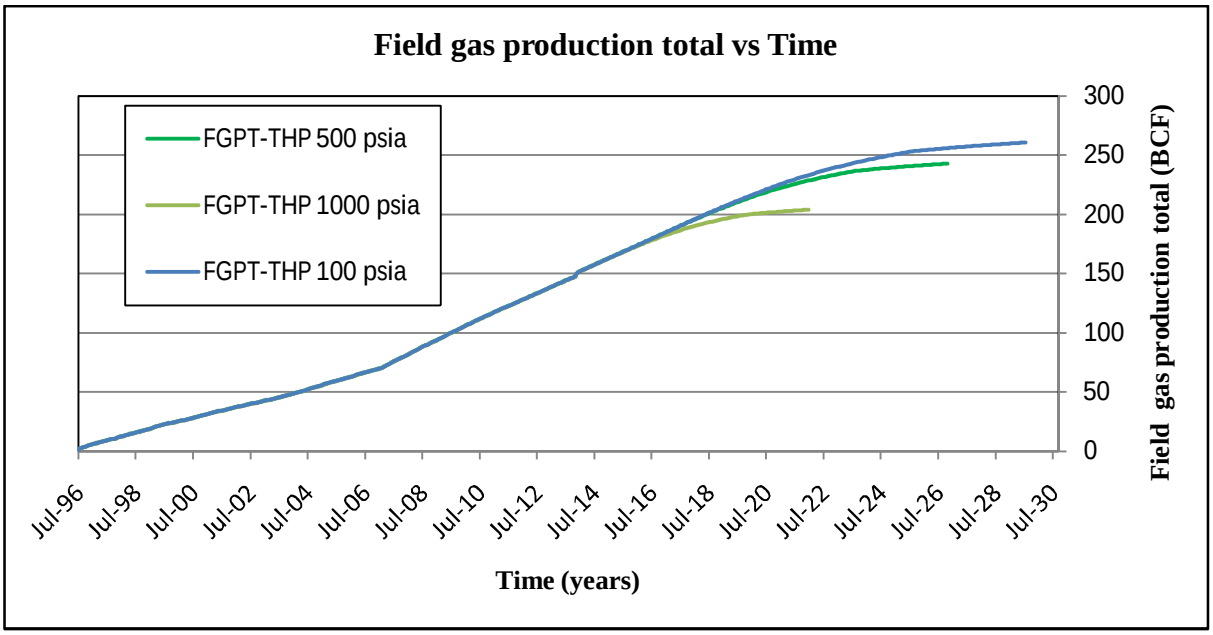

Figure 8.16: Field gas production total for different tubing head pressure

8.14 Forecasting Case-2, Impact of Additional Vertical Well

In this prediction case, drilling of a new vertical well was considered to the lower gas sand. The new well was named NAR-3 and it was considered that production will start from January 2015. The location of the well was seleted based on the gas saturation and pressure of the reservoir. The production rate was set at 10 MMSCF/D. Position of the added well is shown in the Figure 8.17

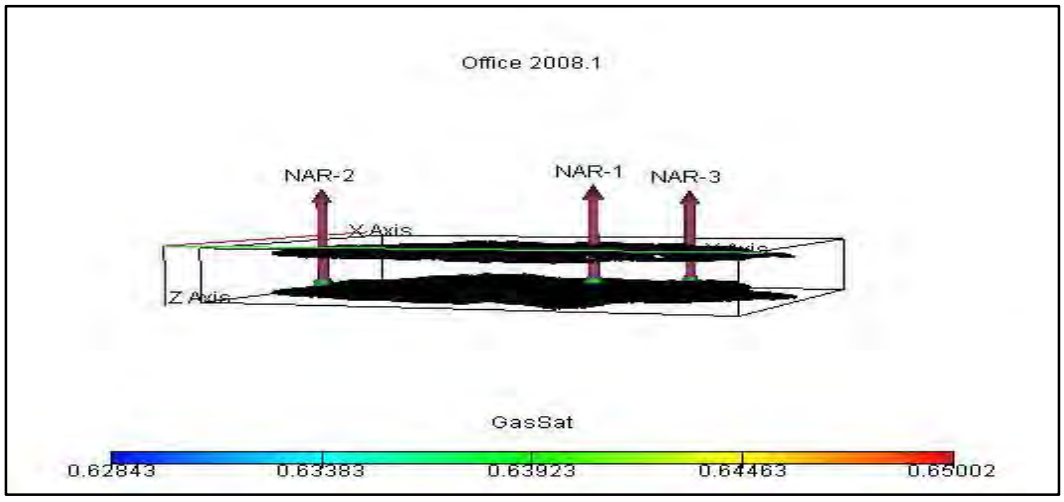

Figure 8.17: 3D view of Narshingdi gas Field after adding a vertical well.

The impact of adding a vertical well on field total production is shown in Figure 8.18. The Figutre 8.18 shows that field production total will be 203.98 BCF at the end of October 2019. This field production total is same as the do nothing scenarios (204.02 BCF) but the production will be more quicker than the do nothing scenarios.

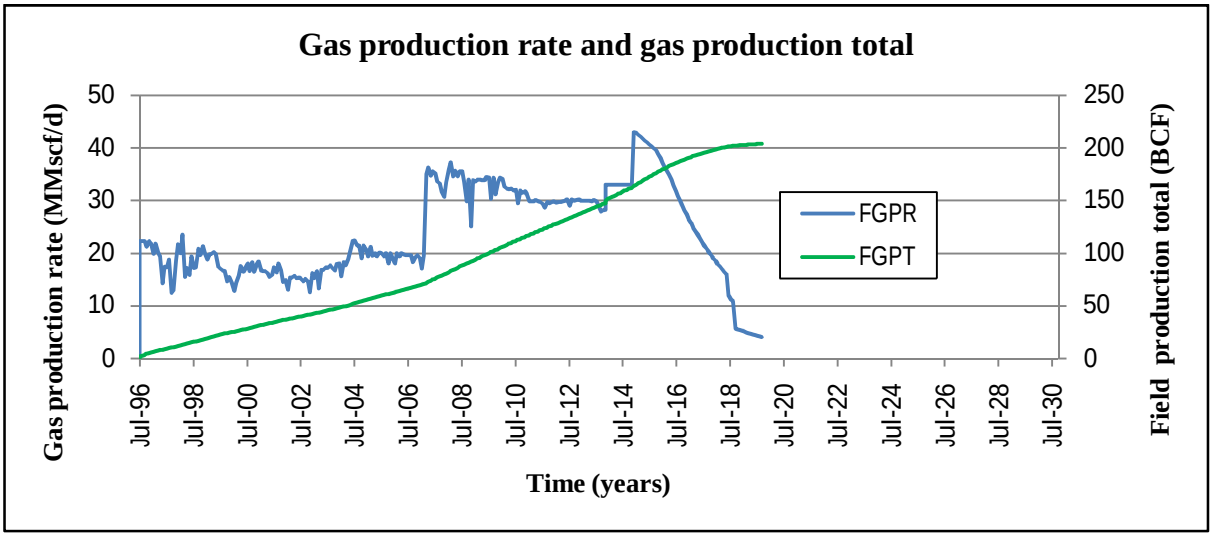

Figure 8.18: Impact of additional vertical well on total production for THP 1000 psia

Well gas production rate with the additional well is shown in Figure 8.19 and this figure suggests that NAR-1, NAR-2and NAR-3 will reach to the economic limit at October 2019, September 2018 and June 2018 respectively.

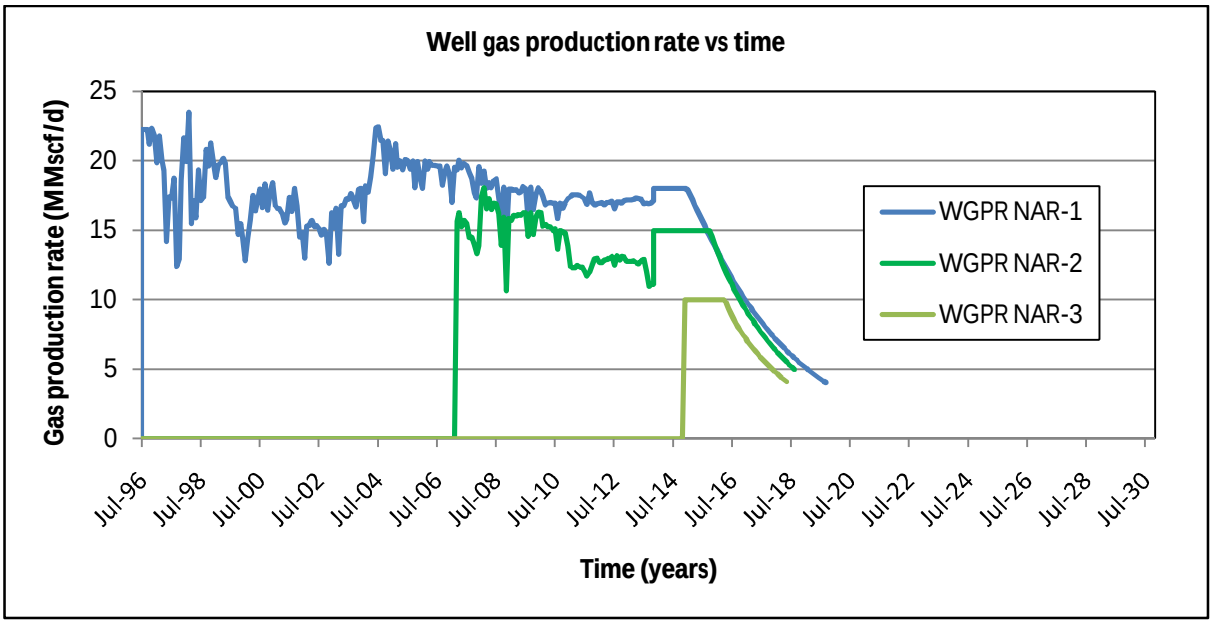

Figure 8.19: Well gas production rate vs time with a additional vertical well

8.15 Effect of Gas Compression with the Additional Vertical Well

Figure 8.20 and 8.21 shows the impact of gas compression on total production with the additional vertical well. Here two different condition are shown first one is lowering the well head pressure to 500 psia and the second one is lowering the well head pressure to 100 psia. Figure 8.20 and 8.21 shows that the field priduction total will be 242.46 BCF and 260.01 BCF with the additional well for tubing head pressure 500 and 100 psia respectively.

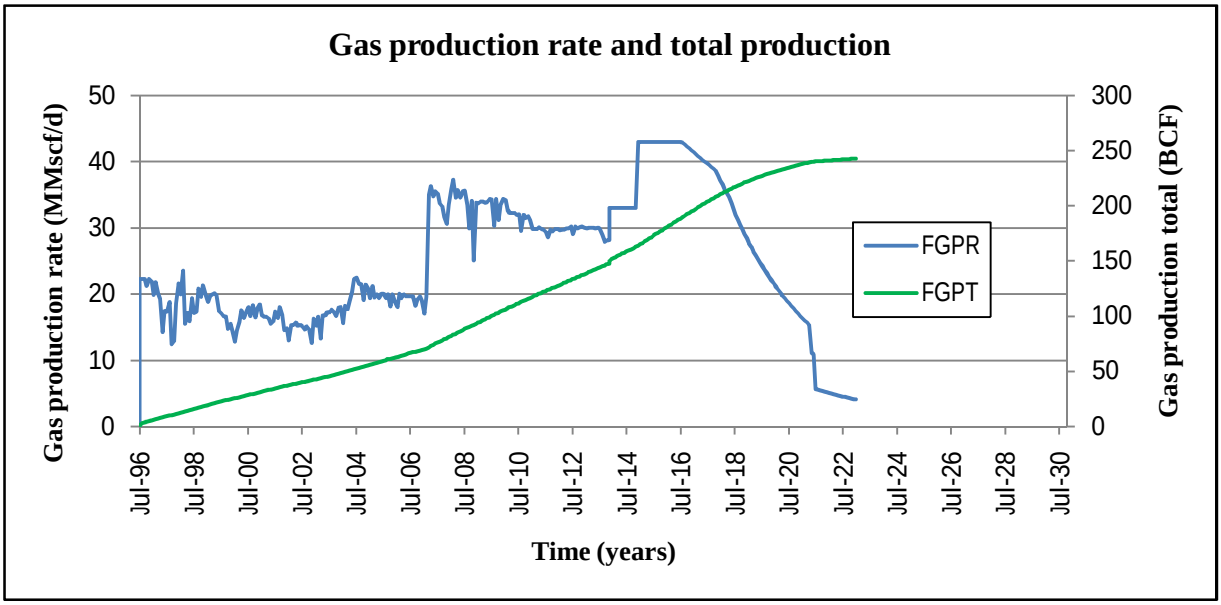

Figure 8.20: Impact of additional vertical well on total production for THP 500 psia

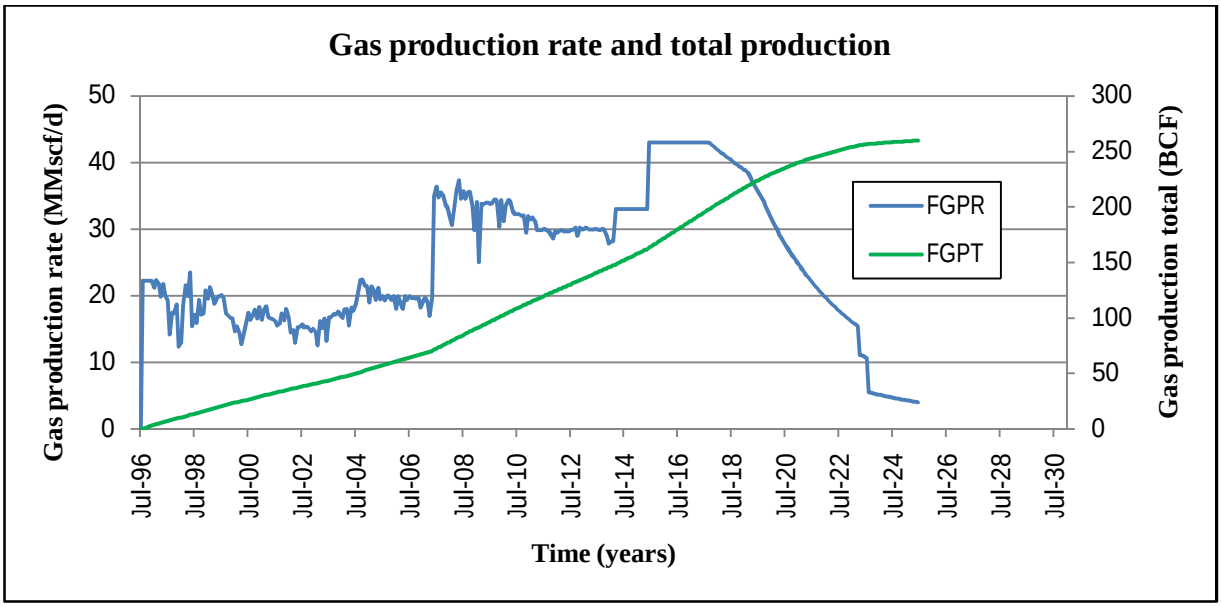

Figure 8.21: Impact of additional vertical well on total production for THP 100 psia

8.16 Comparison of results for two cases

In this section a comparision of field gas production rate, well gas production rate, field total production for two cases are shown in Figure 8.22 and 8.23. Figure 8.22 shows that additional well will increase the total production rate initially but rate will fall below the rate with no additional wells after 2018. For Case-1 field production will continue up to January 2022 and for Case-2 field production will continue up to October 2019 to reach the economic limit.

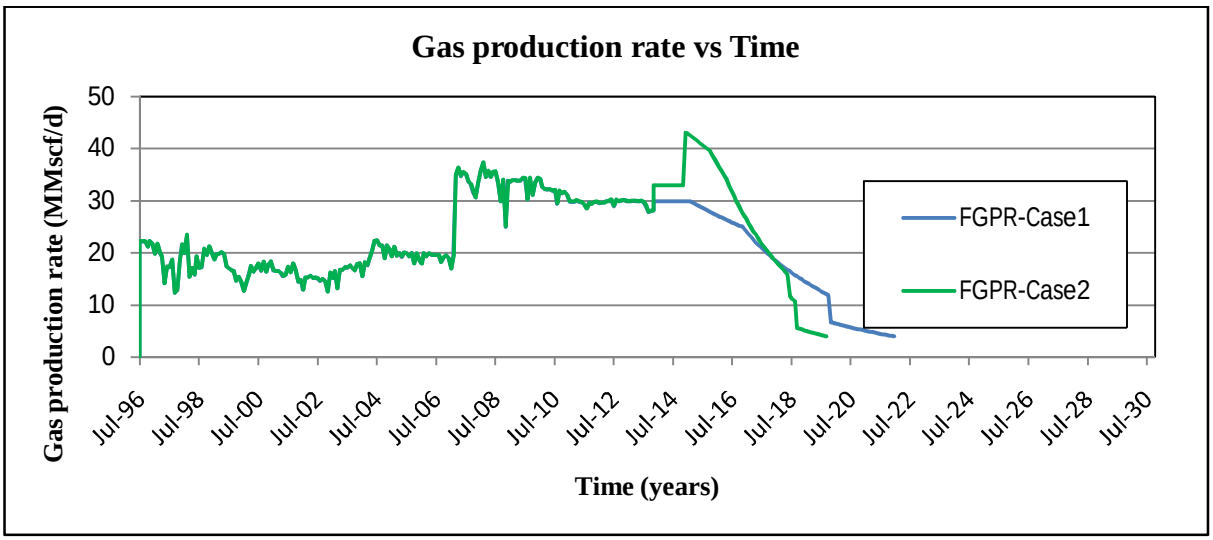

Figure 8.22: Gas production rate vs time

Figure 8.23 shows that there is no impact of a new well on the field total production.

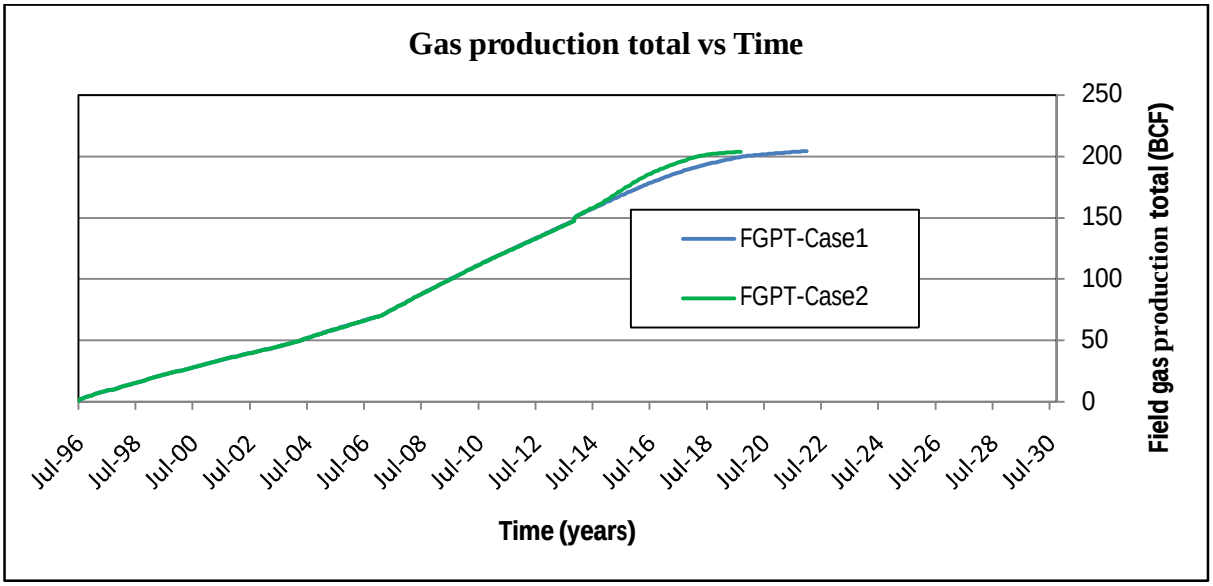

Figure 8.23: Impact of additional well on total production

Figure 8.24 shows the impact of additional vertical well on NAR-1. If another well is drilled then gas production rate of NAR-1 will decrease more rapidly than the existing situation. NAR-1 will reach to the economic limit January 2022 and October 2019 for Case-1 and Case-2 respectively.

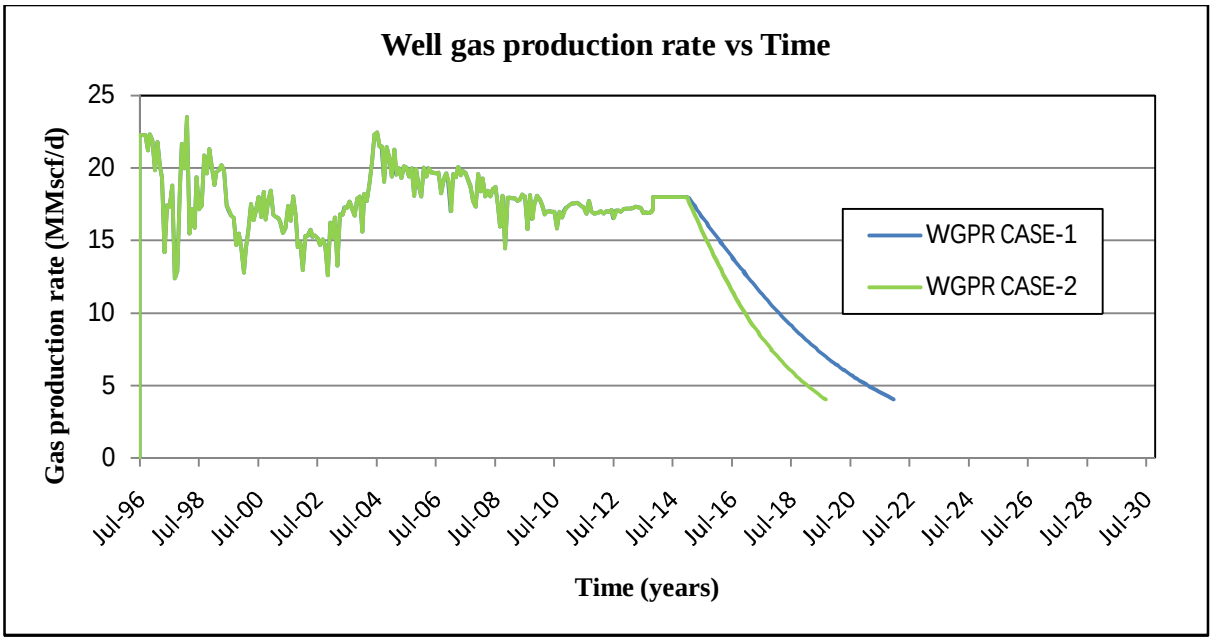

Figure 8.24: Impact of additional well on rate of NAR-1

Figure 8.25 shows the impact of additional vertical well on NAR-2. NAR-2 will reach to the economic limit October 2019 and September 2018 for Case-1 and Case-2 respectively.

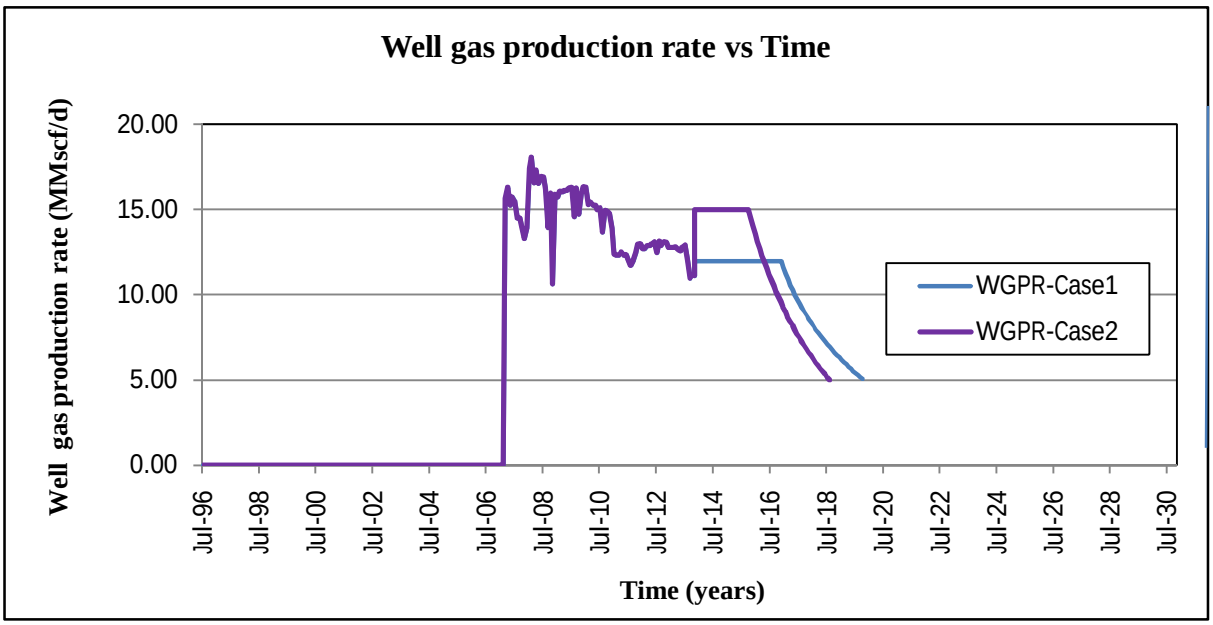

Figure 8.25: gas production rate for two cases in NAR-2

8.17 Result Summary for Two Different Cases

Case 1: do nothing scenario for THP's 1000, 500 and 100 psia.

Case-2: prediction scenario with additional vertical well for THP's 100, 500 and 100 psia.

Table 8.5 Lower Gas Sand Forecast Simulation Results at THP=1000 psia

Forecast Cases	GIIP (BCF)	FGPT (BCF)	RF(%)	Field life (years)	End of simulation
Case-1	302.72	204.02	67.40	26 (1996- 2022)	Minimum economic gas rate
Case-2	302.72	203.98	67.38	23 (1996- 2019)	Minimum economic gas rate

Table 8.6 Lower Gas Sand Forecast Simulation Results at THP=500 psia

Forecast Cases	GIIP (BCF)	FGPT (BCF)	RF(%)	Field life (years)	End of simulation
Case-1	302.72	242.60	80.14	30 (1996- 2026)	Minimum economic gas rate
Case-2	302.72	242.46	80.09	27 (1996- 2023)	Minimum economic gas rate

Table 8.7 Lower Gas Sand Forecast Simulation Results at THP=100 psia

Forecast Cases	GIIP (BCF)	FGPT (BCF)	RF(%)	Field life (years)	End of simulation
Case-1	302.72	260.47	86.04	33 (1996- 2029)	Minimum economic gas rate
Case-2	302.72	260.01	85.89	28 (1996- 2024)	Minimum economic gas rate

CHAPTER 9

RESULTS AND DISCUSSIONS

9.1 Results

The Monte Carlo simulation approach for upper gas sand shows that the P_{90}, P_{50} and P_{10} GIIP values are 69.24, 95.21 and 127.51 BCF. Reservoir simulation study shows that the GIIP is 83.53 BCF.

Result summary of all methods is shown in Table 9.1 for Lower Gas Sand:

Table 9.1 Result summary

<table>
<tr><td colspan="2" rowspan="2">Name of the method</td><td colspan="3" rowspan="2">GIIP (BCF)</td><td rowspan="2">Reserve (BCF)</td><td rowspan="2">RF (%)</td></tr>
<tr></tr>
<tr><td colspan="2" rowspan="2">Volumetric method
(Monte Carlo Simulation)</td><td>P_{90}</td><td>P_{50}</td><td>P_{10}</td><td rowspan="2"></td><td rowspan="2"></td></tr>
<tr><td>225.953</td><td>289.096</td><td>371.553</td></tr>
<tr><td rowspan="2">Material Balance</td><td>SBHP Approach</td><td colspan="3">350</td><td>275</td><td>78.57</td></tr>
<tr><td>SIWH Approach</td><td colspan="3">300</td><td></td><td></td></tr>
<tr><td rowspan="3">Flowing Gas Material Balance</td><td>Bottom Hole Pressure Approach</td><td colspan="3">366</td><td></td><td></td></tr>
<tr><td>Well head pressure Approach</td><td colspan="3">382</td><td></td><td></td></tr>
<tr><td>AWMB</td><td colspan="3">390</td><td></td><td></td></tr>
<tr><td rowspan="3">Advanced decline Curve Analysis</td><td>Blasingame type curve</td><td colspan="3">413</td><td>292</td><td>69.88</td></tr>
<tr><td>Agarwal – Gardener type curve</td><td colspan="3">421</td><td>297</td><td>69.88</td></tr>
<tr><td>NPI type curve</td><td colspan="3">413</td><td>294</td><td>69.88</td></tr>
<tr><td colspan="2">Reservoir Simulation</td><td colspan="3">302.72</td><td>204.02</td><td>67.40</td></tr>
</table>

GIIP: The GIIP values of different methods vary from 300 BCF to 421 BCF. Different reasons of this variation will be explained.

Reserve: Recoverable reserve estimated from material balance, advanced decline curve analysis and reservoir simulation are 275, 290 and 204.02 BCF respectively.

Field life: The field life was calculated by the reservoir simulation approach and it show that the field life is 26 years (1996 to 2022) at a minimum economic rate of 4 and 5 MMSCFD for NAR-1 and NAR-2 in case of abandonment tubing head pressure 1000 psia.

Effect of compressor: Recovery factor will be 67.40, 80.14, 86.04% and field life will be 26, 30, and 33 years for abandonment THP 1000, 500, 100 respectively.

Reservoir Performance: Average reservoir permeability calculated from the type curve analysis using Topaze software is 35.6 md for LGS. Skin factor was also calculated the value of skin factor is 0.282

Reservoir area: Reservoir drainage area calculated from the type curve analysis is around 9900 acre for NAR-1 and this area is within the range of the area used in Monte Carlo Simulation.

9.2 Discussions on Result

The reasons for the variations in the values of GIIP are:

The probabilistic methods have several inherent problems. They are affected by all input parameters, including the most likely and maximum values for the parameters. The main input parameter for Monte Carlo simulation for volumetric reserve estimate is reservoir area and the reservoir thickness. Geological and geophysical mapping give an indication of a poll shape and orientation but typically the confidence in the hydrocarbon in place calculation using this value is not high.

Material Balance method uses the actual reservoir performance data (static reservoir pressure), and is therefore generally accepted as the most accurate procedure for estimating original gas in place. Average reservoir pressure or static reservoir pressure can be found from the well test analysis but regular pressure survey are not conducted in Narshingdi gas field so no pressure data were available for Narshingdi field. Static bottom hole pressure data calculated from static well head pressure data was used in material balance analysis.

The FMB is a good alternative of conventional material balance and very helpful for GIIP calculation. Daily production data can give more precise result of GIIP but the pressure data used here is monthly data taken from the BGFCL was recorded at the last day of the month.

Rate transient analysis gives us significant information in several areas: GIIP, permeability, skin, reservoir drainage area etc. and these results depend on the type curve matching. A small variation in type curve marching change the result significantly. In case of type curve analysis daily basis data improves the result but in this analysis monthly data was used. To get the more accurate result it needs to use the daily basis data. Regular well test analysis can give the more accurate result of permeability, skin and reservoir drainage area.

The major goal of reservoir simulation is to predict future performance of the reservoir and find ways and means of optimizing the recovery of the hydrocarbons under various operating conditions. In this study the history of Narshingdi gas field was matched and the future of the field was predicted. The geo model used here was too old, (built in 2008) so several modifications were needed to match the history of tubing head pressure with the simulated tubing head pressure. An updated geo model with the latest information of the reservoir can improve the simulation result.

CHAPTER 10

CONCLUSIONS AND RECOMMENDATIONS

The production history of lower gas sand suggests that there is no aquifer support at the lower gas sand. The material balance study also confirms that the lower gas sand is volumetrically closed and there is no external pressure support.

All the available methods of reserve estimation were performed to calculate the GIIP of the LGS, these result suggest that the GIIP of the LGS is 350 BCF (with an exception of ± 15%). So this result should be used to design the production facilities and preparation for the gas contacts.

The Monte Carlo simulation approach shows that the P_{90} (proved), P_{50} (proved + probable) and P_{10} (proved + probable + possible) reserve for the upper gas sand is 69, 95 and 127 BCF respectively. So the upper gas sand is also potential for production.

Reservoir simulation study shows that NAR-2 and NAR-1 will reach the economic limit on October 2019 and January 2022 respectively if the abandonment THP is maintained at 1000 psia. This study also shows that the use of compressor will increase the field life and it will also increase the ultimate recovery and recovery factor.

If the abandonment THP is maintained at 500 psia then NAR-2 and NAR-1 will reach the economic limit on September 2023 and November 2026. In this case, recovery factor will increase by 13%. If the THP is further lowered using the compressor to 100 psia then NAR-2 and NAR-1 will reach to economic limit on August 2025 and August 2029 respectively. In this case recovery factory will increase by 18.64%.

This study shows that the water production from the lower gas sand is insignificant and uniform (1 bbl/MMscf).

Reservoir simulation study also shows that drilling one more vertical well in the lower gas sand will not be beneficial as it will not increase the recoverable reserve. No additional well

is needed to produce from the upper gas sand. The well NAR-1 and NAR-2 should be used to produce from the upper gas sand when the lower gas sand will go in abandonment.

Recommendations

Regular pressure survey should be performed to understand the reservoir behavior more accurately.

Natural energy of a volumetric reservoir declines rapidly and recovery maximization may be possible by using artificial lifts. Compressor should be used in the wells to produce gas at lower tubing head pressure requirements. A detailed feasibility study should be carried out before any installations.

There is an uncertainty in the fluid contact of the lower gas sand; this uncertainty should be resolved by reviewing the interpretation of both NAR-1 and NAR-2 well log data.

Once the production starts from the upper gas sand, a simulation study may be carried out to determine the upper sand gas more accurately.

NOMENCLATURE

AWMB	Approximate Wellhead Material Balance
Bbl(s)	Barrels
Bbl/MMSCF	Barrels per Million Standard Cubic Feet
BHP	Bottom Hole (static) Pressure
BHT	Bottom Hole Temperature
CDF	Cumulative Density Function
CGR	Condensate Gas Ratio
EUR	Expected Ultimate Recovery
FBHP	Flowing Bottom Hole Pressure
FGIP	Field Gas In Place
FGPR	Field Gas Production Rate
FGPT	Field Gas Production Total
FPR	Field Reservoir Pressure
ft	Feet
ftss	Feet Below Sea Level
GDT	Gas down to
GIP	Gas In Place
GIIP	Gas Initially In Place
GPR	Gas Production Rate
GPRH	Gas Production Rate History
GWC	Gas Water Contact
Kr	Relative Permeability
Krg	Relative Permeability of Gas
Kw	Relative Permeability of Water
LGS	Lower Gas Sand
MD	Measured Depth

mD	millidarcies
MDT	Modular Formation Tester
Mscf/day	Thousand Standard Cubic Feet per Day
MMscf/day	Millions Standard Cubic Feet per Day
NPI	Normalized Pressure Integral
NTG	Net to Gross Ratio
FPR	Field Pressure
P_i	Initial Reservoir Pressure
psia	Pounds per Square Inch Absolute
PVT	Pressure Volume Temperature
P_{ab}	Abandonment Pressure
rb	Reservoir Barrels
rb/Mscf	Reservoir Barrels per Thousand Standard Cubic Feet
RFT	Repeat Formation Tester
RGIP	Region Gas In Place
RF	Recovery Factor
scf/d	Standard Cubic Feet per Day
S_{wc}	Connate Water Saturation
stb	Stock Tank Barrels
Sw	Water Saturation
Rt	True Resistivity of the Formation
THP	Tubing Head Pressure
THPH	Tubing Head Pressure Historical
TVDSS	True Vertical Depth (sub-sea)
WBHPH	Well Bottomhole Pressure Historical
WGR	Water Gas Ratio
WGRH	Water Gas Ratio Historical

WCGR	Well Condensate Gas Ratio
WCGRH	Well Condensate Gas Ratio History
WGPR	Well Gas Production Rate
WGPRH	Well Gas Production Rate History
WHP	Well Head Pressure
WWGR	Well Water Gas Ratio
WWGRH	Well Water Gas Ratio History
WTHP	Well Tubing Head Pressure
WTHPH	Well Tubing Head Pressure History
SIWHP	Shut In Well Head Pressure
SIBHP	Shut In Bottom Hole Pressure
SCAL	Special Core Analysis
SGS	Sequential Gaussian Simulation

REFERENCES

1. http://www.glossary.oilfield.slb.com/ (accessed 10 December 2014).

2. Chowdury, Z. and Gomes, E. 2000. Material Balance Study of Gas Reservoir by Flowing Well Method, A Case Study of Bakhrabad Gas Field, Paper SPE 64456 was prepared for presentation at the SPE Asia Pacific Gas Conference and Exhibition held in Brisbane, Australia, 16-18 October 2000.

3. Lee, J. and Wattenbargar, R. A. 1996.*Gas Reservoir Engineering*, Volume 5, SPE text book series.

4. RPS Energy. 2009. Narshingdi Geological study, Petrobangla, Dhaka (November 2009)

5. Gustavson Associates. 2011. Updated Report on Bangladesh Gas Reserve Estimation 2010, Hydrocarbon Unit, Energy and Mineral Resources Division, Government of the People's Republic of Bangladesh (February 15,2011)

6. Akter, F. 2009. *Reserve estimation study of Narshingdi gas field using ECLIPSE-100.* M.Sc. Thesis, Norwegian University of Science and Technology, Trondheim, Norway (June 28, 2009)

7. Lisa, D. and Geol, P. 2014. Reserve estimation for geologist, part-3 volumetric estimation, Fekete Associate Inc.

8. Ikoku, C. U. 1984. *Natural Gas Reservoir Engineering*, the Pennsylvania University, Krieger publishing company Malabar, Florida

9. Truong, T. 2002. An Improved Method for Reserves Estimation, SPE, HCMC U. of Technology SPE 101939-STU

10. Murtha, J. 1997. Monte Carlo Simulation; Its status and Future, J Pet Technol 49(4): SPE-37932-MS. Doi 10.2118/37932-MS

11. Behrenbruch, P. Turner, G.J, and Bachouse, A.R. 1985. Probabilistic Hydrocarbon Reserve Estimation: A Novel Monte Carlo Approach, Paper SPE 13982, was prepared for the offshore Europe 85 conference on conjunction with the society of Petroleum Engineers of AIME, held in Aberdeen 10-13 September 1985.

12. Risk theory-Fekete 2014, http://www.fekete.com/SAN/TheoryAndEquations/HarmonyTheory Equation..... (accessed in 8 December 2014)

13. Wikipedia.2014. Triangular distribution (9 November 2014 revision), http://en.wikipedia.org./w./index.php?title=Traiangular_distrobution&oldid=633114585 (accessed 10 December 2014)

14. Jahn,F. Cook,M and Graham, M. 1998. Hydrocarbon Exploration and Production, Dps development in petroleum science series, Elsevier Science B.V., Amsterdam, Netherlands.

15. Dake, L.P. 1978. *Fundamental of Reservoir Engineering*, Developments in Petroleum Science, 8, Elsevier Science Publishers B.V., The Hague, Netherlands

16. Kumar, S. 1987. *Gas Production Engineering*, volume 4, Gulf Publishing Company, Huston Texas.

17. Choudhury, Z. *Reservoir Engineering Study of Bakhrabad Gas Field*. MSc. Thesis, Bangladesh University of Science and Technology, Dhaka, Bangladesh (August 2009

18. Matter, L. and Mcneil, R. 1998. The Flowing Gas Material Balance; The Journal of Canadian Petroleum Technology, vol 37, No 2, February 1998.

19. Transient type curve analysis, Fekete associate Inc.2014

20. Fekete Software Training Course, FASTRTA. 2014

21. Chen,Z. 2007. Reservoir simulation mathematical techniques in oil recovery university of Calgary. Calgary, Canada.

22. Rwchungura,R. Dadashpour, M. and Kleppe.J. 2011. Advanced History Matching Techniques Reviewed. Paper SPE 142497 presented at the SPE Middle East Oil and Gas Show and Conference held in Manama, Bahrain, 25-28 September, 2011.

23. Olumide, G. 2006. *History Matching with 4D Seismic and Uncertainty Assessment, Department of Petroleum Engineering and Applied Geophysics*. MSc. Thesis, Norwegian University of Scoence and technology, Trondheim, Norway. (Spring, 2006.)

24. Nan, C. 2012. History Matching of Reservoir Simulation Models. Prepare for Norne Village, Institute if Petroleum Technology, IPT, Norwegian University of Science and Technology, Trondheim, Norway. February, 2012

25. Almuallim, H. Edwards, K. and Ganzer, L. 2010. History-Matching With Sensitivity-Based Parameter Modifications at Grid-Block Level. Paper SPE 131627 presented at the EUROPEC/EAGE Annual Conference and Exihibtion held in Barcelona, Spain, 14-17 June 2010.
26. ECLIPSE 100 References Manual 2001A, Schlumberger, Geoquest.
27. ECLIPSE, Version 2008.1 Reference Manual, 2008, UK: Schlumberger.

Appendix-1

Static bottom- hole pressure (SBHP) estimated from shut in well head pressure

Average Temperature and Z-Factor Method

Depth, z= 10443ft, well head temperature, Twh = 140º F, reservoir temperature 205ºF, Ppc=667.8383 psia, Tpc=357.3084 ºR

First trial

$$Pws = Pwh + 0.25\left(\frac{Pwh}{100}\right)\left(\frac{z}{100}\right)$$

$$= 3480 + \frac{0.25*3480*10423}{100*100}$$

$$= 4386 \text{ psia}$$

$$Tav = \frac{140+460+205+460}{2}$$

$$= 632.5^{o}R$$

$Tpr = \frac{632.5}{357.3084} = 1.8$, $Ppr = \frac{3933}{667.8383} = 5.88$ Now using the chart Zav =0.93

$$s = \frac{0.0375*\gamma g*z}{Zav*Tav} = \frac{0.0375*0.6*10423}{0.93*632.5} = 0.39868$$

$$Pws = Pwh\, e^{s/2} = 3480\, e^{0.39868/2} = 4248 \text{ psia}$$

Second trial,

Pwh = 4248 psia

$Pav = \frac{4248+3480}{2} = 3863$, $Ppr = \frac{3933}{667.8383} = 5.79$, Tpr = 1.8 now from the plot Zav=0.93

$$s = \frac{0.0375*\gamma g*z}{Zav*Tav} = \frac{0.0375*0.6*10423}{0.93*632.5} = 0.39868$$

$$Pws = Pwh\, e^{s/2} = 3480\, e^{0.39868/2} = 4248 \text{ psia}$$

So the static bottom hole pressure is 4248 psia.

Similarly the the following shut in well head pressure is converted to the static bottom hole pressure.

Date	Shut in well head pressure (psia)	Static bottom hole pressure (psia)	Cumulative production, BCF
Before Production		4575	0
04/24/1997	3480	4248	5.576200
06/25/1997	3400	4150	6.636490
03/24/2002	3050	3740	36.10290
07/22/2002	3042	3720	37.97120
10/23/2003	2780	3416	46.15360
01/20/2006	2705	3320	62.40200
09/22/2006	2634	3233	67.15280
10/22/2006	2600	3200	67.69290
09/23/2007	2508	3088	73.77850
01/10/2008	2450	3022	82.50000
11/30/2009	2325	2870	105.1767
09/30/2010	2231	2753	114.7852

Appendix 2: Production performance prediction for 10 years (2014 to 2023) for case 1

Time (years)	FGPR (MMscf/d)	FGPT (BCF)	FPR (psia)	FGIP (BCF)	WGPR (MMscf/d) NAR-1	WGPR (MMscf/d) NAR-2
Jan-14	30.0000	149.472	2531.3535	236.77	18.00	12
Feb-14	30.0000	150.372	2522.1763	235.87	18.00	12
Mar-14	30.0000	151.272	2513.0002	234.97	18.00	12
Apr-14	30.0000	152.172	2503.8250	234.07	18.00	12
May-14	30.0000	153.072	2494.6504	233.17	18.00	12
Jun-14	30.0000	153.972	2485.4763	232.27	18.00	12
Jul-14	30.0000	154.872	2476.3044	231.37	18.00	12
Aug-14	30.0000	155.772	2467.1360	230.47	18.00	12
Sep-14	30.0000	156.672	2457.9753	229.57	18.00	12
Oct-14	30.0000	157.572	2448.8311	228.67	18.00	12
Nov-14	30.0000	158.472	2439.7007	227.77	18.00	12
Dec-14	30.0000	159.372	2430.5815	226.87	18.00	12
Jan-15	30.0000	160.272	2421.4749	225.97	18.00	12
Feb-15	29.9064	161.169	2412.4016	225.07	17.91	12
Mar-15	29.6457	162.058	2403.4097	224.19	17.65	12
Apr-15	29.3966	162.940	2394.4915	223.30	17.40	12
May-15	29.1535	163.815	2385.6460	222.43	17.15	12
Jun-15	28.9129	164.682	2376.8726	221.56	16.91	12
Jul-15	28.6727	165.542	2368.1716	220.70	16.67	12
Aug-15	28.4364	166.395	2359.5417	219.85	16.44	12
Sep-15	28.2033	167.241	2350.9822	219.00	16.20	12
Oct-15	27.9725	168.081	2342.4922	218.16	15.97	12
Nov-15	27.7403	168.913	2334.0723	217.33	15.74	12
Dec-15	27.5111	169.738	2325.7217	216.51	15.51	12
Jan-16	27.2848	170.557	2317.4397	215.69	15.28	12
Feb-16	27.0613	171.368	2309.2251	214.87	15.06	12
Mar-16	26.8366	172.174	2301.0789	214.07	14.84	12
Apr-16	26.6131	172.972	2293.0005	213.27	14.61	12
May-16	26.39269	173.7642	2284.9888	212.48	14.39	12
Jun-16	26.17501	174.5495	2277.0425	211.69	14.18	12

Time (years)	FGPR (MMscf/d)	FGPT (BCF)	FPR (psia)	FGIP (BCF)	WGPR (MMscf/d) NAR-1	WGPR (MMscf/d) NAR-2
Jul-16	25.95822	175.3282	2269.1616	210.92	13.96	12
Aug-16	25.74025	176.1004	2261.3472	210.14	13.74	12
Sep-16	25.52489	176.8662	2253.5974	209.38	13.52	12
Oct-16	25.31217	177.6255	2245.9121	208.62	13.31	12
Nov-16	25.10191	178.3786	2238.2908	207.87	13.10	12
Dec-16	24.89131	179.1253	2230.7341	207.12	12.89	12
Jan-17	24.29933	179.8543	2223.3599	206.39	12.68	11.61892
Feb-17	23.71092	180.5656	2216.1675	205.68	12.47	11.23844
Mar-17	23.16092	181.2605	2209.1453	204.98	12.27	10.89349
Apr-17	22.63761	181.9396	2202.2832	204.30	12.07	10.57252
May-17	22.13677	182.6037	2195.5747	203.64	11.86	10.27498
Jun-17	21.65601	183.2534	2189.0151	202.99	11.66	9.99626
Jul-17	21.18981	183.8891	2182.5984	202.35	11.46	9.728672
Aug-17	20.74218	184.5113	2176.3176	201.73	11.27	9.475999
Sep-17	20.31065	185.1207	2170.1687	201.12	11.07	9.235902
Oct-17	19.88976	185.7173	2164.146	200.53	10.88	9.006876
Nov-17	19.47542	186.3016	2158.248	199.94	10.69	8.783639
Dec-17	19.07419	186.8738	2152.4717	199.37	10.50	8.569776
Jan-18	18.68547	187.4344	2146.8123	198.81	10.32	8.364637
Feb-18	18.3079	187.9836	2141.2668	198.26	10.14	8.167112
Mar-18	17.93911	188.5218	2135.8323	197.72	9.96	7.976099
Apr-18	17.57183	189.049	2130.5088	197.20	9.78	7.788466
May-18	17.21533	189.5654	2125.2927	196.68	9.61	7.60755
Jun-18	16.86835	190.0715	2120.1814	196.17	9.44	7.432519
Jul-18	16.53054	190.5674	2115.1721	195.68	9.27	7.263048
Aug-18	16.20134	191.0534	2110.2622	195.19	9.10	7.09874
Sep-18	15.87667	191.5297	2105.4497	194.71	8.94	6.93794
Oct-18	15.55403	191.9964	2100.7351	194.25	8.77	6.779967
Nov-18	15.2401	192.4536	2096.1152	193.79	8.61	6.626835
Dec-18	14.93401	192.9016	2091.5876	193.34	8.46	6.478052
Jan-19	14.63546	193.3406	2087.1504	192.90	8.30	6.333442
Feb-19	14.34413	193.771	2082.8005	192.47	8.15	6.192767

Time (years)	FGPR (MMscf/d)	FGPT (BCF)	FPR (psia)	FGIP (BCF)	WGPR (MMscf/d) NAR-1	WGPR (MMscf/d) NAR-2
Mar-19	14.05969	194.1928	2078.5361	192.05	8.00	6.055749
Apr-19	13.77386	194.606	2074.3569	191.64	7.85	5.920673
May-19	13.49397	195.0108	2070.2617	191.23	7.71	5.788059
Jun-19	13.22103	195.4074	2066.248	190.84	7.56	5.659079
Jul-19	12.95462	195.7961	2062.3149	190.45	7.42	5.533527
Aug-19	12.69463	196.1769	2058.4602	190.07	7.28	5.411223
Sep-19	12.44068	196.5501	2054.6819	189.69	7.15	5.291969
Oct-19	12.19263	196.9159	2050.9773	189.33	7.02	5.17562
Nov-19	6.75	199.9256	2043.7904	188.62	6.75	
Dec-19	6.62	200.1242	2040.3063	188.28	6.62	
Jan-20	6.50	200.3191	2036.8926	187.94	6.50	
Feb-20	6.37	200.5103	2033.548	187.61	6.37	
Mar-20	6.25	200.6979	2030.271	187.29	6.25	
Apr-20	6.13	200.8819	2027.0599	186.97	6.13	
May-20	6.02	201.0625	2023.9133	186.66	6.02	
Jun-20	5.90	201.2396	2020.8311	186.35	5.90	
Jul-20	5.79	201.4131	2017.8121	186.06	5.79	
Aug-20	5.67	201.5834	2014.8549	185.76	5.67	
Sep-20	5.56	201.7503	2011.958	185.48	5.56	
Oct-20	5.46	201.9139	2009.121	185.20	5.46	
Nov-20	5.35	202.0744	2006.342	184.92	5.35	
Dec-20	5.25	202.2319	2003.6199	184.66	5.25	
Jan-21	5.15	202.3863	2000.9532	184.39	5.15	
Feb-21	5.05	202.5377	1998.3407	184.14	5.05	
Mar-21	4.95	202.6862	1995.782	183.88	4.95	
Apr-21	4.85	202.8317	1993.2767	183.64	4.85	
May-21	4.75	202.9743	1990.8236	183.39	4.75	

Time (years)	FGPR (MMscf/d)	FGPT (BCF)	FPR (psia)	FGIP (BCF)	WGPR (MMscf/d) NAR-1	
Jun-21	4.66	203.1141	1988.4213	183.16	4.66	
Jul-21	4.57	203.2511	1986.0687	182.93	4.57	
Aug-21	4.48	203.3854	1983.7646	182.70	4.48	
Sep-21	4.39	203.517	1981.5082	182.48	4.39	
Oct-21	4.30	203.646	1979.2985	182.26	4.30	
Nov-21	4.22	203.7725	1977.1348	182.04	4.22	
Dec-21	4.13	203.8965	1975.0161	181.84	4.13	
Jan-22	4.05	204.0182	1972.9412	181.63	4.05	